



# Etude des patrons de variation intraspécifique et de covariation chez les éléments conodontes

Louise Souquet

## ► To cite this version:

Louise Souquet. Etude des patrons de variation intraspécifique et de covariation chez les éléments conodontes. Sciences de la Terre. Université de Lyon, 2018. Français. NNT: 2018LYSEN083 . tel-02418606

**HAL Id: tel-02418606**

<https://theses.hal.science/tel-02418606>

Submitted on 19 Dec 2019

**HAL** is a multi-disciplinary open access archive for the deposit and dissemination of scientific research documents, whether they are published or not. The documents may come from teaching and research institutions in France or abroad, or from public or private research centers.

L'archive ouverte pluridisciplinaire **HAL**, est destinée au dépôt et à la diffusion de documents scientifiques de niveau recherche, publiés ou non, émanant des établissements d'enseignement et de recherche français ou étrangers, des laboratoires publics ou privés.



Numéro National de Thèse: 2018LYSEN083

**THESE de DOCTORAT DE L'UNIVERSITE DE LYON**  
opérée par  
**l'Ecole Normale Supérieure de Lyon**

**Ecole Doctorale N° 341**  
**Evolution Ecosystèmes Microbiologie Modélisation**

**Spécialité de doctorat:** Paléoenvironnement et évolution  
**Discipline:** Sciences de la Terre

Soutenue publiquement le 18/12/2018, par :  
**Louise SOUQUET**

---

**Étude des patrons de variation intraspécifique  
et de covariation chez les éléments conodontes**

---

Devant le jury composé de :

ZOLLIKOFER, Christoph, Professeur, Universität Zürich, Rapporteur  
CORRADINI, Carlo, Professeur, Università degli studi di Cagliari, Rapporteur  
PONCE DE LEÓN, Marcia, Senior researcher, Universität Zürich, Examinatrice  
KHILA, Abderrahman, Directeur de recherche, ENS de Lyon, Examinateur  
GOUDEMARD, Nicolas, Professeur, ENS de Lyon, Directeur de thèse



## Remerciements

Tout d'abord, je tiens à remercier mon directeur de thèse Nicolas Goudemand pour avoir financé ce doctorat, ainsi qu'à la direction et aux membres de l'IGFL pour m'avoir accueilli au sein du laboratoire. Un grand merci à l'équipe administrative de l'institut, la plus efficace que je n'ai jamais vu.

Ensuite, je remercie chaleureusement toutes les personnes m'ayant aidé de près ou de loin pendant ce travail de thèse: Catherine Girard de m'avoir offert ma première expérience de terrain et donné accès à son matériel, ainsi que pour son implication, ses discussions, ses conseils, et son expertise pendant ces trois dernières années; Pauline Guenser sans qui une grande partie de ce travail n'aurait pas été possible; Cyril Charles pour avoir toujours été présent pour répondre à mes nombreuses questions; Giles Escarguel pour avoir piloté mon comité de thèse avant tant de bienveillance; Pauline Joncour de m'avoir permis de sortir victorieuse de plusieurs affrontements avec R; Mathilde Bouchet-Combe pour son aide inestimable avec le microtomographe, ainsi que son soutien indéfectible depuis le premier jours; Morgane Brosse pour son travail sur les neogondolellids, ainsi que son accueil à Zurich, et ses leçon d'utilisation du MEB; Michele Mazza et Manuel Rigo d'avoir fournis une partie du matériel, ainsi que pour leurs commentaires utiles sur les manuscrits; Carlo Corradini pour m'avoir appris à maîtriser la taxonomie des Siphonodella. Je tiens aussi à dire un grand merci à toutes les personnes de mon équipe et de l'équipe Viriot que j'ai eu la chance de cotoyer et qui m'ont beaucoup apporté humainement et scientifiquement ces trois dernières années: Marc, Samuel, Fidji, Roland, Ludivine, Jeremie, Thomas, Laurent et Béatrice. Sans vous je ne serais pas allé bien loin. Merci à Sabrina Renaud d'avoir été mon mentor depuis le master et de m'avoir tant appris.

Pour finir, je remercie du fond du cœur tous mes proches pour leurs encouragements, leur soutien, leur compréhension et leur patience tout au long de cette thèse.

## Résumé

L'évolution est le produit de deux grands facteurs: l'environnement et le développement. Il est donc important de déterminer l'impact de ces deux forces lorsque l'on s'intéresse à l'évolution morphologique d'un organe. Pour cela, il est utile d'étudier l'évolution en temps profond, seul moyen d'observer les mécanismes en action sur de longs intervalles de temps et les réponses à des variations environnementales majeures. Le but de ce travail de thèse est de mieux comprendre l'évolution d'une espèce fossile: le conodonte. Ce vertébré marin dépourvu de mâchoire possède un appareil buccal composé de structures minéralisées semblables à des dents, appelées éléments conodontes. Leur fort taux d'évolution, leur enregistrement fossile long et sub-continu, et la taille importante de leurs populations font de ces éléments conodontes un modèle de choix pour répondre aux questions évolutives en temps profond. Dans la littérature, peu d'études ont tentées de quantifier la forme de ces éléments, et aucune dans un cadre développemental. Grâce à la découverte de fossiles exceptionnellement préservés, ainsi qu'à l'établissement d'une méthodologie pour quantifier les patrons de variation morphologique et de covariation de ces éléments, plusieurs facettes de l'évolution de la forme chez ces éléments ont pu être étudiées. Nous avons entre autre établis l'existence de covariations entre certains traits morphologiques, illustrant les contraintes faisant pression sur ceux-ci. Certaines contraintes sont considérées comme développementales et d'autres potentiellement mécaniques. Des directions évolutives sont également mises en évidence, contraintes par le développement qui canalise ainsi l'évolution. A l'échelle inter-genre, nous avons démontré un lien entre les changements environnementaux (notamment des variations de température) et ces directions évolutives. Ces résultats démontrent un effet croisé des forces développemen-

tales (contraignant les morphologies possibles) et les forces environnementales (sélectionnant les morphologies en fonction des changements de conditions) dans l'évolution des éléments conodontes. Nous proposons des événements d'hétérochronie comme mécanisme sous-jacent à cette évolution, potentiellement contrôlés par la température océanique. La quantification de la forme est également utilisée pour tenter de clarifier la taxonomie des neogondolellides au Trias inférieur. Ces travaux démontrent le potentiel du conodonte en tant qu'organisme modèle pour étudier l'évolution en temps profond.



## Table des matières:

Remerciements	3
Introduction	9
Chapitre 1 : Le corps basal, découverte récente et nouvelles perspectives	19
- Article publié dans Palaeogeography, Palaeoclimatology, Palaeoecology	
Chapitre 2: Conodontes, morphométrie et forces évolutives	51
1 - Croissance et analyse quantitative de la forme des conodontes	51
2- Déterminer les forces évolutives en présence	54
Chapitre 3: Impact de l'environnement et du développement sur l'évolution d'un assemblage d'éléments conodontes du Trias	59
- Article accepté dans Paleobiology	
Chapitre 4 :Forces évolutives et morphologie des conodonts: impact de l'environnement et des contraintes développementales	95
- Article en préparation	
Chapitre 5: Utiliser la morphométrie géométrique et l'analyse de clusters pour démêler la taxonomie des neogondolellides du Griesbachien.	127
- Article en préparation	
Conclusion et perspectives	151



# Introduction

Le terme « Evolution » est aujourd’hui entré dans le langage courant, et prend des définitions différentes selon l’emploi. En biologie, l’Evolution désigne à la fois le patron de variation phénotypique, c’est à dire le changement observé d’un organisme, et les processus qui produisent ces patrons (Gingerich, 2001). Les patrons de variation phénotypiques peuvent être (plus ou moins) facilement observés, quantifiés et étudiés aujourd’hui. Cela est d’autant plus vrai lorsqu’on s’intéresse à la morphologie des organismes. En effet, l’incroyable diversité de formes du vivant et son évolution ont toujours été une source d’émerveillement et un terreau fertile pour bon nombre de questionnements chez les biologistes, et ce depuis bien avant l’époque de Darwin. La morphologie d’un organe est souvent la première observation d’un organisme. Elle est historiquement une manière de saisir synthétiquement les organismes vivants et leurs métamorphoses, car la morphologie « doit contenir l’enseignement de la forme, de la formation et de la transformation des corps organiques » (Goethe, 1817). De plus, la forme est souvent encore aujourd’hui la seule information disponible concernant un organisme, par exemple pour certaines espèces rares, protégées, ou fossiles. Etudier l’évolution des formes du vivant est donc une mine d’information exploitée depuis bien longtemps. Aujourd’hui, il est possible d’étudier et de quantifier de plus en plus précisément ces formes, notamment grâce à l’essor de la morphométrie géométrique et des techniques d’imagerie en trois dimensions. Mais déterminer les processus évolutifs sous-jacents et leurs mécanismes est une tâche bien plus ardue. Historiquement, la synthèse Néo-Darwinienne de l’Evolution établit qu’elle se définit par la diffusion dans une population d’un caractère donné conférant à l’organisme qui le porte

une meilleure valeur sélective, permettant la sélection de ce caractère par sélection naturelle parmi la variation aléatoire naturelle de l'espèce. Les facteurs environnementaux étaient alors considérés comme étant la principale force dirigeant l'évolution, à travers la pression directe qu'ils exercent sur les organismes. Darwin a d'ailleurs été le premier à mettre en évidence l'effet des ressources alimentaires disponibles sur la forme du bec chez le pinson des Galapagos (Darwin, 1859), exemple d'adaptation aujourd'hui bien connu. Depuis, de nombreux cas d'adaptation morphologique à des changements environnementaux ont été mis en évidences dans de nombreuses familles. Mais l'apparition de la biologie évolutive du développement (evo-devo) a démontré que le concept Néo-Darwinien de l'évolution n'est pas exact. La sélection n'est en réalité pas la seule source de non-stochasticité des patrons de variation évolutifs, le rôle important du développement des organismes ayant été démontré comme biaisant la variation phénotypique observée et l'évolution des morphologies. En 1980, Alberch (Alberch, 1980) a résumé cette idée par cette phrase: "In evolution, selection may decide the winner of a given game but development non-randomly defines the players". Cela signifie que l'évolution est en fait le résultat de deux grands mécanismes : le développement et la sélection. Tout d'abord, l'univers des formes possibles que peut prendre un organe est limité par les contraintes développementales, c'est-à-dire par la manière dont les règles universelles de la physique et de la chimie contraignent leur développement embryonnaire et leur croissance. Et seulement par la suite, la sélection filtre les phénotypes déjà existants en fonction de leur valeur sélective. Ces deux processus sont donc complémentaires et intimement liés, les contraintes développementales et les conditions environnementales s'avérant donc être deux forces évolutives majeures.

La question que nombre de chercheurs se posent alors est la suivante : quel est le rôle relatif du développement (facteurs intrinsèques) et de l'environnement (facteurs extrinsèques) dans l'évolution d'un organisme? Tel est la toile de fond de ce travail de thèse.

Dans ce cadre, conduire des études en temps profond est crucial car c'est le seul moyen d'appréhender "the actual course of life's history"(Gould, 1980). L'abondance de données paléoenvironnementales facilite la recherche de corrélation entre des variations climatiques ou biotiques, et les changements morphologiques observés. Cependant, étudier la morphogénèse en temps profond représente un défi en raison du manque de données génétiques et cellulaires disponibles. Dans cette thèse, nous avons tenté d'établir un cadre d'étude pour répondre à cette question en temps profond. Pour cela, un bon modèle biologique est requis, dont les critères sont : (1) Un fort taux d'évolution permettant une base de variation morphologique à étudier ainsi qu'une bonne résolution temporelle des espèces fossiles ; (2) Un registre fossile long et subcontinu pour pouvoir suivre l'évolution dans le temps avec un minimum de hiatus ; (3) Des populations importantes pour avoir plus de chances d'observer de la variabilité et avoir une meilleure puissance statistique. Le modèle choisi dans cette étude est donc le conodont, car il remplit tous ces critères. Il représente donc un bon modèle pour répondre aux questions évolutives en temps profond.

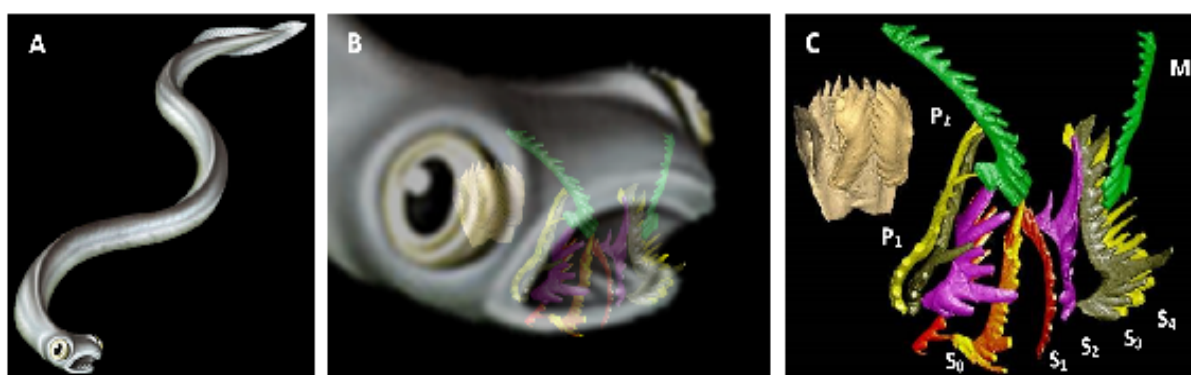


**Figure 1:** Le conodont; (A) Reconstruction artistique de l'animal complet, (B) Vue de la position des éléments conodontes placés à l'intérieur de la tête ; (C) Reconstruction de l'appareil du genre *Novispathodus* en position ouverte.

Découverts en 1856 par C.H. Pander (Pander, 1856), les conodontes sont un groupe éteint d'animaux marins dépourvus de mâchoire (Fig.1A). Les dernières analyses phylogéniques les placent au sein des premiers vertébrés (Aldridge et al., 1993; Donoghue, 1998; Donoghue et al., 2000; Janvier, 2015; Murdock et al., 2013; Purnell et al., 1995). Ils sont principalement connus dans le registre fossile par leurs structures buccales phosphatées semblables à des dents (Fig.1B) appelées éléments conodontes et dont la taille moyenne est de l'ordre du millimètre. Plus rarement, des empreintes de tissus mous de l'animal complet ont également été retrouvées. Les éléments conodontes (Fig.1C) sont largement distribués géographiquement et très abondants dans les restes fossiles tout au long de leur 300 millions d'années d'existence, de la fin du Cambrien à la fin du Trias. Ces éléments sont arrangés en un appareil masticateur (Hinde, 1879). Celui-ci présente une symétrie bilatérale et est généralement composé de 15 éléments séparés en deux groupes distincts. L'ensemble des éléments antérieurs (appelés éléments S et M) servaient probablement à attraper la nourriture, tandis que les deux paires d'éléments plus robustes positionnés plus postérieurement (appelés éléments P) pouvaient permettre de mâcher la nourriture (Goudemand et al., 2011) (Fig.1C). Les éléments constituants la paire occupant la position la plus postérieure sont appelés éléments P1 (Purnell et al., 2000) et présentent un taux d'évolution particulièrement fort mis en évidence par des variations morphologiques importantes (Sweet, 1988). Ainsi, ces éléments P1 représentent des marqueurs de choix pour les analyses biostratigraphiques et ont, depuis leur découverte, été largement étudiés et décrits dans ce but. À ce jour, seulement quelques études sont parvenues à explorer la forme et l'évolution des conodontes de manière quantitative (Barnett, 1972, 1971; Girard et al., 2004; Murphy and Cebecioglu, 1984; Murphy and Springer, 1989; Ritter, 1989; Roopnarine et al., 2004). De plus, dans ces études, la pluspart des patrons évolutifs décrits sont interprétés dans un cadre fonctionnel d'adaptation à l'environnement. Il en résulte un manque de connaissances sur leur

développement et la manière dont celui-ci constraint leur forme. Pourtant, leurs formes reflètent à la fois les contraintes développementales subies lors de leur morphogénèse, et les contraintes environnementales directes exercées par l'environnement via les ressources alimentaires disponibles et leur fonction masticatrice. Par conséquent, le potentiel des conodontes pour étudier les mécanismes évolutifs et leurs forces directrices est très prometteur et reste entièrement à exploiter.

Le but de ce travail de thèse est de quantifier les partons de variation morphologiques des éléments de différentes espèces de conodontes. Ces résultats sont par la suite analysés et interprétés en termes de réponse à l'environnement, mais aussi de développement, par exemple en mettant en évidence des covariations entre des traits morphologiques pouvant être interprétés comme l'empreinte de certaines contraintes durant le développement. Ainsi, il est possible de comprendre quels traits morphologiques peuvent être adaptatifs, et lesquels ne le sont pas, tout en retracant l'histoire évolutive des éléments conodontes.

L'origine du premier chapitre est la découverte d'éléments conodontes du Trias inférieur en Oman, dont la préservation exceptionnelle a permis la conservation du corps basal sur tous les éléments de l'appareil buccal du conodonte. La morphologie de cette structure est décrite et mise en relation avec celle de la couronne. Ces résultats nous permettent de mieux comprendre la fonction, le développement et la macroévolution des éléments conodontes.

Le second chapitre a pour but d'introduire les méthodes et concept clés des chapitres suivants. La complexité des études de morphométrie géométrique sur un organe à croissance continue dont la morphologie varie au cours de l'ontogénie est discutée, un cadre d'étude est proposé. Le débat concernant le rôle de l'environnement et du développement en tant que principales forces évolutives, concept important pour les chapitres 3 et 4 est ici introduit et mis en

relation avec les connaissances actuelles concernent les conodontes.

Le troisième chapitre introduit la notion d'axe principal de variation phénotypique (pmax) et son impact potentiel comme «facilitateur» de l'évolution. Cette théorie est testée sur un groupe d'espèces du Trias supérieur. La morphologie des éléments est quantifiée, puis les patrons de variation intra- et inter-spécifiques sont analysés et mis en relation avec des perturbations environnementales, et des covariations sont mises en évidence entre certains caractères morphologiques, permettant d'inférer les mécanismes de l'évolution à l'œuvre dans cet assemblage.

Le quatrième chapitre s'inscrit dans la continuité du chapitre précédent. Il propose de comparer deux assemblages d'éléments conodontes distant dans le temps, l'espace et l'évolution, pour démêler les effets de l'environnement et du développement dans l'évolution des morphologies. Les patrons communs observés entre les deux groupes d'espèces (groupe provenant du Carbonifère inférieur et groupe provenant du Trias) et leur lien avec les variations de température permettent de mettre en lumière un axe principal d'évolution contraint par le développement, le long duquel les espèces peuvent évoluer dans un sens ou dans l'autre en fonction de l'environnement. Un possible mécanisme d'hétérochronie en lien avec la température est également proposé et discuté.

Le cinquième chapitre est une étude préliminaire s'intéressant à l'utilisation de la morphométrie géométrique et d'analyses multivariées dans la taxonomie des éléments conodontes. Basé sur un assemblage de neogondolellides du Trias inférieur, ce chapitre tente de quantifier la forme globale des éléments basés sur une matrice de caractères taxonomiques couramment utilisés et sur une analyse de contours, et de reconnaître les différentes espèces grâce à une analyse de clustering. La validité des espèces décrites est alors discutée ainsi que des caractères

taxonomiques correspondant.

## Références

- Alberch, P., 1980. Ontogenesis and morphological diversification. *American zoologist* 20, 653–667.
- Aldridge, R.J., Briggs, D.E.G., Smith, M.P., Clarkson, E.N.K., Clark, N.D.L., 1993. The anatomy of conodonts. *Phil. Trans. R. Soc. Lond. B* 340, 405–421.
- Barnett, S.G., 1972. The evolution of *Spathognathodus remsciedensis* in New York, New Jersey, Nevada, and Czechoslovakia. *Journal of Paleontology* 900–917.
- Barnett, S.G., 1971. Biometric determination of the evolution of *Spathognathodus remsciedensis*: a method for precise intrabasinal time correlations in the Northern Appalachians. *Journal of Paleontology* 274–300.
- Darwin, C., 1859. On the origins of species by means of natural selection. London: Murray 247.
- Donoghue, P.C., 1998. Growth and patterning in the conodont skeleton. *Philosophical Transactions of the Royal Society of London B: Biological Sciences* 353, 633–666.
- Donoghue, P.C., Forey, P.L., Aldridge, R.J., 2000. Conodont affinity and chordate phylogeny. *Biological Reviews* 75, 191–251.
- Gingerich, P.D., 2001. Rates of evolution on the time scale of the evolutionary process, in: Microevolution Rate, Pattern, Process. Springer, pp. 127–144.
- Girard, C., Renaud, S., Korn, D., 2004. Step-wise morphological trends in fluctuating environments: evidence in the Late Devonian conodont genus *Palmatolepis*. *Geobios* 37, 404–415.
- Goethe, J.W. von, 1817. On Morphology: The Purpose Set Forth. Originally published in German in 63–66.
- Goudemand, N., Orchard, M.J., Urdy, S., Bucher, H., Tafforeau, P., 2011. Synchrotron-aided reconstruction of the conodont feeding apparatus and implications for the mouth of the first vertebrates. *Proceedings of the National Academy of Sciences* 108, 8720–8724.
- Gould, S.J., 1980. The evolutionary biology of constraint. *Daedalus* 39–52.
- Hinde, G.J., 1879. On conodonts from the Chazy and Cincinnati Group of the Cambro-Silurian, and from the Hamilton and Genesee-Shale divisions of the Devonian, in Canada and the United States. *Quarterly Journal of the Geological Society* 35, 351–369.
- Janvier, P., 2015. Facts and fancies about early fossil chordates and vertebrates. *Nature* 520, 483.
- Murdock, D.J., Dong, X.-P., Repetski, J.E., Marone, F., Stampanoni, M., Donoghue, P.C.,

2013. The origin of conodonts and of vertebrate mineralized skeletons. *Nature* 502, 546.

Murphy, M.A., Cebecioglu, M.K., 1984. The *Icriodus steinachensis* and *I. claudiae* lineages (Devonian conodonts). *Journal of Paleontology* 58, 1399–1411.

Murphy, M.A., Springer, K.B., 1989. Morphometric study of the platform elements of *Amydrotaxis praehjohnsoni* n. sp. (Lower Devonian, Conodonts, Nevada). *Journal of Paleontology* 63, 349–355.

Pander, C.H., 1856. Monographie der fossilen fische des silurischen systems des Russisch-baltischen gouvernements. Buchdr. der K. Akademie der wissenschaften.

Purnell, M.A., Aldridge, R.J., Donoghue, P.C., Gabbott, S.E., 1995. Conodonts and the first vertebrates. *Endeavour* 19, 20–27.

Purnell, M.A., Donoghue, P.C., Aldridge, R.J., 2000. Orientation and anatomical notation in conodonts. *Journal of Paleontology* 74, 113–122.

Ritter, S.M., 1989. Morphometric patterns in Middle Triassic *Neogondolella mombergensis* (Conodonta), Fossil Hill, Nevada. *Journal of Paleontology* 63, 233–245.

Roopnarine, P.D., Murphy, M.A., Buening, N., 2004. Microevolutionary dynamics of the Early Devonian conodont *Wurmiella* from the Great basin of Nevada. *Palaeontologia Electronica* 8, 1–16.

Sweet, W.C., 1988. The Conodonta: morphology, taxonomy, paleoecology, and evolutionary history of a long-extinct animal phylum. Clarendon Press Oxford.





## Chapitre 1 :

### Le corps basal, découverte récente et nouvelles perspectives

En 1929, Kirk découvre que les conodontes se composent en fait de deux parties. La première est celle précédemment décrite par Pander (1856), qui est similaire à la couronne d'émail des dents de vertébrés. Les études de micro-usures dentaires ont montré qu'elle émerge au moins en partie des tissus mous et participe à la fonction d'alimentation. La seconde partie est appelé corps basal. Elle est comparée à la racine en dentine des dents de vertébrés. Le corps basal des éléments conodontes est une structure lamellée dont la structure est voisine de celle de la couronne, mais bien plus faiblement minéralisée, et donc moins susceptible d'être préservé dans le registre fossile. Les éléments ayant conservé un corps basal ne sont retrouvés que dans certains cas exceptionnels. A cause de cette faible préservation, très peu d'informations sont connues sur le corps basal, et les quelques études actuelles s'y intéressant se concentrent principalement sur sa composition. En effet, le centre d'intérêt de nombreux chercheurs travaillant avec les conodontes est d'établir une base biochronologique stable, ou de reconstruire la paléoécologie et les paléoenvironments des espèces fossiles grâce à la géochimie. Dans ce genre de cadre d'étude, la présence de corps basal n'est pas souhaitée. Il masque certains caractères taxonomiques utiles en remplissant la cavité basale des éléments, et ainsi empêchant paradoxalement une assignation taxonomique « complète ». Il biaise aussi les mesures géochimiques diminuant la précision des résultats (Trotter *et al.*, 2008). A ce jour, aucun corps basal associé à un élément S ou M n'a été documenté après le Dévonien, ce qui a permis l'émergence d'une hypothèse expliquant ce manque par une tendance évolutive des éléments vers un corps basal non minéralisé. Pourtant le corps basal, tout comme la dentine des dents, a un rôle crucial dans le développement et le fonctionnement de l'organe. Une meilleure connaissance du corps basal est donc nécessaire pour tester les précédentes hypothèses développementales et fonctionnelles proposées. Dans cette étude, nous présentons la découverte d'éléments de la famille des neospathodids provenant de roches de l'Oman datant selon les estimations du Smithien (Trias in-

férieur), et dont les éléments conodontes ont au moins partiellement préservé leur corps basal. En particulier, cet assemblage contient des éléments du genre *Novispathodus* en abondance, incluant des éléments S et M présentant une préservation du corps basal. Cette découverte est d'une importance majeure pour la compréhension de la fonction, du développement et de la macroévolution des conodontes.

# **Exceptional basal-body preservation in some Early Triassic conodont elements from Oman**

## **Authors**

Louise Souquet<sup>1</sup> and Nicolas Goudemand<sup>1</sup>

<sup>1</sup>Univ. Lyon, Ecole Normale Supérieure de Lyon, Centre National de la Recherche Scientifique, Université Claude Bernard Lyon 1, Institut de Génomique Fonctionnelle de Lyon, UMR 5242, 46 Allée d'Italie, F-69364 Lyon Cedex 07, France.

\* Corresponding author

[louise.souquet@ens-lyon.fr](mailto:louise.souquet@ens-lyon.fr)

[nicolas.goudemand@ens-lyon.fr](mailto:nicolas.goudemand@ens-lyon.fr)

## **Abstract**

Conodont elements are composed of two main parts: the crown and the basal bodies. The basal body of conodonts is a laminated structure that is less densely mineralized than their crown, hence less likely to be preserved. Elements with preserved basal body are found only in exceptional cases in the fossil record. To date, no S or M element with preserved basal body has ever been documented for post-Devonian conodonts, which had raised the question of an evolutionary trend towards unmineralized basal bodies in conodonts. Here we report the discovery, in Smithian (Early Triassic) rocks of Oman, of neospaphodid conodont elements whose basal body is partly preserved. We demonstrate the presence of basal body in all elements, including S and M elements, of *Novispathodus*, and most likely of all gondolelloideans, thereby suggesting that the absence of basal body in post-Devonian conodonts was due to a preservational bias only. We further show that the morphology and extent of the basal body in *Novispathodus* are in agreement with previous predictions and do not contradict a cyclostome-like functional model of the apparatus. Based on a review of the occurrences of basal bodies in the literature, we suggest a general pattern for the morphology of the basal body in conodont elements that may reflect the mechanical constraints associated with feeding motions.

## **Keywords**

Vertebrate skeleton, evolution, developmental constraints, functional model, *Novispathodus*, apparatus.

## 1. Introduction

Conodonts are extinct jawless animals that thrived in most marine environments from the Late Cambrian to the very end of the Triassic (Aldridge et al., 1993; Sweet, 1988). The feeding apparatus of complex euconodonts was usually composed of 15 teeth-like elements: a bilaterally symmetrical basket of so-called S and M elements located at the anterior part of the mouth was apparently used to grasp food, whereas two pairs of posterior and relatively robust elements (the so-called P elements) were used to process the food (Goudemand et al., 2011; Purnell and Donoghue, 1997). Conodont elements comprise two main parts made of two types of tissues: the crown, which constitutes most of the elements in euconodonts, and the basal body (Fig. 1). Conodont elements and vertebrate teeth “have evolved independently and convergently” (Murdock et al., 2013) and are therefore not homologous, but considered as analogous. Crown tissue is an enamel-like tissue, whereas basal body compares best to dentin (Donoghue, 1998). Both tissues are mineralized with apatite and layered with internal lamellae that result from the intermittent appositional growth of the element (Donoghue, 2001, 1998; Donoghue and Purnell, 1999; Gross, 1960, 1957; Jeppsson, 1979; Müller and Nogami, 1971; Sweet, 1988). Yet, basal body’s laminated structure is less densely mineralized than the crown. Apatite crystallites in the basal body are smaller, randomly oriented, and less tightly packed than those of the crown (Donoghue, 1998). Moreover the surface between crown and basal body is a surface of weakness (Sweet, 1988), leading to dissociation upon death.

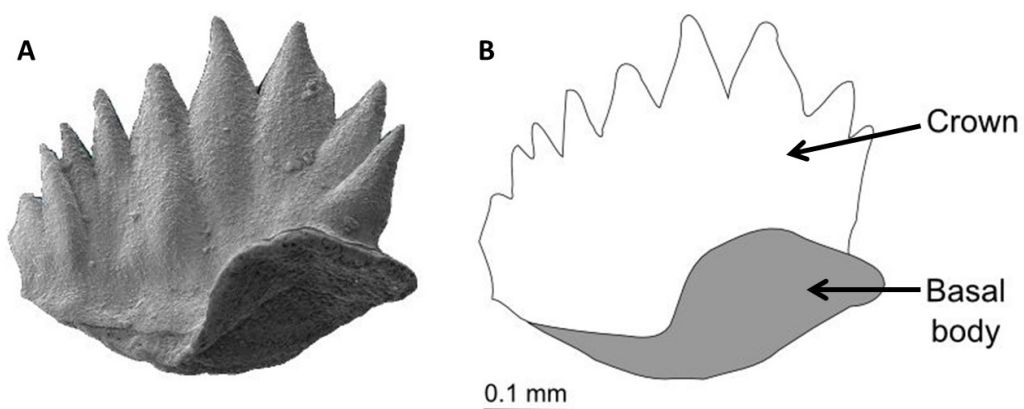


**Figure 1 :** Representation of a conodont P1 element and its two principal parts: the crown and the basal body. A: Picture of the element. B: Scheme of the same element with basal body highlights in grey.

As a consequence basal body tissues are less likely to be preserved and are found only exceptionally in the fossil record. Although knowledge about the basal body is crucial for testing functional and developmental hypotheses, even in those rare cases where they are preserved, they are usually poorly described, if at all. Indeed, for many conodont workers whose goal is to use conodonts to establish biochronological schemes or to reconstruct paleoecologies or paleoenvironments via geochemistry, basal bodies are a pain rather than a bless: they fill in the basal cavity, whose outline is a major taxonomical trait, paradoxically impeding ‘full’ taxonomical assessments, and they may decrease the precision of some geochemical measurements (Trotter et al., 2008).

Ramiform elements (usually S or M elements) with basal body preservation are particularly rare (Jeppsson, 1969; Miller and Märss, 1999; Nicoll, 1980, 1977). In the post-Devonian literature especially, although the basal body of some P elements has been illustrated occasionally (Goel, 1977; Jiang et al., 2011; Nogami, 1968; Orchard et al., 1994), the basal bodies of S and M elements have hitherto remained unknown. This has fueled debates about the possible development of these conodont tissues, because, in vertebrates, enamel secretion is induced by the presence of mineralized dentine (Donoghue, 1998; Smith, 1992) and thus one would expect that the mineralization of the enamel-like crown tissue was associated with the presence of a mineralized dentin-like basal body.

Furthermore, the most recent functional model of the conodont feeding apparatus (Goudemand et al., 2011) was based on the three-dimensional reconstruction of some Triassic apparatuses (in particular *Novispathodus*) for whom the morphology of the basal bodies is unknown. Goudemand *et al.* (2011) suggested that the feeding apparatus of conodonts worked in a way that is similar if not homologous to that of extant cyclostomes (hagfishes and lampreys): a pulley-like mechanism whereby the S elements rotated around a presumed homologous lingual cartilage. If confirmed this model would lend strong support for the current hypothesis that conodonts are likely stem-cyclostomes. Yet, although the model proposed by Goudemand *et al.* (*ibid*) was partially corroborated by the discovery of new Triassic natural assemblages (Huang et al., 2018), there is still no direct evidence for the speculated lingual cartilage. Furthermore,

one of the assumptions of this model was that the basal bodies of the corresponding S elements were relatively thin and were not to interfere with the reconstructed movements of the elements: a hypothesis that could not be tested hitherto.

In addition, the morphology of the basal body is likely to be informative for assessing the role of functional and developmental constraints on the morphological evolution of conodont elements. Some authors have applied analytical tools such as finite element analysis (Jones et al., 2012a, 2012b; Martínez-Pérez et al., 2016, 2014; Murdock et al., 2014) and geometric morphometrics (Jones and Purnell, 2007; Renaud and Girard, 1999) to quantify aspects of the conodont biomechanics and patterns of intra and inter-specific variation respectively. The usually missing basal part of the elements may or may not support the conclusions that are drawn using the crown only on complex elements.

Here we report the recent discovery of Triassic conodont elements, including, S and M elements, whose basal body is preserved. We discuss the developmental importance of basal body in Triassic elements, we explore the variation and possible covariation of this structure in our sample and in the literature, and we assess the viability of the *Novispathodus* functional model.

## 2. Geological settings

The described elements were extracted from rock samples collected on an exotic block of marine, Lower Triassic limestone located in the Batain Plain, Eastern Oman (Fig. 2). The block, about 1.2 meters in diameter, contains abundant ammonoids and conodonts that are diagnostic of the Induan-Olenekian boundary (IOB, or Dienerian-Smithian boundary). The in detail description of this block and of its paleontological content is beyond the scope of the present paper and will be the topic of another publication. Here we focus on those elements whose basal body is preserved. Those are found in the top half of the block and, based on the presence of *Novispathodus waageni* sensu lato, are considered to be early Olenekian (Smithian) in age.

The Batain Plain, located South of the city of Sur, Eastern Oman, extends over 4000km<sup>2</sup> in the northeastern corner of Oman. The Batain nappes are represented by allochthonous Permian to Maastrichtian marine sediments, as well as volcanic rocks and the Eastern Oman Ophiolite Nappes, obducted onto the Oman continental margin at the Cretaceous/Tertiary boundary (Hauser et al., 2002). They consist of several units and formations, among which the Triassic Sal and the Jurassic Guwayza Formations. The conglomerate interbeds in the Guwayza Formation contain reworked boulders of marine limestones from the Sal Formation of Early and Middle Triassic age (Hauser et al., 2002), of which the studied block is a typical example. These boulders are evidence for the partial destruction of the proximal Triassic Batain basin in Late Jurassic times (Hauser et al., 2002).

The studied outcrop is located about 20 km northwest of the Ad Daffah village, in the northern part of the Batain Plains (GPS coordinates: 22°22'18.5"N, 59°39'46.0"E, Fig. 2: A). The boulder was found about five meters away from the top of a small hill.

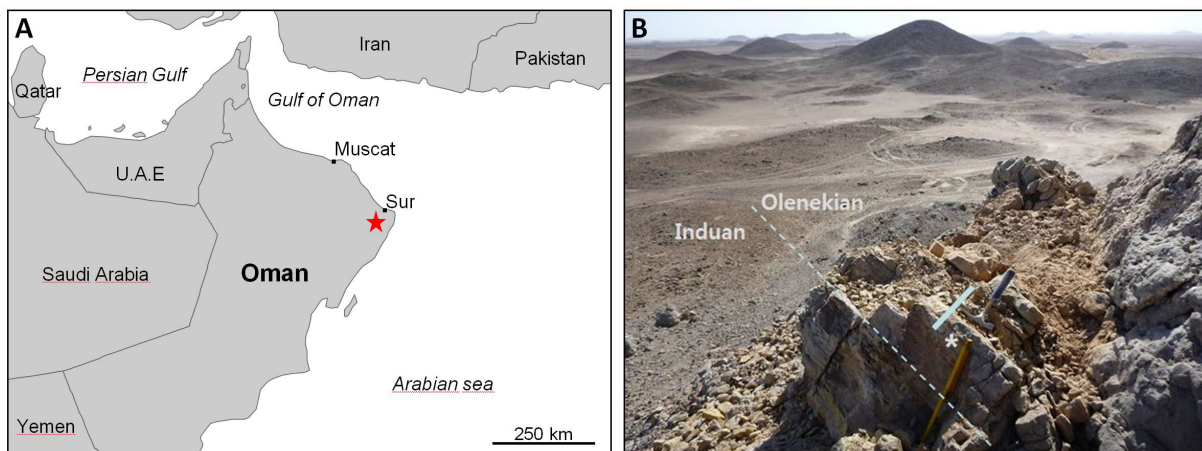


**Figure 2:** A: Location map of the studied material. The star indicates the Ad Daffah locality. B: Onsite view of the studied exotic block. The lithology of this metric limestone block is sub-homogeneous. The material discussed here comes from the Smithian (Olenekian) top of the block (the interval corresponding to the solid bar with a \*, next to the hammer).

### **3. Methods**

The conodonts were extracted using standard acid digestion techniques (Jeppsson et al., 1999). The discussed specimens are from four different but contiguous samples. For each sample, about one kilogram of rocks was dissolved in buffered ten percent acetic acid. The insoluble residues were then treated for concentration by heavy liquid separation using Sodium-Polytungstate (Jeppsson et al., 1999). The picking of the elements was done under a Motic binocular. The preservation of the specimens is pristine, with most denticles still intact, surfaces clean of debris and a color alteration index (CAI) of 1. Hence these elements were subjected to minimal post-depositional transport and minimal heating (Epstein et al., 1977). Pictures of the elements were taken at the University of Zurich using a Jeol JSM-6010 environmental SEM, without metallic coating, which enables easier distinction of the basal body.

### **5. Taxonomy**

The described material corresponds to a very small portion of the abundant assemblages (several thousands of elements) that we retrieved. Elements of *Novispathodus* ex gr. *waa-geni* compose most of these assemblages. Elements of the genera *Neospathodus*? *Wapitiodus*, *Guangxidella*, *Discretella*, ‘*Cornudina*’, and *Smithodus* are also present, although much less frequent. This association is typical of the Smithian (early Olenekian).

Class Conodonta Pander, 1856

Division Prionodontida Dzik, 1976

Order Ozarkodinida Dzik, 1976

Superfamily Gondolelloidae (Lindström, 1970)

Family Gondolellidea Lindström, 1970

Subfamily Novispathodinae Orchard, 2005

Genus *Novispathodus* Orchard, 2005

For the crown part of the elements, the multielement diagnosis is as described by Orchard (2005) and subsequently revised by Goudemand et al. (2012).

The M element is breviform digyrate (Fig. 5: a,b). One partly broken element has straight erect sharp denticles and a narrow angle between the two processes that is completely filled with basal body. The other element, likely from a different species than the latter element, possesses short discrete rounded denticles and a wide blunt angle between the two processes. A thin regular strip of basal body extends on the basal side along the processes, but it is unclear whether it is complete or not.

The alate S<sub>0</sub> element bears two symmetrical antero-lateral processes branching from a point anterior to the cusp (Fig. 5: c). Basal body is visible on the basal side of the lateral processes. The basal body of the herein illustrated specimen seems to have been initially more extended.

The S<sub>1</sub> element is weakly digyrate with one much shorter anterolateral process that bears one or two small denticles (Fig. 5: h-i, p-s). Some elements bear a nearly complete basal body that fills the basal cavity of the crown, and extends along the posterior process where it divides into two lips separated by a groove. In lateral view, the outline of the basal body is smooth and subparallel to the basal margin along the larger anterolateral process.

The breviform digyrate S<sub>2</sub> element has two long curved anterolateral processes (which are broken in the illustrated specimens) (Fig. 5: d-g, l-o). The basal body fills the narrow, acute angled space under the basal cavity.

The S<sub>3-4</sub> elements are bipennate elements (Fig. 5: w). The posterior process is attached but it may often be broken (as is the case in the illustrated specimens). The lower margin of the posterior process is usually sinuous. The basal body extends along the entire length of the process and its height seems to increase in the concave, posteriormost portion of the sinuous posterior process.

The  $P_2$  angulate high-bladed elements have an anterior process twice as long as the posterior one (Fig. 5: t-v). The basal body is very reduced, forming a thin layer filling the space between the two processes. This results in a straight flat lower margin of the entire element in lateral view.

*Novispathodus waageni* (Sweet, 1970)(Fig. 3, 4)

In lateral view, the  $P_1$  element presents a subquadrate form, with a laterally compressed blade, an arched crest composed by 7 to 14 slightly reclined denticles with a fan-like organization. In his original description, Sweet (1970) notes that this variable species often presents a sensibly upturned basal margin in the posterior half of the elements. We observe what seems to be a morphological continuum between slightly and strongly upturned morphologies. In all variants the outline of the basal body mostly follows that of the lower margin of the crown, except at mid-length where it is U-shaped. It is not clear yet whether the variation on the shape of the U may correlate with any trait of the crown. The point where the basal body seems to disappear (in lateral view) within the crown is variable. Note however that the anterior part of the basal body is frequently broken. In aboral view, the lower surface of the basal body presents a slight depression at the position of the pit. There starts a groove that extends to the anterior end of the element, just as the groove of the crown.

*Novispathodus* aff. *waageni* (Fig. 4: b-f)

These short segminate  $P_1$  elements are most similar to those of *N. waageni* but they bear erect and less numerous denticles and the posterior denticles do not decline in height as smoothly as in *N. waageni*. The basal body is much reduced.

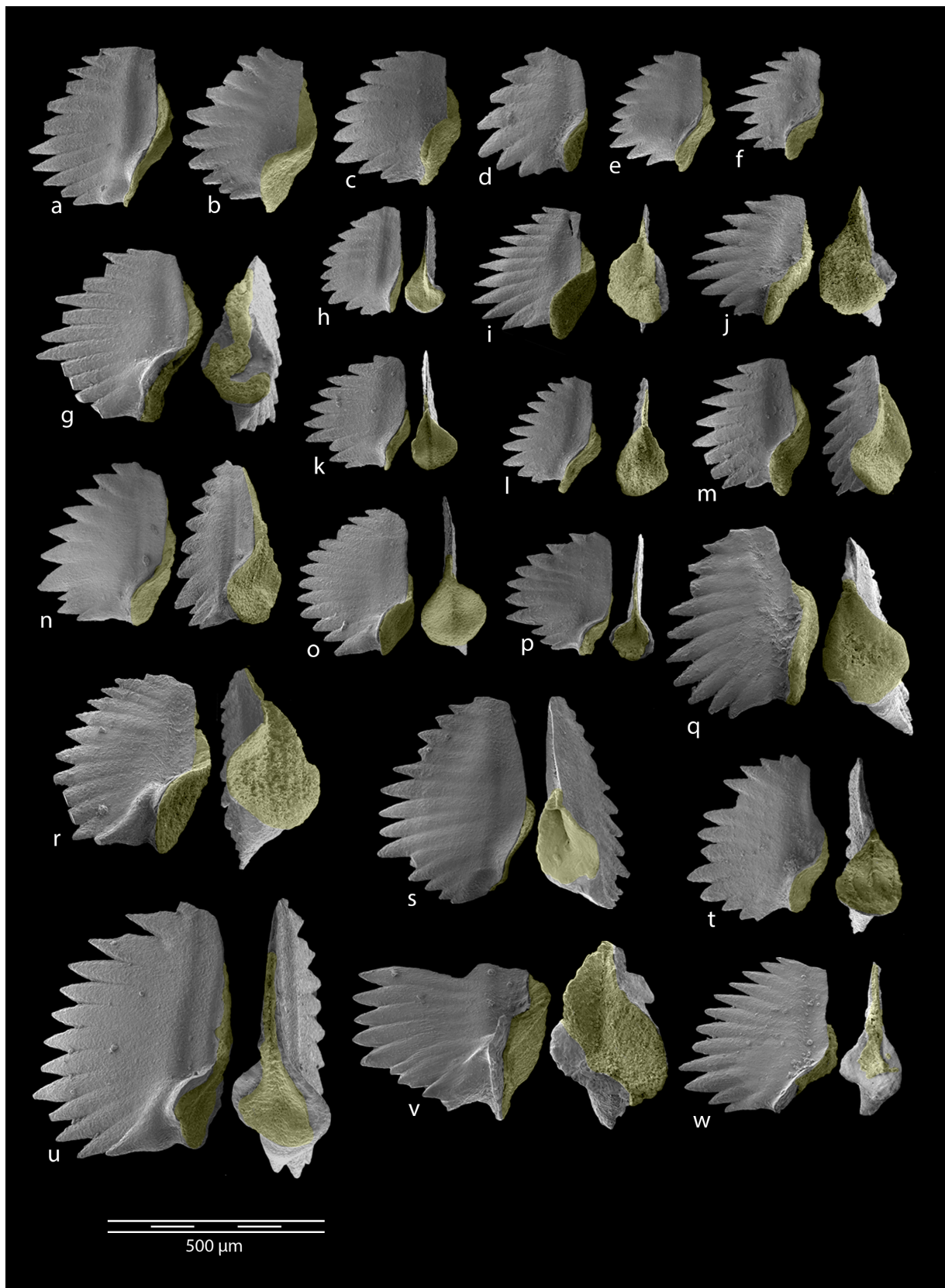


**Figure 3:** *Novispathodus waageni*. All P1 elements in lateral and aboral views. The basal body is highlighted in false yellow color. Scale bar 500  $\mu\text{m}$ .

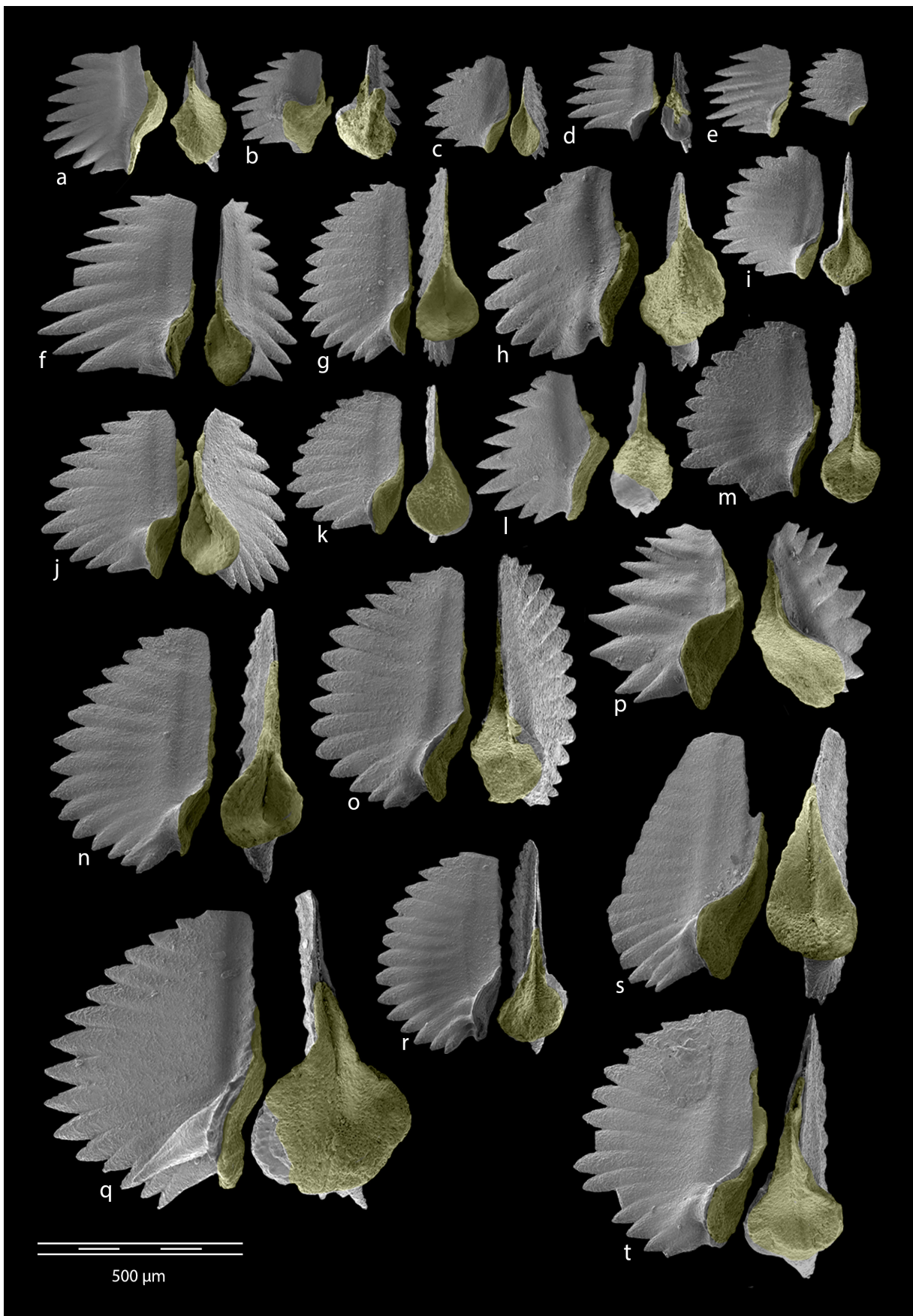


**Figure 4:** a, g-t: *Novispadodus waageni*. b-f: *Novispadodus aff. waageni*. All P1 elements in lateral and aboral views. The basal body is highlighted in false yellow color. Scale bar 500  $\mu\text{m}$ .

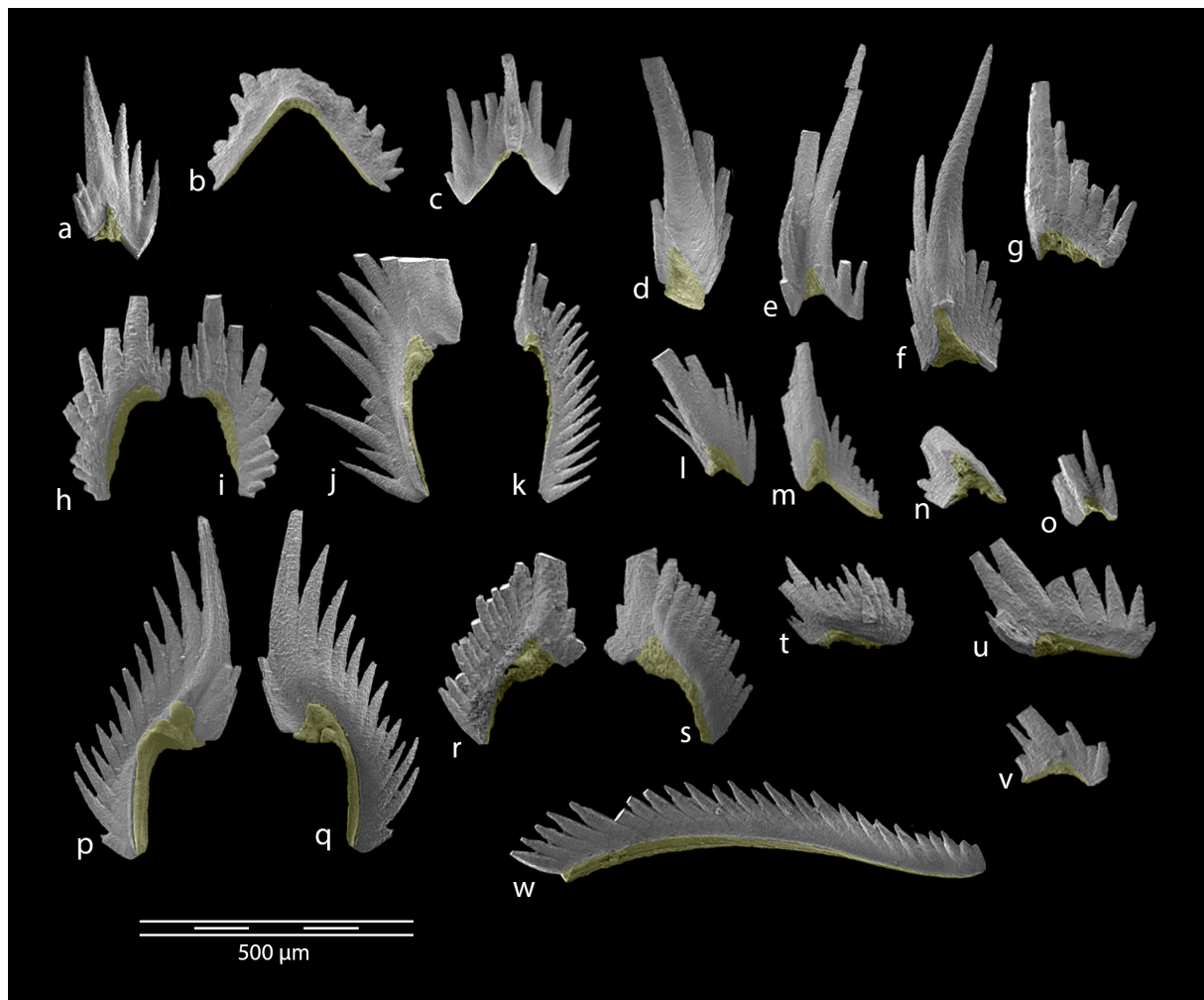


**Figure 5:** Novispathodus ramiform elements. a,b: M. c: S0. h, i, j, k, p, q, r, s: S1. d, e, f, g, l, m, n, o: S2. t, u, v: P2. w: S3-4. The basal body is highlighted in false yellow color. Scale bar 500  $\mu\text{m}$ .

## 4. Results

Remains of basal body are easily identified because they are white and opaque, while the crown part is usually creamy yellow and often translucent. They are very frequent although they consist in many cases of only small patches on the aboral side of the elements. Some much less frequent elements do exhibit basal bodies that we consider as complete, based on a superficial investigation of the surface smoothness and the apparent absence of breakage surfaces. This is particularly true for P elements, for which the basal body is also usually thicker, potentially explaining this differential preservation.

### 4.1. Presence of basal body in *Novispathodus* elements

The P elements of *Novispathodus* being the predominant form in these assemblages, it is likely that the frequent S and M elements found associated with them also belong predominantly to *Novispathodus*. A comparison with the multi-element reconstruction of Orchard (2005), revised by Goudemand *et al.* (2012), confirms this hypothesis (see descriptions in the Taxonomy part below).

All eight element types of the apparatus of *Novispathodus* are represented by at least one individual with at least partial basal body preservation (see Fig. 3, 4, 5, not all illustrated). This constitutes the first evidence of the presence of basal body in S or M elements younger than the Carboniferous, and hence the first evidence for the entire superfamily Gondolelloidea. The Gondolelloidea are the predominant conodont group from the mid-Permian to the end of the Triassic (Orchard, 2005). As mentioned above, besides *Novispathodus*, several genera belonging also to this superfamily are represented in the studied material and for most there exists at least a few individuals that show at least traces of basal body (not illustrated).

### 4.2. Extent of basal body in Gondolelloidea

Even in specimens where the basal body seems to be preserved completely, the basal body is much reduced compared to the crown. In most cases it barely extends beyond the margin of the basal cavity. In S and M elements (Fig. 5) its extent is maximal under the basal cavity,

in P elements (Fig. 3, 4) at element's mid-length, just in front of the cavity. On the aboral side of processes of ramiform elements it is reduced to a thin layer.

#### *4.3. Basal body morphology*

In S and M elements (Fig. 5, 6, 7), the subconical basal body fills the basal cavity and, between any two processes, the smooth curve defined by its edges suggest a hyperbola whose asymptotes are the lower margins of the processes. In other words, if we consider the lower margin of the crown as the geometrical reference, the basal body has a smooth, concave outline that converges with the crown outline along the processes.

In P elements on the contrary, the basal body has a smooth, convex outline (Fig. 3, 4, 6, 7): in lateral view, it forms a broad parabola with maximum curvature facing aborally. The base of the parabola is located at mid-length of the element and the sides recurved to align with the lower margin of the crown.

## **6. Discussion**

### *6.1. Lack of basal body in post-Devonian conodonts is not the result of an evolutionary loss*

Because the growth lamellae are continuous between the crown and the basal body (Müller and Nogami, 1971), it is thought that the basal body and the crown developed in concert. Yet, the apparent absence of basal body in many taxa (in particular, until today, in all Late Paleozoic and Triassic S and M conodont elements) had raised the question of whether this was due to a preservational bias, or reflected an actual evolutionary trend towards unmineralized basal bodies, and, in the latter case, how this could be explained developmentally (Donoghue, 1998).

During development of the vertebrate dermal skeleton, enamel secretion is induced by the presence of mineralized dentine (Smith 1992, Donoghue 1998). This ensures outward secretion and growth of the corresponding odontodes, the basic building blocks of the vertebrate

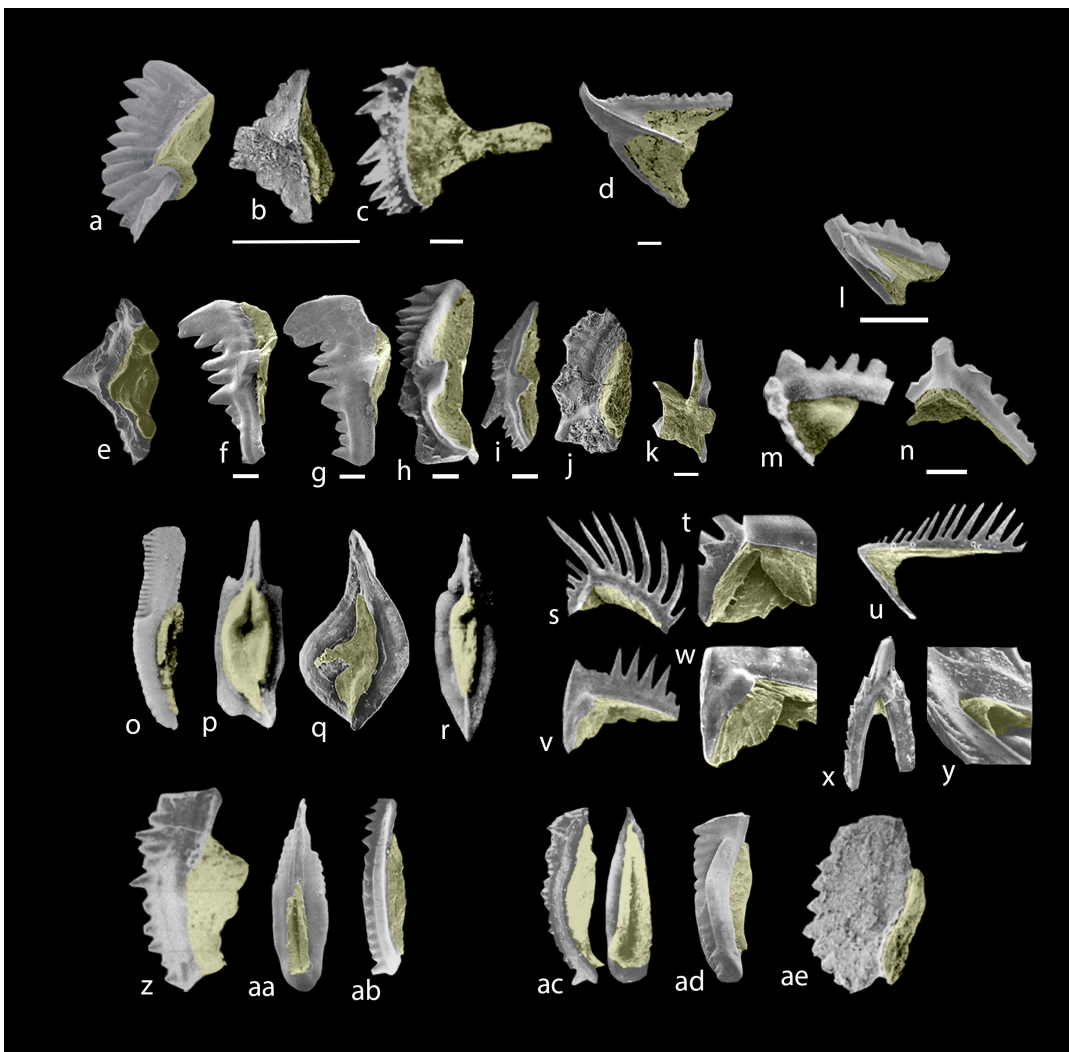


**Figure 6:** Published elements with subcomplete preservation of the basal body. a: *Jumudontus gananda*, P element. b: aff *Microzarkodina* sp., P element. c: *Archeognathus primus?*, P element. d: *Omanognathus daiqaensis*, S3 element. e: *Ozarkodina?* *hemensis* sp. nov., P2 element. f, g: *Ozarkodina* cf. *cornidentata*, P1 elements. h: *Polygnathoides siluricus*, P1 element. i: *Polygnatoides siluricus*, P2 element. j: *Ozarkodina?* *hemensis*, P1 element. k: *Kockelella variabilis variabilis*, P1 element. l: *Arianagnathus jafariani*, Sb1 dextral element. m: *Oulodus elegans*, ramiform element. n: *Ctenognathodus* sp., S1-2 element. o: *Polygnathus kennettensis*, P1 element. p: *Polygnathus linguiformis linguiformis*, P1 element. q: *Palmatolepis* sp., P1 element. r: *Polygnathus* aff. *trigonicus*, P1 element. s,t: *Oulodus angulatus*, M element (t: enlarged view). u: *Hibbardella angulata*, Sa element. v,w: *Hibbardella angulata*, “N” element (w: enlarged view). x,y: *Apatognathus varians klappereri*, Sa element (y: enlarged view). z: *Clarkina* cf. *bitteri*, P1 element. aa: *Mesogondolella nankingensis*, P1 element. ab: *Mesogondolella postserratia*, P1 element. ac: *Gondolella naviculla*, P1 element in lateral and lower view. ad: *Clarkina carinata*, P1 element. ae: *Novispatherodus waageni*, P1 element.

a-d: Ordovician. e-n: Silurian. o-y: Devonian. z-ab: Permian. ac-ae: Triassic. False yellow color highlights the basal body. Scale bars 250 µm. Some scales were missing. Adapted from Pyle et al. 2003 (a), Miller et al. 2017 (b,d), Mosher and Bodenstein 1969 (c), Miller and Märss 1999 (e,j), Slavík and Carls 2012 (f,g), Slavík et al. 2010 (h,i,k), Männik et al. 2013 (l,n), Jeppson 1969 (m), Savage 1976 (o), Sparling 1983 (p,r), Uyeno 1991 (q), Nicoll 1977 (s,t,u,v,w), Nicoll 1980 (x,y), Kozur 1992 (z), Kozur and Mostler 1995 (aa,ab), Nogami 1968 (ac), Orchard et al., 1994 (ad), Goel 1977 (ae).

dermal skeleton (Ørvig, 1967). If an enamel-like tissue is secreted by the epithelial cells before mineralization of the underlying dentine-like tissue, as is the case with enameloid (Smith, 1995, 1992), we expect growth to occur in the opposite direction: inwards instead of outwards. As a consequence, unless at least a thin layer of basal body is mineralized at the crown-basal body junction in conodont elements, the observed enamel-like outward growth of the crown tissue can hardly be explained.

Indeed, although the ultrastructural evolution of early conodont elements seems to exclude an homology between lamellar crown tissue and enamel (Kemp, 2002; Kemp and Nicoll, 1996, 1995; Murdock et al., 2013; Reif, 2006; Schultze, 1996; Trotter et al., 2007), it is very likely that conodont elements developed in a way that is analogous, if not homologous to vertebrate odontodes. Odontodes are formed through epithelial-ectomesenchymal interaction, via formation of a placode, invagination of the corresponding volume of epithelium into the mesenchyme, and subsequent mineralization at the epithelial-mesenchymal interface. (Smith, 1995) first attempted to homologize conodont elements with odontodes. Later, Donoghue (1998) who reviewed in details the growth and patterning of conodont elements, proposed instead that each conodont element may be homologous to an odontocomplex (or polyodontode), not to a single odontode. Since conodont's crown tissue has apparently evolved independently of enamel (Murdock et al., 2013), it is not clear to what extent this putative homology may hold. Yet, a deep homology may actually exist, in terms of underlying processes, between these two organs.

Donoghue (1998) suggested that odontodes were “flexible enough to allow any of their component tissues (enamel, dentine, bone) [...] to be present independently of the others” (1998, p. 658), which would have explained the absence of basal body in some conodont taxa. This statement may be true in general, but it seems that the biophysical, mineralization constraint mentioned above excludes the possibility of independence between enamel and dentine, and likewise between an enamel-like tissue and its dentine-like counterpart, in outward growing odontodes (or odontode-like organs), such as conodont elements.

Consequently the apparent absence of mineralized basal body in Late Paleozoic and Triassic conodonts was intriguing and one could have argued that conodont elements (of that

age at least) must have developed in a way that is fundamentally different from that of any other known vertebrate odontode. Although the main evidence for a vertebrate affinity of conodonts is based on the soft tissues homology and does not rest on a putative homology of their feeding elements with those of other vertebrates (Aldridge et al., 1993; Blieck et al., 2010; Donoghue et al., 2000; Donoghue and Rücklin, 2016; Janvier, 2015; Krejsa et al., 1990; Murdock et al., 2013; Purnell, 1995; Purnell et al., 1995; Sansom et al., 1992; Turner et al., 2010), this may have even been used to suggest that conodonts are not vertebrates. Based on the evidence presented here, and as far as we currently know, *Novispathodus* elements, and possibly all conodonts elements, still do conform to the development of vertebrate odontodes.

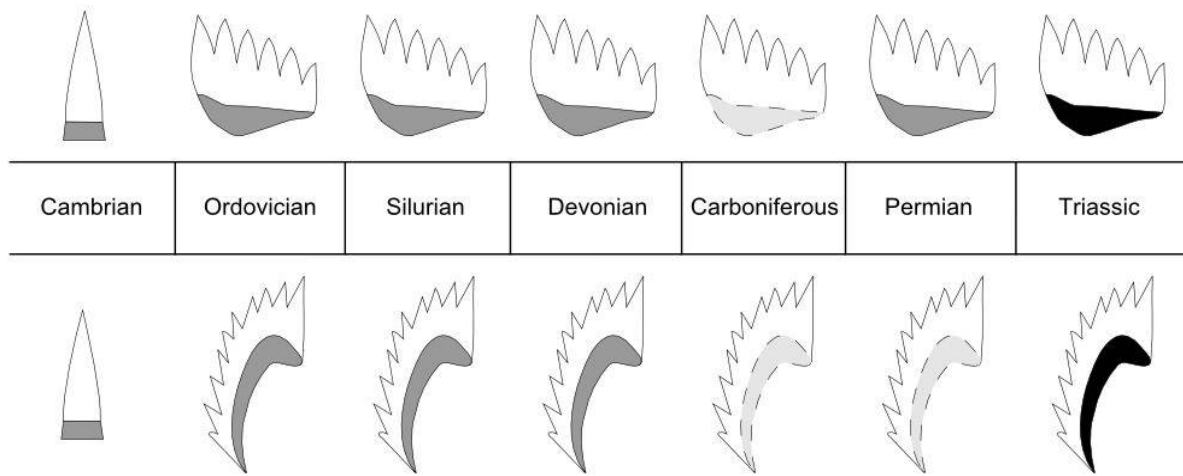


**Figure 7:** Presence of basal body through time. Cambrian elements are coniform. Euconodont (complex conodont) elements are here schematized, the actual morphologies differ from this simplified representation. Top: P elements; Bottom: S or M elements. Note the difference of curvature of the lower outline of the basal body between the P and S or M elements. Dark grey, continuous outline: presence of basal body already documented in the literature (Goel 1977, Kozur 1992, Kozur and Mostler 1995, Männik et al. 2013, Miller and Märss 1999, Miller et al. 2017, Mosher and Bodenstein 1969, Nicoll 1977, Nicoll 1980, Orchard 1994, Pyle et al. 2003, Savage 1976, Slavík et al. 2010, Slavík and Carls 2012, Sparling 1983, Uyeno 1991); Soft grey, dashed outline: presence of basal body hitherto not documented but here inferred

## *6.2. The extent of the basal body in *Novispathodus* agrees with the current, cyclostome-like functional model of the conodont apparatus*

In the description of their functional model of the conodont apparatus, (Goudemand et al., 2011) wrote that in “S or M elements, the basal body, when present, smoothes out the lower margin (ventral outline) of the element [...]. In *Novispathodus*, the lower margins of the S elements are already smooth (low 3D curvature), and we therefore assume that their respective basal bodies, if mineralized, were relatively thin and filled up the basal grooves but did not alter the shape of their lower margins substantially” (p. 8723). They also illustrated the apparatus of *Novispathodus* with elements reconstructed using their hypothesis for the extent of the basal body (their additional figure S<sub>1</sub>). Except for the sinuous posterior part of the posterior process in S<sub>0</sub> and S<sub>3-4</sub> elements, the observed extent of the basal body in *Novispathodus* is in full agreement with their predictions. Because the posterior part of the posterior process of these elements is not critical for the validity of their model, we conclude that the observed morphology of the basal body does not come into conflict with their model, which therefore still holds at least for *Novispathodus*.

## *6.3. A pattern of covariation between the morphologies of crown and basal body?*

In order to discuss the universality within euconodonts of the observed morphological covariation between the crown and the basal body -- that is, a convex basal body associated with a sub-flat lower margin of the crown and a concave basal body associated with a concave lower margin of the crown --, we reviewed the literature for illustrated examples of basal body preservation in non-coniform elements. Note that many different names have been given to the basal body: basal filling, basal plate, basal attachment, basal structure, basal organ. Note also that in several cases the authors do not mention the presence of basal body even though basal body can be sometimes distinguished in the illustrations. Therefore, we do not claim to have identified all the published occurrences. Moreover, there were cases where the preservation of the basal body was too partial to be included in the following discussion.

For the ramiform elements, we were able to retrieve illustrations for twelve taxa only:

the Ordovician *Archeognathus primus* and *Iowagnathus grandis* (Liu et al., 2017), *Microzarkodina* sp., *Omanognathus* sp. and *Aldridgeognathus manniki* (Miller et al., 2018), the Silurian *Arianagnathus jafariani* and *Ctenognathodus* sp. (Männik et al., 2015), *Oulodus elegans* (Jeppsson, 1969), *Ozarkodina hemensis* (Miller and Märss, 1999), *Kockeella* (Slavík et al., 2010), and the Devonian *Hibbardella angulata* (Nicoll, 1977) and *Apatognathus* sp. (Nicoll, 1980). Nevertheless, the outline of the basal body is always mostly concave in lateral view. We also observe a general decrease in size (height and thickness) of the basal body over time, but this qualitative observation would deserve more attention as we may expect the extent of basal body to vary as a multivariate function of geometry (e.g. angle between processes), size and mechanical properties (e.g. elasticity of the tissues before mineralization), parameters that may in turn depend on, for instance, the position of the element within the apparatus or phylogeny.

Pectiniform elements with basal body preservation are much more frequent in the literature. We noted in particular: for the Ordovician, *Archeognathus primus* (Liu et al., 2017; Moshher and Bodenstein, 1969), *Jumudontus gananda* (Pyle et al., 2003), *Microzarkodina* sp. (Miller et al., 2018); for the Silurian, *Ozarkodina derenjalensis* (Männik et al., 2015), *Ozarkodina hemensis* (Miller and Märss, 1999), *Polygnathoides siluricus*, *Ozarkodina typica*, *Ozarkodina cf.cornidentata* and *Wurmiella excavata* (Slavík et al., 2010; Slavík and Carls, 2012); for the Devonian, *Polygnathus kennettensis* (Savage, 1976), *Palmatolepis* sp. (Uyeno et al., 1991), *Polygnathus linguiformis linguiformis* (Sparling, 1983), *Hibbardella angulata* (Nicoll, 1977); for the Permian, *Clarkina bitteri* (Kozur, 1992), *Jinogondolella nankingensis*, *J. postserrata* and *J. shannoni* (Kozur and Mostler, 1995), and for the Triassic, *Gladigondolella malayensis* (Nogami, 1968), *Clarkina carinata* (Orchard et al., 1994) and *Novispathodus waageni* (Goel, 1977). Specimens of *Novispathodus waageni* with preserved basal body presented by Goel (1977) are only illustrated on the latteral view. It is unclear if the observed variability of the basal body, especially its extent, is due to breakages or is a real morphological feature. The visible part of the basal body are similar to the ones described in this paper.

The outline of the basal body has always a convex profile in lateral view. Except for the very early history of conodonts, we do not observe a temporal decrease of the basal body in

pectiniform elements. Yet, and this is striking when one observe the example of *Archeognathus*, complex conodont elements may have evolved from simple, coniform elements via an increase of mineralization of the crown and/or the basal body and subsequent fusion of otherwise isolated (coniform) denticles and formation of a bar (compare *Archeognathus* in (Liu et al., 2017) and in (Klapper and Bergstroem, 1984). It is worth noting but this is also what is observed during the growth of some complex conodont elements (Donoghue, 1998).

#### *6.4. May the morphology of the basal body inform us about the mechanical constraints acting on the elements?*

Since the basal body may have served as an attachment surface for the underlying soft tissues (Branson and Mehl, 1933; Mosher and Bodenstein, 1969; Sweet, 1955), it is likely that its morphology reflects somehow the mechanical constraints associated with feeding. In some cases, especially in early conodont taxa such as the Ordovician *Archeognathus* (Liu et al., 2017), the basal body may actually be more informative than the crown: in *Archeognathus*, the crown is reduced to a ‘simple’ comb-like bar, whereas the relatively conspicuous basal body exhibits a large root-like extension that may be interpreted more easily in terms of biomechanics.

In that respect, the concave vs. convex outline may also reflect distinct mechanical, functional constraints on the elements: although the motion of pectiniform elements tends to be oriented mostly along an oral-aboral axis (Jones et al., 2012), the current functional model of the ramiform S and M elements suggests pivotal motions where the main pulling forces were exerted along the processes (Goudemand et al., 2011). Hence it might not be surprising that the basal body of pectiniform elements extends essentially along the oral-aboral axis and the one of ramiform elements defines a minimal surface at the intersection of the processes. Detailed finite element analyses (FEA) might help us to test this functional hypothesis in the future and, if it holds, then the morphology of the basal body (along with the morphology of the cusp, see (Goudemand et al., 2011; Murdock et al., 2013; Purnell and Donoghue, 1997)) might even be used someday to infer the movements of a given element.

## 7. Conclusion

The discovery of abundant Early Triassic *Novispathodus* elements, including S and M elements, with preserved basal bodies has several implications for our understanding of conodont macroevolution. The apparent absence of basal body in post-Devonian ramiform conodonts (until now) is probably due to a preservation bias only and not to an evolutionary trend towards unmineralized basal bodies. The morphology and extent of the basal body in *Novispathodus* are in agreement with previous predictions and do not contradict a cyclostome-like functional model of the apparatus. Finally, the review of basal body occurrences in the literature suggests a general pattern for the morphology of the basal body in conodont elements that may reflect the mechanical constraints associated with the feeding motions. Although the histology of both crown and basal tissues has been studied to some extent in Paleozoic forms, much is still to be done to understand the likely couplings between the features of their respective ultrastructures, their respective sizes and morphologies and how these couplings may originate from putative developmental and functional constraints. It would be interesting also to assess whether these couplings may or may not have evolved through conodont history.

## Acknowledgments

We thank Aymon Baud (Lausane), Romain Jattiot and Hugo Bucher (Paleontological Institute and Museum, Univ. Zurich, Switzerland; PIMUZ) for their help on the field. We also thank Morgane Brosse (PIMUZ) for her help with the SEM and associated image processing, and Marc Leu (PIMUZ) for having processed some of the rocks.

Funding: This work was supported by a French ANR @RAction grant (ACHN project EvoDevOdonto).

## References

- Aldridge, R.J., Briggs, D.E.G., Smith, M.P., Clarkson, E.N.K., Clark, N.D.L., 1993. The anatomy of conodonts. *Phil. Trans. R. Soc. Lond. B* 340, 405–421.

Blieck, A., Turner, S., Burrow, C.J., Schultze, H.-P., Rexroad, C.B., Bultynck, P., Nowlan, G.S., 2010. Fossils, histology, and phylogeny: why conodonts are not vertebrates. *Episodes* 33, 234–241.

Branson, E.B., Mehl, M.G., 1933. Conodonts from the Jefferson City (Lower Ordovician) of Missouri. *University of Missouri Studies* 8, 53–64.

Donoghue, P.C., 2001. Microstructural variation in conodont enamel is a functional adaptation. *Proceedings of the Royal Society of London B: Biological Sciences* 268, 1691–1698.

Donoghue, P.C., 1998. Growth and patterning in the conodont skeleton. *Philosophical Transactions of the Royal Society of London B: Biological Sciences* 353, 633–666.

Donoghue, P.C., Forey, P.L., Aldridge, R.J., 2000. Conodont affinity and chordate phylogeny. *Biological Reviews* 75, 191–251.

Donoghue, P.C., Purnell, M.A., 1999. Growth, function, and the conodont fossil record. *Geology* 27, 251–254.

Donoghue, P.C., Rücklin, M., 2016. The ins and outs of the evolutionary origin of teeth. *Evolution & development* 18, 19–30.

Epstein, A.G., Epstein, J.B., Harris, L.D., 1977. Conodont color alteration: an index to organic metamorphism.

Goel, R.K., 1977. Triassic conodonts from Spiti (Himachal Pradesh), India. *Journal of Paleontology* 1085–1101.

Gouemand, N., Orchard, M.J., Tafforeau, P., Urdy, S., Bruehwiler, T., Brayard, A., Galfetti, T., Bucher, H., 2012. Early Triassic conodont clusters from South China: revision of the architecture of the 15 element apparatuses of the superfamily Gondolelloidea. *Palaeontology* 55, 1021–1034.

Gouemand, N., Orchard, M.J., Urdy, S., Bucher, H., Tafforeau, P., 2011. Synchrotron-aided reconstruction of the conodont feeding apparatus and implications for the mouth of the

first vertebrates. *Proceedings of the National Academy of Sciences* 108, 8720–8724.

Gross, W., 1960. Über die Basis bei den Gattungen *Palmatolepis* und *Polygnathus* (Conodontida). *Paläontologische Zeitschrift* 34, 40–58.

Gross, W., 1957. Über die Basis der Conodonten. *PalZ* 31, 78–91.

Hauser, M., Martini, R., Matter, A., Krystyn, L., Peters, T., Stampfli, G., Zaninetti, L., 2002. The break-up of East Gondwana along the northeast coast of Oman: evidence from the Batain basin. *Geological Magazine* 139, 145–157.

Huang, J., Hu, S., Zhang, Q., Donoghue, P.C., Benton, M.J., Zhou, C., Martínez-Pérez, C., Wen, W., Xie, T., Chen, Z.-Q., 2018. Gondolellloid multielement conodont apparatus (*Nicoraella*) from the Middle Triassic of Yunnan Province, southwestern China. *Palaeogeography, Palaeoclimatology, Palaeoecology*.

Janvier, P., 2015. Facts and fancies about early fossil chordates and vertebrates. *Nature* 520, 483.

Jeppsson, L., 1979. Conodont element function. *Lethaia* 12, 153–170.

Jeppsson, L., 1969. Notes on some Upper Silurian multielement conodonts. *Geologiska Föreningen i Stockholm Förhandlingar* 91, 12–24.

Jeppsson, L., Anehus, R., Fredholm, D., 1999. The optimal acetate buffered acetic acid technique for extracting phosphatic fossils. *Journal of Paleontology* 73, 964–972.

Jiang, H., Lai, X., Yan, C., Aldridge, R.J., Wignall, P., Sun, Y., 2011. Revised conodont zonation and conodont evolution across the Permian–Triassic boundary at the Shangsi section, Guangyuan, Sichuan, South China. *Global and Planetary Change* 77, 103–115.

Jones, D., Evans, A.R., Rayfield, E.J., Siu, K.K., Donoghue, P.C., 2012. Testing microstructural adaptation in the earliest dental tools. *Biology letters* 8, 952–955.

Jones, D., Purnell, M., 2007. 14 A New Semi-Automatic Morphometric Protocol for Conodonts and Taxonomic Application.

Kemp, A., 2002. Hyaline tissue of thermally unaltered conodont elements and the enamel of vertebrates. *Alcheringa* 26, 23–36.

Kemp, A., Nicoll, R.S., 1996. A histochemical analysis of biological residues in conodont elements. *Modern Geology* 20, 287–302.

Kemp, A., Nicoll, R.S., 1995. Protochordate affinities of conodonts. *Courier Forschungsinstitut Senckenberg* 182, 235–245.

Klapper, G., Bergstroem, S.M., 1984. The enigmatic Middle Ordovician fossil *Archeognathus* and its relations to conodonts and vertebrates. *Journal of Paleontology* 949–976.

Kozur, H., 1992. Boundaries and Stage subdivision of the Mid-Permian (Guadalupian Series) in the light of new micropaleontological data. *International Geology Review* 34, 907–932.

Kozur, H., Mostler, H., 1995. Guadalupian (Middle Permian) conodonts of sponge-bearing limestones from the margins of the Delaware Basin, West Texas. *Geologia Croatica* 48, 107–128.

Krejsa, R., Bringas, P., Slavkin, H., 1990. A neontological interpretation of conodont elements based on agnathan cyclostome tooth structure function, and development. *Lethaia* 23, 359–378.

Liu, H.P., Bergström, S.M., Witzke, B.J., Briggs, D.E., McKay, R.M., Ferretti, A., 2017. Exceptionally preserved conodont apparatuses with giant elements from the Middle Ordovician Winneshiek Konservat-Lagerstätte, Iowa, USA. *Journal of Paleontology* 91, 493–511.

Männik, P., Miller, C.G., Hairapetian, V., 2015. A new early Silurian prioniodontid conodont with three P elements from Iran and associated species. *Acta Palaeontologica Polonica* 60, 733–746.

Martínez-Pérez, C., Rayfield, E.J., Botella, H., Donoghue, P.C., 2016. Translating taxonomy into the evolution of conodont feeding ecology. *Geology* 44, 247–250.

- Martínez-Pérez, C., Rayfield, E.J., Purnell, M.A., Donoghue, P.C., 2014. Finite element, occlusal, microwear and microstructural analyses indicate that conodont microstructure is adapted to dental function. *Palaeontology* 57, 1059–1066.
- Miller, C.G., Heward, A.P., Mossoni, A., Sansom, I.J., 2018. Two new early balognathid conodont genera from the Ordovician of Oman and comments on the early evolution of priodontid conodonts. *Journal of Systematic Palaeontology* 16, 571–593.
- Miller, C.G., Märss, T., 1999. A conodont, thelodont and acanthodian fauna from the Lower Pridoli (Silurian) of the Much Wenlock Area, Shropshire. *Palaeontology* 42, 691–714.
- Mosher, L.C., Bodenstein, F., 1969. A unique conodont basal structure from the Ordovician of Alabama. *Geological Society of America Bulletin* 80, 1401–1402.
- Müller, K.J., Nogami, Y., 1971. Über den Feinbau der Conodonten.
- Murdock, D.J., Dong, X.-P., Repetski, J.E., Marone, F., Stampanoni, M., Donoghue, P.C., 2013. The origin of conodonts and of vertebrate mineralized skeletons. *Nature* 502, 546.
- Murdock, D.J., Rayfield, E.J., Donoghue, P.C., 2014. Functional adaptation underpinned the evolutionary assembly of the earliest vertebrate skeleton. *Evolution & development* 16, 354–361.
- Nicoll, R.S., 1980. The multielement genus *Apatognathus* from the Late Devonian of the Cannig Basin, Western Australia. *Alcheringa* 4, 133–152.
- Nicoll, R.S., 1977. Conodont apparatuses in an Upper Devonian palaeoniscoid fish from the Cannig Basin, Western Australia. *Bureau of Mineral Resources Journal of Australian Geology and Geophysics* 2, 217–228.
- Nogami, Y., 1968. Trias-Conodonten von Timor, Malaysien und Japan (Palaeontological Study of Portuguese Timor, 5).
- Orchard, M., 2005. Multielement conodont apparatuses of Triassic Gondolelloidea. 73–101. *Conodont biology and phylogeny: interpreting the fossil record. Special Papers in Palaeontology*.

laeontology 73, 218.

Orchard, M.J., Nassichuk, W.W., Rui, L., 1994. Conodonts from the Lower Griesbachian Otoceras Latilobatum Bed of Selong, Tibet and the Position of the Permian—Triassic Boundary.

Ørvig, T., 1967. Phylogeny of tooth tissues: evolution of some calcified tissues: evolution of some calcified tissues in early vertebrates. Structural and chemical organization of teeth 45–110.

Purnell, M.A., 1995. Large eyes and vision in conodonts. *Lethaia* 28, 187–188.

Purnell, M.A., Aldridge, R.J., Donoghue, P.C., Gabbott, S.E., 1995. Conodonts and the first vertebrates. *Endeavour* 19, 20–27.

Purnell, M.A., Donoghue, P.C., 1997. Architecture and functional morphology of the skeletal apparatus of ozarkodinid conodonts. *Philosophical Transactions of the Royal Society of London B: Biological Sciences* 352, 1545–1564.

Pyle, L.J., Barnes, C.R., Ji, Z., 2003. Conodont fauna and biostratigraphy of the Outram, Skoki, and Owen Creek formations (Lower to Middle Ordovician), Wilcox Pass, Alberta, Canada. *Journal of Paleontology* 77, 958–976.

Reif, W.-E., 2006. Conodonts, odontodes, stem-groups, and the ancestry of enamel genes. *Neues Jahrbuch für Geologie und Paläontologie-Abhandlungen* 405–439.

Renaud, S., Girard, C., 1999. Strategies of survival during extreme environmental perturbations: evolution of conodonts in response to the Kellwasser crisis (Upper Devonian). *Palaeogeography, Palaeoclimatology, Palaeoecology* 146, 19–32.

Sansom, I.J., Smith, M.P., Armstrong, H.A., Smith, M.M., 1992. Presence of the earliest vertebrate hard tissue in conodonts. *Science* 256, 1308–1311.

Savage, N.M., 1976. Middle Devonian species of *Polygnathus* from the Kennett Formation, northern California. *Journal of Paleontology* 374–379.

Schultze, H.P., 1996. Conodont histology: An indicator of vertebrate relationship? *Modern Geology* 20, 275–286.

Slavík, L., Carls, P., 2012. Post-Lau Event (late Ludfordian, Silurian) recovery of conodont faunas of Bohemia. *Bulletin of Geosciences* 87, 815–832.

Slavík, L., Kříž, J., Carls, P., 2010. Reflection of the mid-Ludfordian Lau Event in conodont faunas of Bohemia. *Bulletin of Geosciences* 85, 395–414.

Smith, M.M., 1995. Heterochrony in the evolution of enamel in vertebrates. *Evolutionary change and heterochrony*.

Smith, M.M., 1992. Microstructure and evolution of enamel amongst osteichthyan fishes and early tetrapods. *Structure, function, and evolution of teeth* 73–101.

Sparling, D.R., 1983. Conodont biostratigraphy and biofacies of lower Middle Devonian limestones, north-central Ohio. *Journal of Paleontology* 825–864.

Sweet, W.C., 1988. *The Conodonta: morphology, taxonomy, paleoecology, and evolutionary history of a long-extinct animal phylum*. Clarendon Press Oxford.

Sweet, W.C., 1970. Uppermost Permian and Lower Triassic conodonts of the Salt Range and Trans-Indus Range, West Pakistan. *Stratigraphic Boundary Problems, Permian and Triassic of West Pakistan* 4, 207–275.

Sweet, W.C., 1955. Conodonts from the Harding Formation (Middle Ordovician) of Colorado. *Journal of Paleontology* 226–262.

Trotter, J.A., GERALD, J.D.F., Kokkonen, H., Barnes, C.R., 2007. New insights into the ultrastructure, permeability, and integrity of conodont apatite determined by transmission electron microscopy. *Lethaia* 40, 97–110.

Trotter, J.A., Williams, I.S., Barnes, C.R., Lécuyer, C., Nicoll, R.S., 2008. Did cooling oceans trigger Ordovician biodiversification? Evidence from conodont thermometry. *Science* 321, 550–554.

Turner, S., Burrow, C.J., Schultze, H.-P., Blieck, A., Reif, W.-E., Rexroad, C.B., Bultynck, P., Nowlan, G.S., 2010. False teeth: conodont-vertebrate phylogenetic relationships revisited. *Geodiversitas* 32, 545–594.

Uyeno, T.T., Orchard, M.J., McCracken, A.D., 1991. Pre-Famennian Devonian conodont biostratigraphy of selected intervals in the eastern Canadian Cordillera. Geological Survey of Canada, Bulletin 417, 129–161.





## **Chapitre 2:**

# **Conodontes, morphométrie et forces évolutives**

### **1. Croissance et analyse quantitative de la forme des conodontes**

Le mode de croissance des éléments conodontes, s'il reste aujourd'hui en partie méconnu, n'en est pas moins particulier. Comme décrit dans le chapitre précédent, les éléments sont constitués de deux tissus minéralisés composés de lamelles d'apatite. Ces dernières sont formées lors d'épisodes périodiques de croissance par accrétion externe, et ce durant toute la vie de l'animal (Donoghue, 2001, 1998; Donoghue and Purnell, 1999; Gross, 1960, 1957; Jeppsson, 1979; Müller and Nogami, 1971; Sweet, 1988). Cette dernière particularité diverge du mode de croissance des odontodes minéralisés chez les autres vertébrés, et permet à l'animal conodonte de réparer ses éléments tout au long de sa vie (Donoghue and Purnell, 1999; Hass, 1941). Une étude récente (Shirley et al., 2018) démontre l'existence de 3 grandes phases de croissance chez les éléments conodontes. Celles-ci sont caractérisées par leurs morphologies, ainsi que par des variations de taux de strontium (Sr) contenu dans les tissus. Cette étude supporte également l'hypothèse d'une rétractation périodique des éléments avec potentiellement une addition de nouveaux centres de croissance (odontodes) pendant ces phases de réparation/croissance. Ainsi, ce mode de croissance particulier entraîne un changement morphologique permanent au cours de la vie d'un individu. Au sein d'une espèce, la forme des éléments peut donc fortement varier, même entre des éléments de taille et de stade de croissance similaires. Couplée à la complexité et la subtilité des variations morphologiques observées chez les éléments conodontes, l'analyse quantitatives de la forme des éléments au sein d'une espèce s'avère constituer un véritable défi. Ainsi par exemple, le denticule terminal d'un élément P1 chez un conodonte juvénile ne sera pas homologue à celui d'un adulte, car celui-ci, en grandissant, aura changé de morphologie, notamment par ajout de denticules supplémentaires. Les éléments conodontes ne présentent donc que très peu de caractères morphologiques pouvant être considérés comme biologiquement homologues, c'est-à-dire se retrouvant chez tous les individus considérés ayant hérité cette similarité d'un ancêtre commun (Smith, 1990).

Hors, dans le cadre théorique de la morphométrie géométrique basée sur des landmarks (i.e. points “homologues”), la notion d’homologie entre les points analysés est très importante, et constitue un prérequis pour assurer la puissance de l’analyse (Bookstein, 1997). Selon sa définition mathématique, un landmark est un point correspondant présent sur tous les objets étudiés, et dont la position est conservée (correspondante) chez tous les individus d’une population, mais aussi entre les différentes populations (Dryden and Mardia, 1998). Le landmark doit donc être choisi de manière à être reconnu sans équivoque sur tous les objets considérés peu importe leur provenance. Cette idée de correspondance a été exportée dans le monde de la biologie en termes d’homologie, comme étant la meilleure façon de s’assurer de la correspondance des points utilisés et de faire le lien avec les processus génétiques et développementaux (Zelditch et al., 2004). Mais cette définition très stricte est difficilement applicable dans le monde du vivant, les homologies n’étant pas toujours présentes ou démontrables. La notion de correspondance nécessite de choisir des landmarks permettant à la déformation observée pour passer d’une configuration à une autre d’avoir un sens biologique et d’être comparable entre tous les spécimens. Ainsi, une véritable homologie histologique n’est pas nécessairement requise si les structures anatomiques sont comparables entre elles, par exemple en termes de fonction impliquant les mêmes points de repères anatomiques (comme l’extrémité de l’aile chez une chauve-souris, un oiseau et un insecte). Bookstein (Bookstein, 1997) a lui-même déterminé trois types de landmarks. Ceux de type 1 sont constitués de points réellement homologues entre tous les spécimens, idéalement à la jonction entre plusieurs tissus. Ceux de type 2 sont des points pouvant être reconnus sur tous les spécimens grâce à leur particularités géométriques, mais n’étant pas nécessairement homologues comme par exemple des points de maximum de courbure. Ceux de type 3 sont caractérisés par des extrémités et dépendent de directions anatomiques. Si certains considèrent que les landmarks de type 2 et 3 ne devraient pas être utilisés en morphométrie géométrique, ils se révèlent souvent être les seuls types de landmarks reconnaissables sur une structure biologique, notamment si elle est constituée d’un seul tissu. Dans la pratique, des compromis peuvent être trouvés, notamment lors d’études à large échelle incluant différentes espèces, ou en présence d’innovations morphologiques, tant qu’une définition explicite de la correspondance de position des landmarks est donnée (Klingenberg, 2008) et que les résultats

sont interprétés avec précaution. Ainsi, l'utilité et la flexibilité de la morphométrie géométrique a pu être démontrée dans divers groupes, y compris chez les conodontes, en utilisant ces différents types de landmarks s'affranchissant de l'homologie biologique (Hogancamp et al., 2016).

Malgré ces avancées, les analyses portant sur la morphologie des conodontes demeurent majoritairement qualitatives. Quelques études ont à ce jour tenté de quantifier la forme des éléments conodontes dans divers buts (Jones and Purnell, 2007): analyses de la taille et de l'allométrie (Chen et al., 2016; Jeppsson, 1976); de l'ontogénie et du taux de survie (Armsstrong, 2005; Murphy and Cebecioglu, 1984; Tolmacheva and Löfgren, 2000; Tolmacheva and Purnell, 2002); tester des hypothèses fonctionnelles (Purnell, 1994, 1993); reconnaître des espèces (Croll et al., 1982; Croll and Aldridge, 1982; Girard et al., 2004; Hogancamp et al., 2016; Klapper and Foster, 1993; Klapper and Foster Jr, 1986; Ritter, 1989; Sloan, 2003; Zimmerman et al., 2018); déterminer des morphologies pouvant être utilisées en biostratigraphie (Barnett, 1972; Lambert, 1994; Murphy and Cebecioglu, 1984; Murphy and Springer, 1989); décrire des tendances évolutives (Barnett, 1971; Girard et al., 2004; Girard and Renaud, 2007; Murphy and Cebecioglu, 1986; Renaud and Girard, 1999; Roopnarine et al., 2004), et proposer des protocoles d'étude en morphométrie (Jones and Purnell, 2007; MacLeod and Carr, 1987). Mais à ce jour, aucune étude quantitative n'a tenté d'interpréter les patrons de variation morphologiques des éléments conodontes dans un contexte développemental.

Les deux chapitres suivants proposent un protocole de quantification de la forme des éléments conodontes en utilisant la morphométrie géométrique basée sur des landmarks et des semilandmarks (points équidistant répartis le long d'une courbe reliant deux landmarks) dans un cadre évolutif. Le cinquième chapitre explore d'autres méthodes de quantification de la forme, cette fois dans un contexte taxonomique et de biostratigraphie.

## 2. Déterminer les forces évolutives en présence

Pour comprendre le rôle des forces évolutives en temps profond, il est essentiel de comprendre l'impact sur les phénotypes de deux forces évolutives majeures: le développement et l'environnement. Cet impact est enregistré dans la variabilité morphologique du registre fossile (Urdy et al., 2013). Il peut ainsi être mis en évidence en étudiant les changements de forme des organismes au cours du temps, et en les reliant à des changements environnementaux, ou à nos connaissances en biologie du développement. Dans le cadre de la synthèse moderne de l'évolution, l'environnement est considéré comme étant la principale force évolutionnaire. Cette théorie fait l'hypothèse que la variation initiale des populations était graduelle, et dans toutes les directions. Les tentatives pour expliquer les patrons macroévolutionnaires en temps profond se sont ainsi principalement concentrés sur les forces extrinsèques (environnementales) comme les variations climatiques ou les modifications physico-chimiques de composition de la biosphère. Cette vision a été grandement débattue depuis la fin des années 1970, notamment grâce à l'introduction du concept de contraintes développementales (Gould, 1977; Thompson, 1917). Le développement se révèle alors être source de structuration et de variation non-aléatoire des phénotypes. Cependant, le rôle relatif des forces intrinsèques à l'organisme (fonction, développement des organes) en macroévolution reste encore mal compris. En particulier: comment les processus développementaux déterminent la variation morphologique des individus dans l'ontogénie, *i.e.* lors du développement et de la croissance des organes, et au cours de l'évolution? En effet, les formes du vivant sont elles aussi contraintes par les règles universelles de la physique, de la chimie et de la géométrie. L'univers des formes possibles pour un organe est ainsi limité par la manière dont ces formes sont générées au cours de l'ontogénie. Les processus développementaux déterminent donc en partie les patrons de variation morphologiques des individus, et ce de manière non linéaire biaisant l'évolution dans certaines directions privilégiées. Alberch résume cette idée en 1980 (Alberch, 1980) par cette phrase: « In evolution, selection may decide the winner of a given game but development non-randomly defines the players» (Dans l'évolution, la sélection peut déterminer le gagnant de la partie, mais c'est le développement qui définit les joueurs de manière non-aléatoire). Une étude intégrée des patrons morphologiques tenant compte de l'impact potentiel de ces deux forces est donc nécessaire pour comprendre

l'évolution des structures biologiques dans son ensemble. Pour cela, la place occupée par les organismes dans l'espace morphologique peut nous renseigner sur les contraintes en action ainsi que la plasticité développementale des populations (Kaneko, 2011).

Les deux chapitres suivants se basent sur la quantification des patrons de variation morphologiques chez les éléments conodontes, à l'échelle intra- et inter-spécifique. Ces patrons sont analysés et interprétés d'un point de vue environnemental et développemental, pour tenter d'avoir cette approche intégrée de l'évolution, et de mieux comprendre le rôle de ces deux forces évolutives.

### 3. Références

- Alberch, P., 1980. Ontogenesis and morphological diversification. *American zoologist* 20, 653–667.
- Armstrong, H.A., 2005. Modes of growth in the euconodont oral skeleton: implications for bias and completeness in the fossil record. *Palaeontological Association*.
- Barnett, S.G., 1972. The evolution of *Spathognathodus remscheidensis* in New York, New Jersey, Nevada, and Czechoslovakia. *Journal of Paleontology* 900–917.
- Barnett, S.G., 1971. Biometric determination of the evolution of *Spathognathodus remscheidensis*: a method for precise intrabasinal time correlations in the Northern Appalachians. *Journal of Paleontology* 274–300.
- Bookstein, F.L., 1997. Morphometric tools for landmark data: geometry and biology. Cambridge University Press.
- Chen, Y., Neubauer, T.A., Krystyn, L., Richoz, S., 2016. Allometry in A nisian (Middle Triassic) segminiplanate conodonts and its implications for conodont taxonomy. *Palaeontology* 59, 725–741.
- Croll, V.M., Aldridge, R.J., 1982. Computer applications in conodont taxonomy: 2. Classificatory methods. *Computer Applications in Geology I & II. Geological Society Miscellaneous Paper* 14, 247–261.
- Croll, V.M., Aldridge, R.J., Harvey, P.K., 1982. Computer applications in conodont taxonomy: characterization of blade elements. *Miscellaneous paper, in: Geological Society of London*. pp. 237–246.
- Donoghue, P.C., 2001. Microstructural variation in conodont enamel is a functional adaptation. *Proceedings of the Royal Society of London B: Biological Sciences* 268, 1691–1698.
- Donoghue, P.C., 1998. Growth and patterning in the conodont skeleton. *Philosophical Transactions of the Royal Society of London B: Biological Sciences* 353, 633–666.
- Donoghue, P.C., Purnell, M.A., 1999. Growth, function, and the conodont fossil record. *Geology* 27, 251–254.
- Dryden, I.L., Mardia, K.V., 1998. Statistical shape analysis. Wiley Chichester.

- Girard, C., Renaud, S., 2007. Quantitative conodont-based approaches for correlation of the Late Devonian Kellwasser anoxic events. *Palaeogeography, Palaeoclimatology, Palaeoecology* 250, 114–125.
- Girard, C., Renaud, S., Korn, D., 2004. Step-wise morphological trends in fluctuating environments: evidence in the Late Devonian conodont genus *Palmatolepis*. *Geobios* 37, 404–415.
- Gould, S.J., 1977. *Ontogeny and phylogeny*. Harvard University Press.
- Gross, W., 1960. Über die Basis bei den Gattungen *Palmatolepis* und *Polygnathus* (Conodontida). *Paläontologische Zeitschrift* 34, 40–58.
- Gross, W., 1957. Über die Basis der Conodonten. *PalZ* 31, 78–91.
- Hass, W.H., 1941. Morphology of conodonts. *Journal of Paleontology* 71–81.
- Hogancamp, N.J., Barrick, J.E., Strauss, R.E., 2016. Geometric morphometric analysis and taxonomic revision of the Gzhelian (Late Pennsylvanian) conodont *Idiognathodus* simulator from North America. *Acta Palaeontologica Polonica* 61, 477–502.
- Jeppsson, L., 1979. Conodont element function. *Lethaia* 12, 153–170.
- Jeppsson, L., 1976. Autecology of late Silurian conodonts. *Conodont paleoecology: Geological Association of Canada Special Paper* 15, 105–118.
- Jones, D., Purnell, M., 2007. Chapter 14 A New Semi-Automatic Morphometric Protocol for Conodonts and a Preliminary Taxonomic Application. *Systematics Association Special Volume* 74, 239.
- Kaneko, K., 2011. Characterization of stem cells and cancer cells on the basis of gene expression profile stability, plasticity, and robustness: dynamical systems theory of gene expressions under cell-cell interaction explains mutational robustness of differentiated cells and suggests how cancer cells emerge. *Bioessays* 33, 403–413.
- Klapper, G., Foster, C.T., 1993. Shape analysis of Frasnian species of the Late Devonian conodont genus *Palmatolepis*. *Journal of Paleontology* 67, 1–35.
- Klapper, G., Foster Jr, C.T., 1986. Quantification of outlines in Frasnian (Upper Devonian) platform conodonts. *Canadian Journal of Earth Sciences* 23, 1214–1222.
- Klingenberg, C.P., 2008. Novelty and “homology-free” morphometrics: what’s in a name? *Evolutionary Biology* 35, 186–190.
- Lambert, L.L., 1994. Morphometric confirmation of the *Mesogondolella idahoensis* to *M. nankingensis* transition. *Permophiles* 24, 28–35.
- MacLeod, N., Carr, T.R., 1987. Morphometrics and the analysis of shape in conodonts. *Conodonts: Investigative Techniques and Applications*. Ellis Horwood Limited, Chichester, England 168–187.
- Müller, K.J., Nogami, Y., 1971. Über den Feinbau der Conodonten.
- Murphy, M.A., Cebecioglu, M.K., 1986. Statistical study of *Ozarkodina excavata* (Branson and Mehl) and *O. tuma* Murphy and Matti (Lower Devonian, delta Zone, conodonts, Nevada). *Journal of Paleontology* 60, 865–869.
- Murphy, M.A., Cebecioglu, M.K., 1984. The *Icriodus steinachensis* and *I. claudiae* lineages (Devonian

conodonts). *Journal of Paleontology* 1399–1411.

- Murphy, M.A., Springer, K.B., 1989. Morphometric study of the platform elements of *Amydrotaxis praejohnsoni* n. sp. (Lower Devonian, Conodonts, Nevada). *Journal of Paleontology* 63, 349–355.
- Purnell, M.A., 1994. Skeletal ontogeny and feeding mechanisms in conodonts. *Lethaia* 27, 129–138.
- Purnell, M.A., 1993. Feeding mechanisms in conodonts and the function of the earliest vertebrate hard tissues. *Geology* 21, 375–377.
- Renaud, S., Girard, C., 1999. Strategies of survival during extreme environmental perturbations: evolution of conodonts in response to the Kellwasser crisis (Upper Devonian). *Palaeogeography, Palaeoclimatology, Palaeoecology* 146, 19–32.
- Ritter, S.M., 1989. Morphometric patterns in Middle Triassic *Neogondolella mombergensis* (Conodonts), Fossil Hill, Nevada. *Journal of Paleontology* 63, 233–245.
- Roopnarine, P.D., Murphy, M.A., Buening, N., 2004. Microevolutionary dynamics of the Early Devonian conodont *Wurmella* from the Great basin of Nevada. *Palaeontologia Electronica* 8, 1–16.
- Shirley, B., Grohganz, M., Bestmann, M., Jarochowska, E., 2018. Wear, tear and systematic repair: testing models of growth dynamics in conodonts with high-resolution imaging. *Proc. R. Soc. B* 285.
- Sloan, T.R., 2003. Results of a new outline-based method for the differentiation of conodont taxa in: Contributions to the Second Australian conodont Symposium (AUSCOS II) held in conjunction with Palaeontology DownUnder-2000 in Orange, Australia, 3–7 July 2000. Courier Forschungsinstitut Senckenberg.
- Smith, G.R., 1990. Homology in morphometrics and phylogenetics, in: Proceedings of the Michigan Morphometrics Workshop. Special Publication Number.
- Sweet, W.C., 1988. The Conodonta: morphology, taxonomy, paleoecology, and evolutionary history of a long-extinct animal phylum. Clarendon Press Oxford.
- Thompson, D.W., 1917. On growth and form. On growth and form.
- Tolmacheva, T., Löfgren, A., 2000. Morphology and paleogeography of the Ordovician conodont *Paracordylodus gracilis* Lindström, 1955: comparison of two populations. *Journal of Paleontology* 74, 1114–1121.
- Tolmacheva, T.Y., Purnell, M.A., 2002. Apparatus composition, growth, and survivorship of the Lower Ordovician conodont *Paracordylodus gracilis* Lindström, 1955. *Palaeontology* 45, 209–228.
- Urdy, S., Wilson, L.A., Haug, J.T., Sánchez-Villagra, M.R., 2013. On the unique perspective of paleontology in the study of developmental evolution and biases. *Biological Theory* 8, 293–311.
- Zelditch, M.L., Swiderski, D.L., Sheets, H.D., Fink, W.L., 2004. Geometric morphometrics for biologists: a primer. 2004. New York and London: Elsevier Academic Press Google Scholar.
- Zimmerman, A.N., Johnson, C.C., Polly, P.D., 2018. Taxonomic and evolutionary pattern revisions resulting from geometric morphometric analysis of Pennsylvanian *Neognathodus* conodonts, Illinois Basin. *Paleobiology* 1–24.



## **Chapitre 3:**

# **Impact de l'environnement et du développement sur l'évolution d'un assemblage d'éléments conodontes du Trias**

En 1996, Schluter (Schluter, 1996) propose pour la première fois un cadre pour l'étude intégré de ces deux forces. Il explique que la direction principale de variance génétique (qu'il nomme Gmax) au sein d'une population correspond à une ligne de moindre résistance à l'évolution. Ainsi, l'évolution sera facilitée, et ainsi plus fréquente dans cette direction plutôt que dans les autres où des contraintes sont appliquées. Comme les matrices de variance-covariance génétiques et phénotypiques sont corrélées (Siahsarvie, 2012), la direction principale de variation phénotypique (appelée Pmax) est alignée avec Gmax. La théorie des lignes de moindre résistance à l'évolution peut alors être étendue au phénotype d'une population. Dans le registre fossile, cela permet d'inférer Gmax à partir d'un phénotype, la morphologie d'un organisme étant souvent la seule information ayant été préservée dans le temps. Ainsi, les patrons de variation morphologiques au sein des populations peuvent être interprétés en tenant compte des contraintes intrinsèques (génétiques/développementales) supposées par Gmax et Pmax, nous renseignant sur les forces évolutives en action. Un patron de variation parallèle à Pmax pourra être considéré comme résultant principalement de l'action des forces intrinsèques à l'organisme. Un patron déviant de la direction de Pmax sera alors interprété comme la conséquence d'une perturbation extrinsèque écologique et/ou environnementale ayant exercé une pression sur les organismes, contraignant leur phénotype à dévier de Pmax (Renaud et al., 2006).

Dans ce chapitre, nous présentons une étude quantitative d'un assemblage apparenté d'éléments P1 de la fin du Trias. En utilisant la morphométrie géométrique, nous explorons la variation morphologique de cet assemblage, mettant en lumière un axe principal de variation phénotypique. Cet axe présent chez toutes les espèces étudiées ici démontre l'existence de contraintes développementales similaires parmi tous les éléments P1 de cet assemblage. Nous démontrons notamment un lien de covariation entre certains traits morphologiques considérés

jusqu'à présent comme indépendants. D'un autre côté, l'évolution entre les formes Carniennes et Noriennes présente une trajectoire divergent significativement du Pmax intraspécifique, suggérant une pression environnementale ou écologique importante.

# **Deciphering the roles of environment and development in the evolution of a Late Triassic assemblage of conodont elements**

Authors: Pauline Guenser<sup>1,2#</sup>, Louise Souquet<sup>1#</sup>, Manuel Rigo<sup>3</sup>, Michele Mazza<sup>4</sup>, Nicolas Goudemand<sup>1\*</sup>

1 Univ Lyon, ENS de Lyon, CNRS, Univ. Claude Bernard Lyon 1, Institut de Génomique Fonctionnelle de Lyon, UMR 5242, 46 Allée d’Italie, F-69364 Lyon Cedex 07, France

2 Current address: Univ Lyon, CNRS, Université Claude Bernard Lyon 1, Laboratoire d’Écologie des Hydrosystèmes Naturels et Anthropisés, UMR 5023, 3-6 rue Raphaël

Dubois – Bâtiments Forel, 69622 Villeurbanne Cedex 43

3 Department of Geosciences, University of Padova, Via G. Gradenigo 6, 35131 Padova, Italy

4 Department of Earth Sciences “Ardito Desio”, University of Milan, Via Mangiagalli 34, 20133 Milan, Italy

# These authors contributed equally to the work.

\* Corresponding author

## **Abstract**

To assess evolutionary processes in deep time, it is essential to understand the roles of development and environment, both recorded through the morphological variability of fossil assemblages. Thanks to their high abundance and temporal resolution, conodont elements are ideal to address this issue. We present the first quantitative study of a Late Triassic assemblage of closely related P1 conodont elements. Using geometric morphometrics such as landmarks and outline analysis, we explored the main axes of phenotypic variation and relate them to classically used morphological characters. The intraspecific variation within most of the considered species is similarly constrained, which highlights, for the first time, a line of least resistance for the evolution of the conodont P1 element. The evolution between Carnian and Norian forms, on the other hand, is shown to have followed a trajectory that is significantly different from this line of least resistance, suggesting the implication of significant environmental or ecological perturbations. Furthermore, we propose that some of morphological traits of conodont elements usually considered independent follow instead laws of covariation.

## **1.**

## 1. Introduction

Attempts at explaining macroevolution in deep time have usually focused on extrinsic (environmental) factors such as climate changes or modifications of the physical and chemical composition of the biosphere. Yet, the question of the relative role of intrinsic (organismal: functional, developmental) factors in macroevolution remains poorly addressed. In particular, how can we explain evolutionary convergences among taxa? Are environmental changes driving such convergences? On the other hand, organisms and their shapes are constrained by the universal rules of chemistry, physics and geometry. The set of theoretically possible forms is thus bounded by the way these forms can be generated during ontogeny. In other words, developmental processes determine the variation of individuals anisotropically, thus possibly biasing evolution into preferential directions.

Because organisms and environment “actively co-determine each other” (Levins and Lewontin, 1985), the dichotomy between intrinsic and extrinsic factors is necessarily reductive, and we should expect that explanatory schemes will involve both types of factors. In 1996, Schlüter (Schlüter, 1996) first proposed that the main direction of genetic variance (termed *Gmax*) within a population corresponds to a ‘line of least resistance’ to evolution, that is, evolution will occur more easily, and thus more frequently, in that direction rather than in any other. Interestingly, as phenotypic and genetic variance-covariance matrices are correlated (Siahsarie, 2012), the main direction of phenotypic variance (*Pmax*) is aligned with *Gmax*. The theory of lines of least resistance can thus be extended to the phenotypic variance of population, extant or fossil (in which case, we prefer the term ‘assemblage’). Moreover, phenotypes do not contain information only about the development of the individuals, but also about their environment. Hence this theoretical framework can be used to assess the relative roles of environmental and developmental processes in evolution, *via* the analysis of the main directions of phenotypic variance in fossil assemblages (Renaud et al., 2006; Hunt, 2007). The *Pmax* can be interpreted in terms of genetic/developmental constraints, and any significant deviation from *Pmax* can be interpreted as being the consequence of an environmental or ecological perturbation. In order to conduct such studies in deep time, one needs a model system whose fossil record spans a large timeframe and comprises large assemblages that are available at a temporal resolution that

compares with the dynamics of paleoenvironmental fluctuations. This is the case of conodonts.

Conodonts are a group of extinct, jawless marine organisms that are considered vertebrates (Donoghue et al., 2000). They are mainly known in the fossil record by their tiny, apatitic teeth-like feeding elements. Their feeding apparatus included an anteriorly located group of so-called S and M elements, which were likely used to grasp food (Goudemand et al., 2011), and, in the posterior part of the mouth, two pairs of so-called P elements, which were used to process the food (Purnell, 1994) (Martinez-Perez et al., 2016). Throughout their 300 Myr of existence (from the Late Cambrian to the Late Triassic), conodonts have one of the best spatio-temporally resolved fossil record and are often used as index fossils for relative dating of sediments and stratigraphic correlation between geological sites. Since conodont elements are also used for geochemistry-based reconstructions of paleoenvironments (Wenzel et al., 2000; Joachimski et al., 2002, 2006; Trotter et al., 2008; Sun et al., 2012), this makes them an ideal model system for deep time evolutionary studies. However, until recently conodonts were used almost exclusively in an “utilitarian” way (for biostratigraphy and paleoenvironment reconstructions) and, despite their huge potential, they have been relatively under-exploited for evolutionary studies, and virtually nothing is known about functional or developmental constraints in conodonts (Purnell, 1994; Donoghue and Purnell, 1999; Girard et al., 2004a; Girard and Renaud, 2007; Goudemand et al., 2011; Murdock et al., 2013; Martinez-Perez et al., 2016). Qualitative descriptions of conodont element variation are ubiquitous in the literature as they are standard in conodont systematics. Yet, they are usually restricted to given species, they rarely focus on patterns of covariation, and the lack of quantification implies that they cannot be statistically evaluated.

Quantitative studies on conodont elements are made difficult by their lifelong accretionary mode of growth (Donoghue, 1998): growth lamellae are periodically added around the elements, resulting in an increase of the number of denticles and a modification of the length-height ratio of the element during ontogeny, thereby hindering definition and identification of homologous landmarks, and hence complicating biologically relevant comparisons (Jones et al., 2009). Previous quantitative analyses on conodont elements were based on classical

and/or geometric morphometrics and quantified interspecific (Croll et al., 1982; Murphy and Cebecioglu, 1984; Klapper and Foster Jr, 1993; Girard et al., 2004b; Chen et al., 2009; Girard and Renaud, 2011) or intraspecific variation (Murphy and Springer, 1989; Ritter, 1989; Jones et al., 2009; Chen et al., 2016). Some authors further described evolutionary trends (Barnett, 1972; Roghi et al., 1995; Girard and Renaud, 2007; Jones, 2009), or linked some morphological evolutions to paleoenvironmental changes (Renaud and Girard, 1999; Girard et al., 2004a; Girard and Renaud, 2008), paleobiogeography (Tolmacheva and Löfgren, 2000), or functional aspects (Purnell, 1994). For instance, Croll and co-workers (Croll et al., 1982) used biometry to describe the  $P_1$  elements of *Ozarkodina*, *Pryantodina*, *Carniodus*, *Microzarkodina* and *Pterospathodus*, and concluded that biometry could be used for classification and identification. Renaud and Girard (Renaud and Girard, 1999) studied the response of *Icriodus* and *Palmatolepis* to Late Devonian extreme paleoenvironmental perturbations in terms of  $P_1$  element's oral outline, showing that the response of the two genera differed in time, which they interpreted as different sensitivities to the environmental perturbation and hence possibly different habitat preferences. Jones (Jones, 2009) used biometry and outline analyses on Silurian material of *Pterospathodus* to test for morphological temporal trends and observed that it involved mainly allometric repatterning. Yet, so far no study has focused on patterns of covariation between different traits of a given element, in order to investigate developmental constraints and putative evolutionary paths of least resistance within the conodont morphospace.

Here we study quantitatively with geometric morphometrics the morphological variation around the Carnian-Norian Boundary (CNB, Late Triassic, ~227 Ma) of  $P_1$  elements from the Pizzo Mondello section (Sicily, Italy) (Mazza et al., 2012b). These conodont elements belong to four genera and seven species: *Carnepigondolella pseudodiebeli* and *C. zoae*; *Hayashiella tuvalica*; *Epigondolella quadrata*, *E. rigoi*, and *E. uniformis*; and *Metapolygnathus communisti*. The material corresponds to a time interval that directly follows the Carnian Pluvial Episode (234-230 Ma), which was marked not only by a conodont extinction (Rigo et al., 2007), but also by a major floral and faunal turnovers (Simms and Ruffell, 1990; Hallam, 1996; Roghi et al., 2010). The corresponding species illustrate one of the last documented conodont evolutionary radiations before their final demise at the Triassic-Jurassic boundary (201.3 Ma)

(Pálfy et al., 2007; Mazza et al., 2012b; Mazza and Martínez-Pérez, 2015). This material has been selected because of its excellent preservation, the relative abundance of elements in each sample/species, and the fact that it had been already the subject of extensive sampling (this section is a candidate for the GSSP of the base of the Norian (Nicora et al., 2007) and several in-depth analyses, including a cladistic analysis (Mazza et al., 2012a), paleoenvironmental reconstructions (Muttoni et al., 2004; Mazza et al., 2010), and several ontogenetic series reconstruction in particular using synchrotron imaging (Mazza and Martínez-Pérez, 2015; Mazza and Martínez-Pérez, 2016). Ancestor-descendant relationships were also hypothesized between most of the species present in the Pizzo Mondello section. Concerning the studied dataset (five genera), two lineages can be recognised, with the genus *Paragondolella* as their presumed common ancestor. Note that an alternative systematics and associated phylogenetic and ancestor/descendant relationship hypotheses have been proposed for a similar conodont assemblage in Black Bear Ridge, British Columbia, Canada (Orchard, 2013) (Orchard, 2014). Yet, these hypotheses are based on a phenetic analysis and have not been tested quantitatively.

Mosher (Mosher, 1968) and, later, Mazza and co-authors (Mazza et al., 2012a) have already proposed hypotheses of putative evolutionary trends based on these taxa during the CNB interval. They suggested the derivation of *Metapolygnathus* and *Epigondolella* from the polyphyletic genus *Carnepigondolella*, through a series of newly derived characters: (1) the shifting of the pit, (2) the shortening of the platform, (3) the shortening of the anterior trough margin, (4) modifications of the lower margin profile of the platform, (5) the apparition of a stronger platform ornamentation (evolution of *Carnepigondolella* into *Epigondolella*), and (6) modifications of the size and relative location of the cusp. Trends (1), (2), (3) and (5) have also been described in Black Bear Ridge (Orchard, 2014) for the lineages crossing the CNB (see Rigo et al., 2018 for a discussion).

In this work, we analyzed the quantitative morphological variation of P1 conodont elements within and between these seven morphospecies and their evolution within 7 Ma around the CNB. We explored this dataset for recurrent patterns, especially patterns of variation and covariation between traits.

## 2. Material & Methods

The samples are housed in the collections of the Dipartimento di Scienze della Terra « A. Desio » (Università degli Studi di Milano). All samples are from the Pizzo Mondello section in the Sicani Mountains, western Sicily, Italy (Mazza et al., 2012b); they are dated between the latest Carnian and the earliest Norian. Conodonts from this section have an average CAI (Colour Alteration Index) of 1-1.5, indicating minimal post-depositional heating (Epstein et al., 1977; Nicora et al., 2007). The specimens were selected to be as complete as possible. A set of 8 to 24  $P_1$  elements per species were 3D-scanned, a total of 132  $P_1$  elements were considered (Table 1). According to the time calibration in (Kent et al., 2017) (fig. 7), the assemblage spreads over 7 Ma (230.5-222 Ma).

Based on the cladistic analysis by (Mazza et al., 2012a) (Figure 1), the five genera considered here are closely related. In particular, *Metopolygnathus* is closest to *C. zoae*, whereas *Epigondolella* is closest to *C. pseudodiebeli*. The affinity of *Hayashiella* remains unclear. These authors also hypothesised that both *Metopolygnathus* and *Epigondolella* would derive from the paraphyletic genus *Carnepigondolella*. Note that *Epigondolella* is considered as polyphyletic since the discovery of evolutionary convergences within this genus (Mazza and Martínez-Pérez, 2016). Furthermore, more recent studies on the phylogeny and evolution of the metapolygnathids (Mazza et al., in press) led to the hypothesis that the lineage *M. praecommunista* – *M. dylani* – *M. parvus* is probably evolutionary closer to the paragondolellids than it is to the carnepigondolellids; whereas the more ornated metapolygnathids (i.e., *M. mersinensis* and *M. mazzai*) would be more closely related to *Carnepigondolella*. This new interpretation is however compatible with the results provided by the previous cladistic analysis. The phylogenetic revision of *Epigondolella* does not affect its relationship with *Carnepigondolella*. *Paragon-dolella polygnathiformis* and *P. praelindae* were the last two conodont species of *Paragon-dolella* to survive the Julian-Tuvalian crisis caused by the Carnian Pluvial Episode. This genus is considered as the last common ancestor of *Norigondolella*, *Carnepigondolella*, *Epigondolella* and *Metopolygnathus*. More precisely, *P. praelindae* is considered as the ancestor of genus *Norigondolella*, whereas *P. noah* is the ancestor of genus *Carnepigondolella* (Mazza et al., 2012a).

Species	Age	Num- ber of ele- ments	On- toge- netic stage
<i>Hayashiella tuvaliaca</i>	Late Carnian	23	GS4 to GS6
<i>Carnepigondoella zoae</i>	Late Carnian	22	
<i>Carnepigondolella pseudodiebeli</i>	Late Carnian	9	GS4, GS5
		4	GS4, GS5
		7	GS4, GS5
<i>Metapolygnathus communista</i>	Car- nian-No- rian boundary interval	24	GS4 to GS6
<i>Epigondolella uniformis</i>	Earliest Norian	8	GS4, GS5
<i>Epigondolella rigoi</i>	Early No- rian	21	GS4, GS5
<i>Epigondolella quadrata</i>	Early No- rian	14	GS4 to GS6

Table 1: List of the studied material: specific determination, age, stratigraphic location (sample number), number of specimens and ontogenetic stage (sensu Mazza and Martinez-Perez (Mazza and Martinez-Perez, 2015)). As *C. tuvaliaca* was not included in that study, the corresponding ontogenetic stages were determined after the illustrations of Mazza and co-workers (Mazza et al., 2012b) (plate 3, Figs. 3-10).

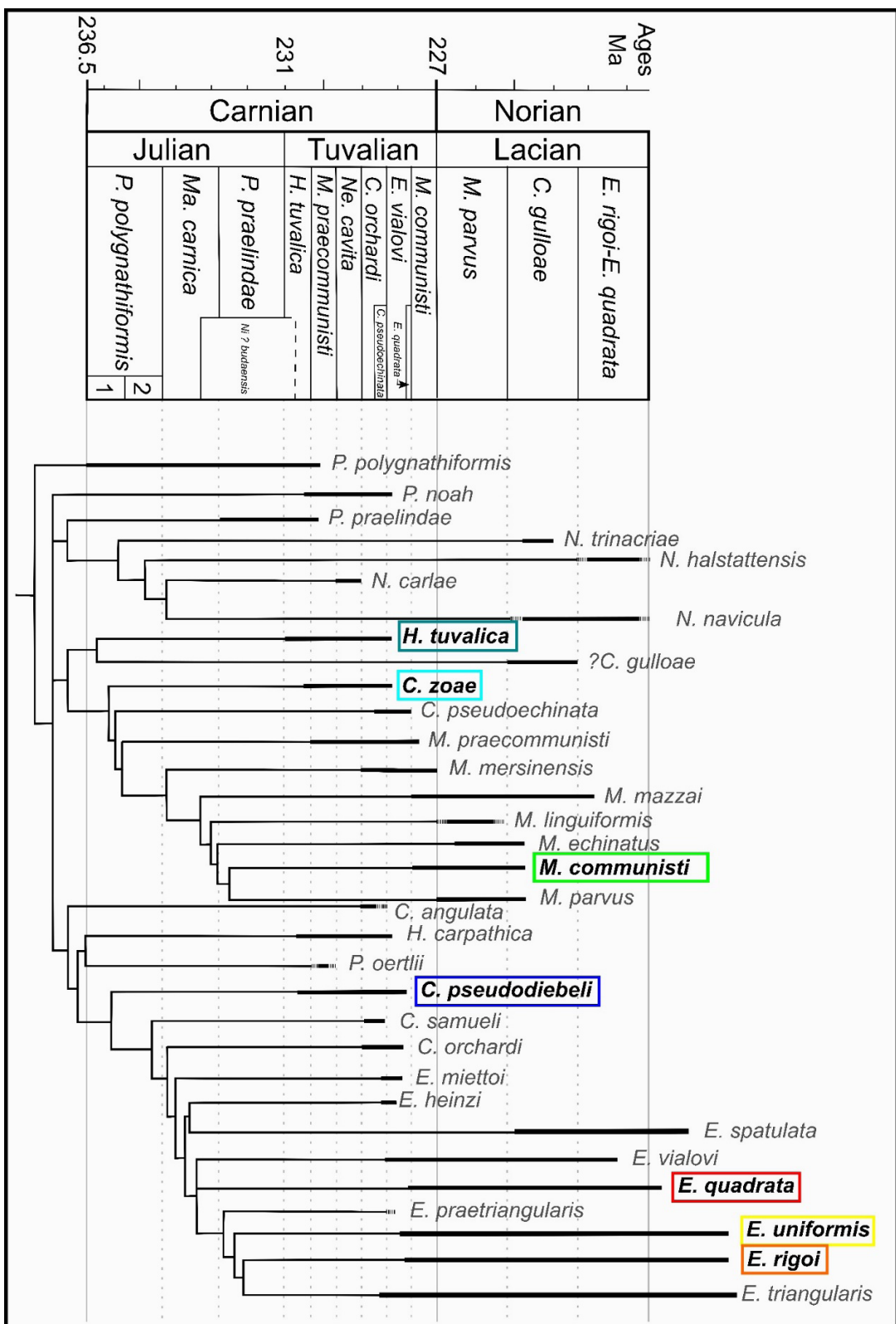


**Figure 1:** Simplified global Strict Consensus Tree Topology stratigraphically calibrated (modified after Mazza and co-workers (2012a) for the cladogram, after Rigo and co-workers (2018) for the species ranges and the biozonation). The taxonomy has been modified according to recent updates (after 2012), and the range of species absent from Rigo et al., 2018 are represented by dashed lines. *Hayashiella tuvalica* includes the Tuvalian forms of *C. nodosa* that was included in Mazza and co-workers study. The colors highlight the species considered in this study.

Additionaly to this assemblage, the holotypes of species of *Paragondolella*, *Carne-pigondolella*, *Metapolygnathus*, *Hayashiella* and *Epigondolella* present in the phylogenetic analysis were also considered in this study. When good enough illustrations of the holotypes, paratypes or lectotypes were not available, well preserved representative specimens were chosen from the litterature related to Pizzo Mondello section (Table 2).

In total, 162 conodont P1 elements were used for this study.

#### *Digitisation*

All elements were glued on wooden sticks using gum arabic and 3D-scanned at 1 µm resolution using the X-ray microtomograph nanotomS (General Electric) of the AniRA-ImmOs platform, SFR Biosciences (UMS 3444), Ecole Normale Supérieure de Lyon, France. Using this technique, multiple elements could be scanned at the same time. 3D reconstructions of the elements were obtained on Amira<sup>®</sup> software (v. 6.3.0), and snapshots of the elements were recorded in the standardized caudo-lateral, oral and aboral views (Figure 2). The nomenclature used in this study follows Purnell and collaborators (Purnell et al., 2000). Besides the fact that this 3D scanning process is as fast as standard SEM (Scanning Electron Microscopy) imaging, one advantage of the 3D scanning is that the standard views can be adjusted precisely, reducing a possible orientation bias for subsequent morphometric analyses. For comparison purposes, the morphological difference between dextral-mirrored and sinistral elements was statistically tested (see results), and all the dextral elements (*sensu* Purnell and co-workers 2000) were mirrored into sinistral elements to avoid morphological bias induced by the planar symmetry (Girard and Renaud, 2008).

#### *Geometric morphometrics*

A set of 6 landmarks was digitized on the aboral view, as well as a 20-sliding-landmark-based curve on the lower margin in lateral view, using tpsDig v. 2.30 (Rohlf and Marcus, 1993; Rohlf, 2006) (Figure 2b). For each data set, a generalised Procrustes analysis was performed using tpsRelw v. 1.67 (Rohlf, 2007). By this method, configurations of landmarks and sliding landmarks were (1) scaled, (2) translated, and (3) rotated in order to minimize the sum

Species	Nature	Source
<i>Carnepigondolella angulata</i>	Holotype	(Mazza et al., 2012a) Fig. 9A
<i>Carnepigondolella carpathica</i>	Holotype	(Mock, 1979) Pl. 1
<i>Carnepigondolella nodosa</i>	Mature growth stage	(Mazza et al., 2012b) Pl. 2 figs. 4a-c
<i>Carnepigondolella orchardi</i>	Mature growth stage	(Mazza et al., 2012b) Pl. 2 figs. 2a-c
<i>Carnepigondolella pseudodiebeli</i>	Mature growth stage	(Mazza et al., 2012b), Pl. 2 fig. 8
<i>Carnepigondolella pseudoechinata</i>	Mature growth stage	(Balini et al., 2010) Pl. 2, fig. 6
<i>Carnepigondolella samueli</i>	Holotype	(Orchard, 1991) Pl. 1, figs. 10-12
<i>Carnepigondolella tuvalica</i>	Holotype	(Mazza et al., 2012b) Pl. 3, figs. 4a-c
<i>Carnepigondolella zoae</i>	Holotype	Orchard 1991
<i>Epigondolella heinzi</i>	Holotype	(Mazza et al., 2012a) Fig. 9C
<i>Epigondolella miettoi</i>	Holotype	(Mazza et al., 2012a) Fig. 9F
<i>Epigondolella praetriangularis</i>	Holotype	(Moix et al., 2007) Pl. 1, figs. 9;10
<i>Epigondolella quadrata</i>	Holotype	(Orchard, 1991) Pl. 2, figs. 1-3
<i>Epigondolella rigoi</i>	Holotype	(Noyan and Kozur, 2007) Fig. 6.4
<i>Epigondolella spatulata</i>	Mature growth stage	(Mazza et al., 2010) Pl. III, figs. 6a-c
<i>Epigondolella triangularis</i>	Mature growth stage	(Balini et al., 2010) Pl. 4, figs 7a-c
<i>Epigondolella uniformis</i>	Holotype	(Orchard, 1991) Pl. 3, figs. 1-3
<i>Epigondolella vialovi</i>	Mature growth stage	(Balini et al., 2010) Pl. 3, figs 6a-c
<i>Metapolygnathus mazzai</i>	Holotype	(Mazza et al., 2012b), Pl. 8, Fig. 12
<i>Metapolygnathus communisti</i>	Holotype	(Hayashi, 1968) reillustrated by Mazza and co-workers (Mazza et al., 2011) Fig. 2B
<i>Carnepigondolella gulloae</i>	Holotype	(Mazza et al., 2012b), Pl. 4, fig. 4a-c
<i>Metapolygnathus echinatus</i>	Mature growth stage	(Mazza et al., 2012b) Pl. 8, figs. 7a-c
<i>Metapolygnathus linguiformis</i>	Mature growth stage	(Balini et al., 2010) Pl. 4, fig. 1

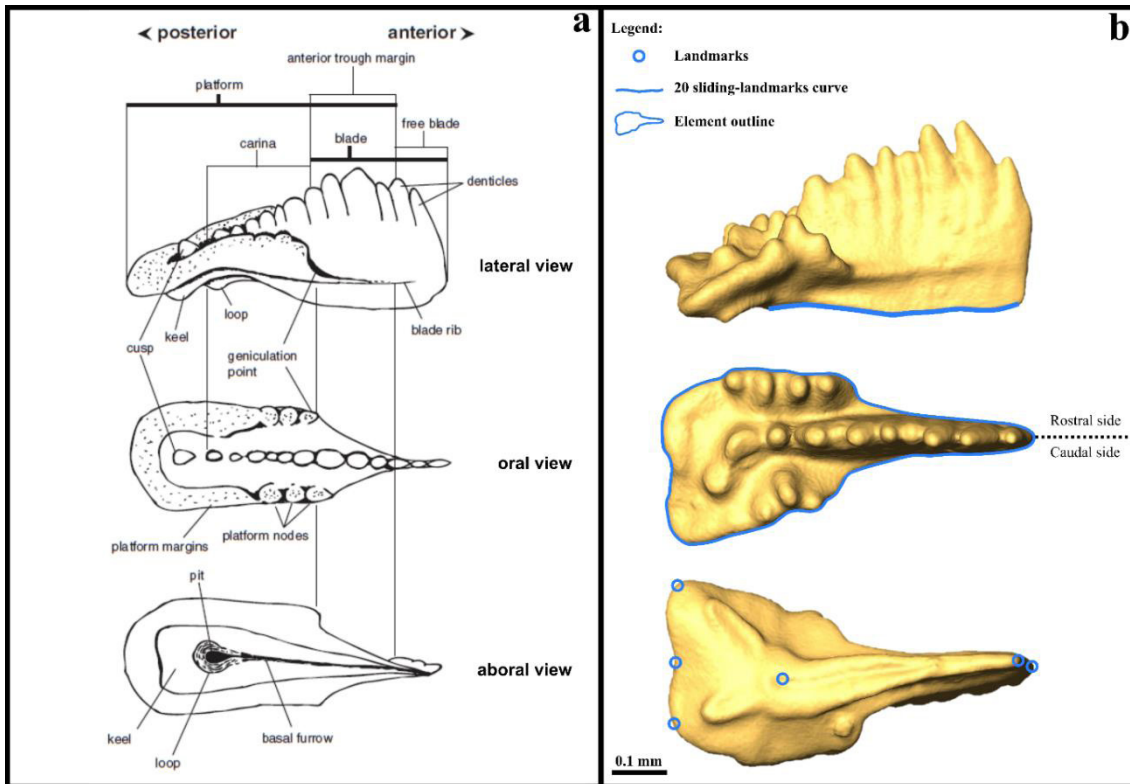
<i>Metapolygnathus mersinensis</i>	Holotype	(Moix et al., 2007) Pl. 1, fig. 14
<i>Metapolygnathus parvus</i>	Holotype	(Kozur, 1972) Pl. 6, fig. 2
<i>Metapolygnathus praecommunisti</i>	Holotype	(Mazza et al., 2011) Fig. 2C
<i>Paragondolella noah</i>	Holotype	(Hayashi, 1968) reillustrated by Mazza and co-workers (Mazza et al., 2011) Fig. 2A
<i>Paragondolella oertlii</i>	Holotype	(Rigo et al., 2018) Fig. 2
<i>Paragondolella polygnathiformis</i>	Indetermined growth stage	(Rigo et al., 2007) Fig. 4.6a-c
<i>Paragondolella praelindae</i>	Sub-mature growth stage	(Mazza et al., 2012b) Pl. 7 figs 13a-c.

Table 2: List of holotypes or representative specimens of each species present in the phylogenetic hypothesis in (Mazza et al., 2012a) considered in the dataset, and the reference for each image. *Norigondolella* was not included because it belongs to a third lineage that was not the scope of the present study.

of squared distances between corresponding landmarks. The resulting coordinates were used as shape variables for the multivariate analyses.

The outline of the element in oral view was extracted and reduced to 24 equally spaced points (origin set at the rostral geniculation point), which were used as input for an elliptic Fourier analysis (Kuhl and Giardina, 1982) using the Momocs package (Bonhomme et al., 2014) in the R software (RStudio Team, 2015). This method decomposes the outline signal into harmonics, each of them described by four Fourier coefficients. Here 8 harmonics were kept, which together describe 99% of the original outlines.

The three sets of variables (landmark and sliding-landmark coordinates, and coefficients of outline harmonics) were summarized using Principal Component Analysis (PCA) on variance-covariance matrices. Then the relationships between the three data sets were investigated using the STATIS method (Lavit et al., 1994), which allows performing the joint analysis of K tables (one per data set, K = 3 in our case) sharing the same rows (specimens). The STATIS method is carried out in two steps (Thioulouse and Chessel, 1987; Blanc et al., 1998). In the first step, called interstructure analysis, one searches for a compromise structure computed as the weighted sum of the K tables. Coefficients are obtained from the singular value decomposition of the matrix of RV-coefficient, which is the multidimensional equivalent of the ordinary



**Figure 2:** a) Definition of P1 morphological terms (from Mazza and co-workers (2012a)); b) Location of the used landmarks, sliding landmarks curve, and outline. The illustrated specimen belongs to *E. rigoi*.

correlation coefficient between two variables (Robert and Escoufier, 1976). The corresponding eigen analysis yields factorial axes that describe the common structure across sets of variables, which is analogous to an average morphospace. During the second step, called intra-structure analysis, the projections of rows and columns of each individual dataset onto the compromise axes are computed as supplementary individuals and supplementary variables, respectively. In addition, the axes of separate PCAs on each dataset can be projected onto the compromise structure too, allowing for the identification of the axes of the separate PCAs best describing the common structure between the three data sets. These PCA axes are then used as shape variables. This procedure helps to minimise the number of relevant variables used in further statistical analyses. For each view, only the PCA axes that together explain at least 80% of the cumulated variance were considered. Finally, these axes were illustrated in terms of morphological variation to better visualise covariations between morphological traits. Statistical tests were performed using the ade4 (Dray et al., 2007) library available in the R software.

A PERMANOVA (Anderson, 2001) was performed on the STATIS compromise scores using PAST v. 3.16 (Hammer et al., 2001) to test the significance of (1) the shape differences between sinistral and dextral-mirrored elements and (2) the intergeneric morphological differences. To assess whether the slopes of reduced major axes (RMA) of each species calculated in the STATIS compromise were significantly different, we used the  $\chi^2$  test for multiple comparison of RMA slopes available in PAST. Correlation between shape variables was tested in R using the Spearman correlation coefficient in order to account for non-normality of these variables, and graphic representations were produced using the R package ggplot2 (Wickham, 2016). In all analysis,  $\alpha=5\%$ .

The datasets generated and/or analysed during the current study are available from the corresponding author on request.

### 3. Results

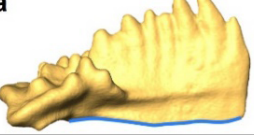
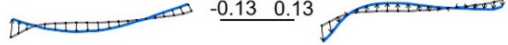
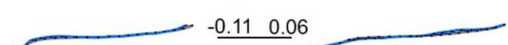
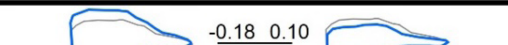
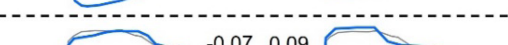
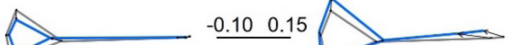
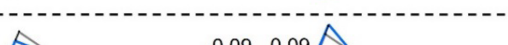
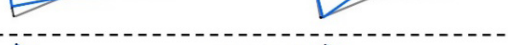
#### *Main patterns of shape variation*

The quantification of the morphological characters of the elements was done on the three standard views. There was no significant morphological difference between dextral-mirrored and sinistral elements for each quantified character (PERMANOVA performed on aligned and harmonic coordinates, p-value > 0.2). Hence, the dextral-mirrored images were included in the dataset and treated equally as sinistral elements in further analyses.

The three data sets were analysed independently using a PCA. For each dataset, only the most significant PCA axes explaining together at least 80% of the cumulated variance are considered.

The analysis of the lower margin in lateral view (Figure 3a) returns two principal axes of morphological variation:

- The first axis (69.6%, ‘lower margin bending’) corresponds to the flexure of the lower margin, ranging from semi-elliptic (upward bending) to ‘wavy’ (associated with a stron-

Views	PCA axes	Shape variation	Name of shape indicator
<b>a</b> 	Axis 1 (69.6%)	 -0.13 0.13	Lower margin bending
	Axis 2 (14.0%)	 -0.11 0.06	Lower margin posterior dip
<b>b</b> 	Axis 1 (38.8%)	 -0.18 0.10	Platform lateral expansion
	Axis 2 (23.8%)	 -0.07 0.09	Squarebovaticity
	Axis 3 (11.0%)	 -0.05 0.06	Cuneospatulaticity
	Axis 4 (6.6%)	 -0.05 0.05	Element longitudinal bending
<b>c</b> 	Axis 1 (42.1%)	 -0.10 0.15	Posterior extension
	Axis 2 (22.8%)	 -0.09 0.09	Posterior width
	Axis 3 (20.6%)	 -0.08 0.13	Posterior asymmetry

**Figure 3:** Selected principal components (shape variables) for each view. a) lateral view, lower margin curve; b) oral view, outline analysis; and c) aboral view, set of six landmarks. For each principal component axis, the percentage of explained variance is given; the extreme morphotypes are represented in blue (associated with the corresponding score along the axis) as superimposed on the consensus shape represented in grey (average shape of the assemblage). The illustrated specimen belongs to *E. rigoi*.

ger downward bending of the posterior end) for the most extreme morphotypes;

- The second axis (14.0%, ‘lower margin posterior dip’) highlights posterior modifications of the lower margin, with a more or less conspicuous dip of the posteriormost end of the anterior process.

The analysis of the element outline in oral view highlights four main axes of variation (Figure 3b):

- The first axis (38.8%, ‘platform lateral expansion’) corresponds to variation in the overall width of the platform.
- The second axis (23.8%, ‘squarebovaticity’) corresponds to variation between elements with a short (about half the length of the element), sub-squared platform and elements with an obovate platform (ovate shape with tapering towards the anterior end).

- The third axis (11.0%, ‘cuneospatulaticity’) illustrates the variation between long wedge-shaped (‘cuneate’) elements and spoon-shaped (‘spatulate’) elements with a relatively short and elliptical platform.
- The fourth axis (6.6%, ‘element longitudinal bending’) corresponds to the overall bending and asymmetry of the element.

In aboral view, the variation of the relative position of the pit can be summarized by three principal components (Figure 3c):

- The first axis (42.1%, ‘posterior extension’) corresponds to a variation of the dimensions of the posterior end of the elements relative to the entire element: the triangle defined by the two posteriormost corners and the pit remains sub-equilateral or isoscele, while the size of this triangle varies between one third and two fifths of the element length.
- The second axis (22.8%, ‘posterior width’) corresponds to variation in the relative length of the posterior part, which gets slightly shorter when the platform gets relatively wider. In other words, it corresponds to lateral expansion of the posterior end of the platform.
- The third axis (20.6%, ‘posterior asymmetry’) illustrates variation in asymmetry of the posterior part of the element: the more asymmetrical, the shorter the posterior end; additionally, the wider side gets deflected anteriorly.

#### *Combined analysis of the three geometric morphometrics data sets*

To explore the overall shape variation within this assemblage and to assess the weight of each shape descriptor on the global variation, we used the STATIS method. We projected for each view the principal components described above onto the 3-table STATIS compromise (built on the three sets of morphometrical variables), and then analysed their relative importance using a correlation circle (Figure 4). The specimens of *Hayashiella*, *Carnepigon-dolella* and their supposed descendants (representatives of *Metapolygnathus* and *Epigondolella*) group in two significantly distinct clusters in the STATIS compromise (PERMANOVA, p-value <0.001). The axis along which these two groups are most discriminated makes an angle of about 45 degrees with the first STATIS component (Figure 4a, C1= 33.5% of the total variance). Furthermore, the main axes of intraspecific variation (i.e., the major axes of each specific

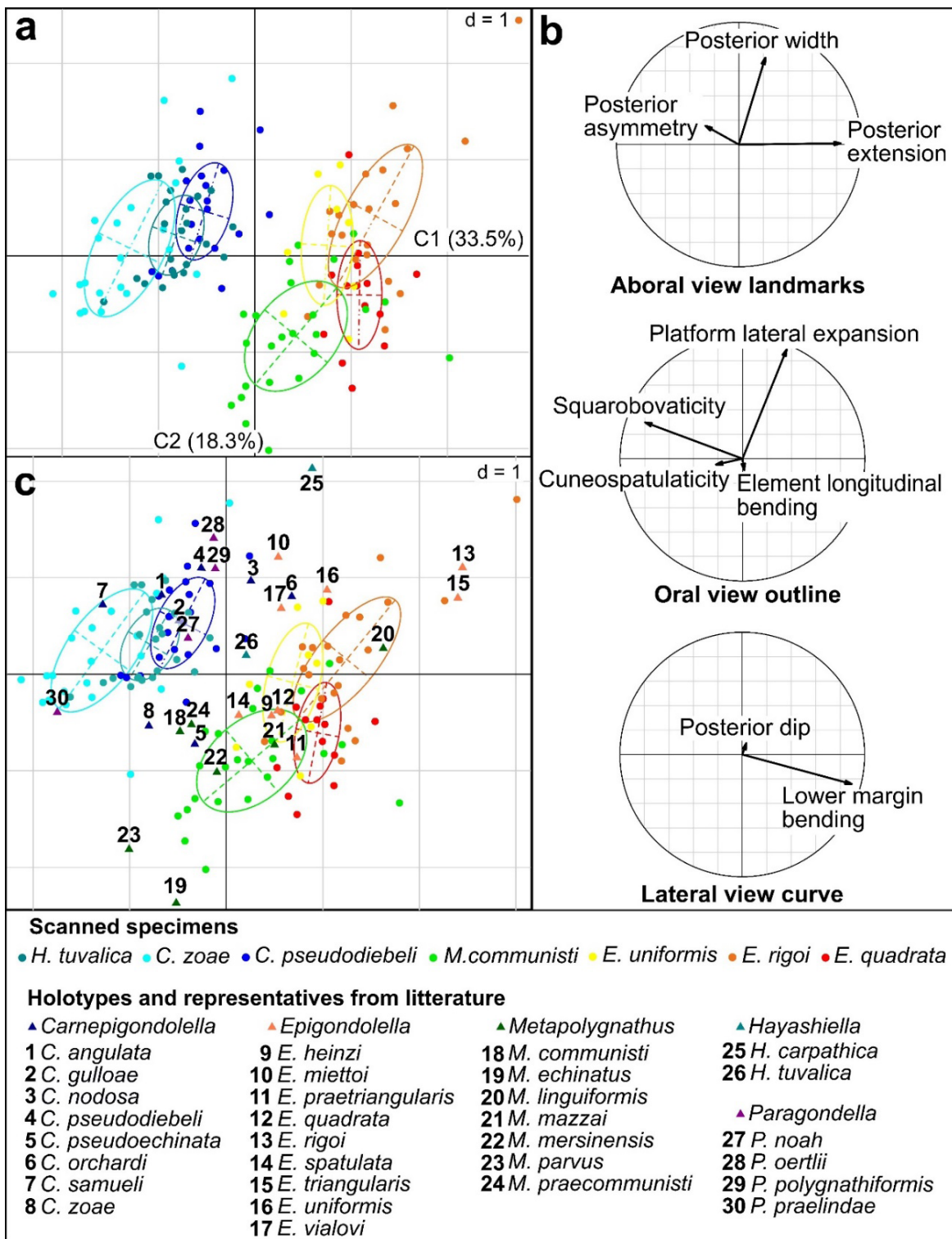


**Figure 4:** a) First two axes of the STATIS compromise showing the best separation of specimens (dots) associated to the three sets of coordinates. Ellipses (63% of dots) identify specimens belonging to a given species (the scale “d” corresponds to the grid size); b) First two axes of a STATIS compromise correlation circle showing the projections of the principal components of separate PCAs selected in Figure 3; c) First two axes of the STATIS compromise with holotypes and representatives of species included in the phylogenetic hypothesis of conodonts from the Pizzo Mondello section. Abbreviations for the legend: C. – Carnepigondolella; H. – Hayashiella; E. – Epigondolella; M. – Metapolygnathus; P. – Paragondolella.

ellipse) do not differ significantly from each other (overall  $\chi^2$ -test for RMA-slope comparison:  $\chi^2 = 6.0$ , p-value = 0.24), highlighting a pattern of intraspecific variation shared by all analyzed taxa (Figure 4a). This common axis of intraspecific variation appears sub-perpendicular to the axis separating the two main clusters.

Using the correlation circles we can interpret these observations in terms of biologically meaningful, morphological parameters (Figure 4b). On the one hand, the parameters that most aligned with the axis separating the ‘Carnian’ ancestors from their presumed ‘Norian’ descendants are the ‘lower margin bending’, the ‘squarobovaticity’ and the ‘posterior asymmetry’. Note also that the non-aligned ‘posterior extension’ has a greater contribution than the ‘posterior asymmetry’ in the morphological transformation associated with this intergeneric axis (the projection of the corresponding arrow on the separation axis is larger than the one for the ‘posterior asymmetry’). In other words, the transition from *Hayashiella* and *Carnepigondolella* to *Epigondolella* and *Metapolygnathus* in this dataset corresponds, in  $P_1$  elements, to a more

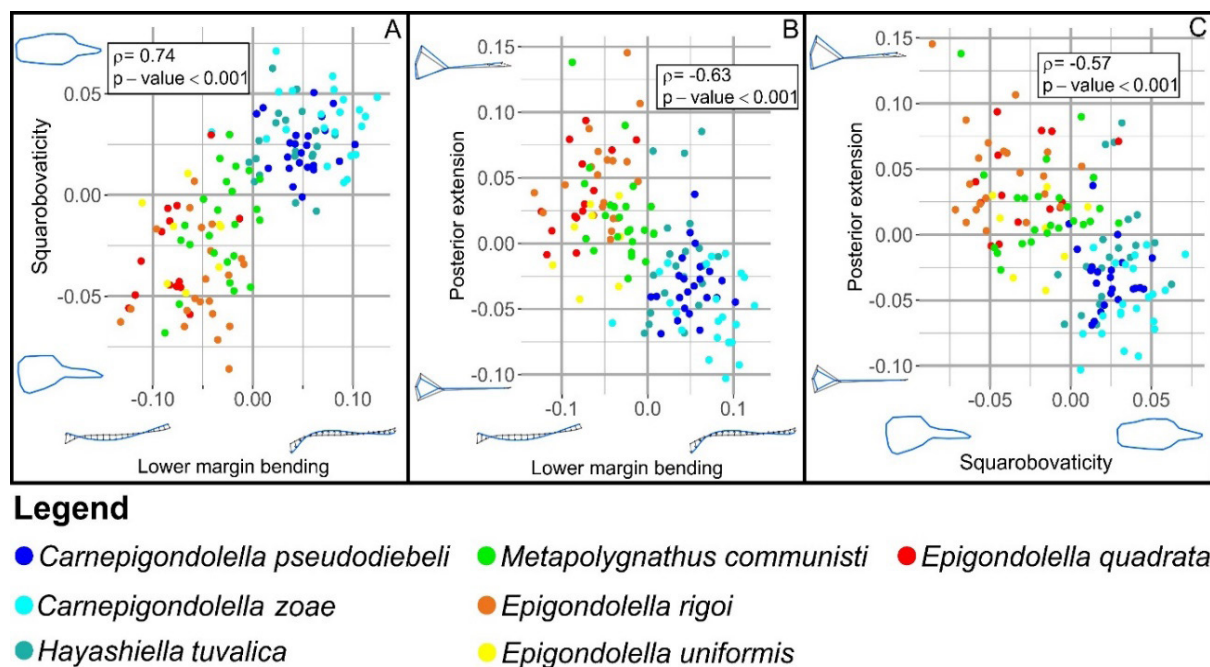


**Figure 5:** Correlations between a) ‘lower margin bending’ and ‘squarobovaticity’; b) ‘lower margin bending’ and ‘posterior extension’; c) ‘squarobovaticity’ and ‘posterior extension’. All correlations are attested by a coefficient of Spearman correlation ( $\rho$ ) and a p-value. Each species is associated to a single colour.

upward bended lower margin, a shorter and more squared platform, and a relatively larger posterior part.

On the other hand, the ‘platform lateral extension’, and the ‘posterior width’ are the parameters that most aligned with the common axis of intraspecific variation. In other words, within a given species, elements tend to show varying degrees of platform lateral expansion associated with modifications of the relative width of the posterior part: the larger the lateral expansion of the platform, the larger the posterior part (in overall size relative to element length) but the narrower the posterior part, and the more elliptic the element.

As is implicit from the patterns of variation described above, most parameters are covarying to some degree. In particular, the ‘lower margin bending’, ‘squarobovacity’, and ‘posterior extension’ are significantly correlated two by two (Spearman correlation test,  $0.57 < |\rho| < 0.74$ , p-values  $< 0.001$ ; Figure 5). Likewise, ‘platform lateral extension’ and ‘posterior width’ are negatively correlated (Spearmann correlation test,  $\rho = -0.52$ , p-value  $< 0.001$ ).

As well for the STATIS compromise (Figure 4a), species are hardly distinguished from one another based on a single pair of characters: the spread of the intraspecific variation is usually much greater than the distance between the means of two given species. The distinction between the Carnian and Norian forms analyzed in this study is driven by the ‘lower margin bending’. In this dataset, carnepigondolellid and hayashiellid forms tend to have a relatively longer platform that is obovate in oral view, a posteriorly located pit, and a wavy lower margin. Epigondolellid forms tend to have a relatively short platform and a large posterior end (squared), a centrally located pit, and a semi-elliptic lower margin. *Metapolygnathus* appears as intermediate between them for the considered descriptors.

In order to best represent the overall morphological variation of *Paragondolella*, *Carnepigondolella*, *Metapolygnathus*, *Hayashiella* and *Epigondolella* at Pizzo Mondello, the holotypes and representatives of 28 conodont species were added to the STATIS analysis (Figure 4c). The holotypes of the studied species fall within the range of variation of the samples, except for those of *H. tuvalica*, *E. quadrata* and *E. uniformis*, which stay close to their species sample variation range. It is unclear whether this shift is due to an orientation bias introduced

by using photographs from the literature that stem from different authors. *Paragondolella* and *Carnepigondolella* are located in the same area, and they are separated from their supposed descendants *Epigondolella* and *Metapolygnathus*.

#### 4. Discussion

This study was focused on the analysis of the morphological variation and covariation of a Late Triassic (late Carnian to early Norian) dataset of  $P_1$  conodont elements. The STATIS analysis shows that the Carnian basal forms clearly differ from the Norian derived forms. The intraspecific and intergeneric morphological variations correspond to two distinct patterns driven by characters that covary at both taxonomical levels (Figure 6). On the other hand, the different species within each of these groups cannot be distinguished using only the morphological traits considered here.

##### *The morphological characters: different implications at different taxonomic levels*

Within each genus, the intraspecific variation usually overlaps in the 3-table STATIS compromise. This can be due to the fact that the ornamentation and morphology of the keel end can not be quantified with the method used in this study, as these characters are not present in all elements, and therefore were not considered in the analysis. Nevertheless, this morphological analysis shows that: (1) a few characters are sufficient to group related species and to reveal the morphological transformations that occurred between the basal and the derived groups (i.e. the ‘lower margin bending’, the ‘squarobovaticity’ and the ‘posterior extension’, Figure 4a); (2) the same morphological transformations were involved in the evolution of two separate lineages (i.e. parallel evolution between *Carnepigondolella-Metapolygnathus* and *Carnepigondolella-Epigondolella*, Figure 4, Figure 5); and (3) the characters driving variation at the intra-specific level (i.e., the ‘posterior width’ and the ‘platform lateral expansion’) differ from those driving morphological variation at the intergeneric level (Figure 4a, b).

This study highlights for the first time a common pattern of intraspecific variation within a conodont assemblage consisting of closely related taxa. All the available adult specimens that

were preserved well enough to conduct the geometric morphometrics analysis were considered, thus avoiding any “cherry picking” bias. Nevertheless, the elements analysed here represent only a portion of the available material as the method requires fully preserved conodonts. Since the specimens had been already determined and hence classified into specific bins, the observed consistency of the intraspecific variation may correspond to a generic concept of conodont species variability, even if unlikely.

#### *Global environmental perturbation as an explanation of the morphological shift*

The studied dataset can also be used to investigate environmental *vs.* developmental drivers of conodont evolution within the analysed time series, by using the theoretical framework of the lines of least evolutionary resistance (Schluter, 1996; Renaud et al., 2006; some morphologies are more readily generated than others due to internal developmental constraints. Such constraints can channel evolutionary changes into directions corresponding to the greatest intraspecific variation. Long term evolutionary outputs, however, depend on the stability of these intraspecific patterns of variation over time and from the interplay between internal constraints and selective regimes. To address these questions, the relationship between the structure of phenotypic variance covariance matrices and direction of morphological evolution was investigated using teeth of fossil rodents. One lineage considered here leads to Stephanomys,

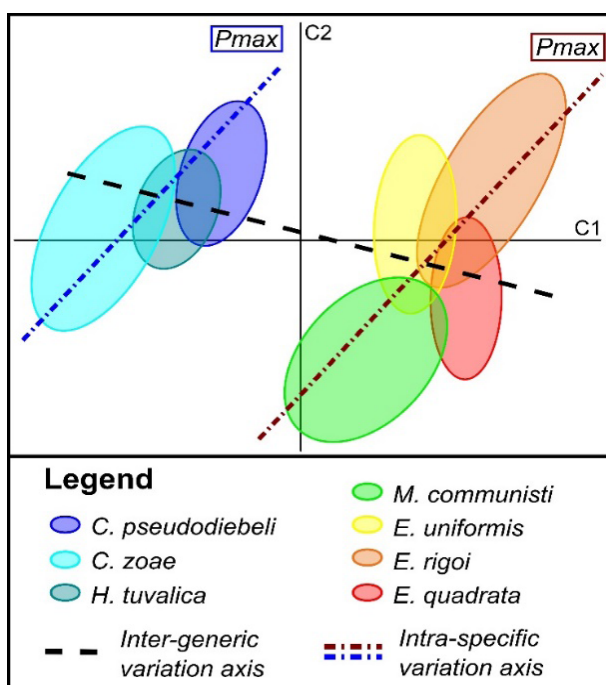


**Figure 6:** Illustration of the inter- vs intra-specific patterns of variation based on the STATIS compromise. The ellipses identify species.

a highly specialized genus characterized by a dental pattern supposedly favoring grass eating. Stephanomys evolved in the context of directional selection related to the climatic trend of global cooling causing an increasing proportion of grasslands in southwestern Europe. The initial divergence (up to ~6.5 mya Hunt, 2007). According to this theory, species would evolve preferentially along the main axis of intraspecific phenotypic variance ( $P_{max}$ ). Further, any significant deviation from the  $P_{max}$  trajectory can be interpreted as reflecting the influence of non-random selective factors such as environmental pressures.

The fact that the main intergeneric axis of phenotypic variance is almost perpendicular to  $P_{max}$  in two separate lineages strongly suggests that the evolution of these Norian forms was driven by an external perturbation (Figure 6). The location within the morphospace of the

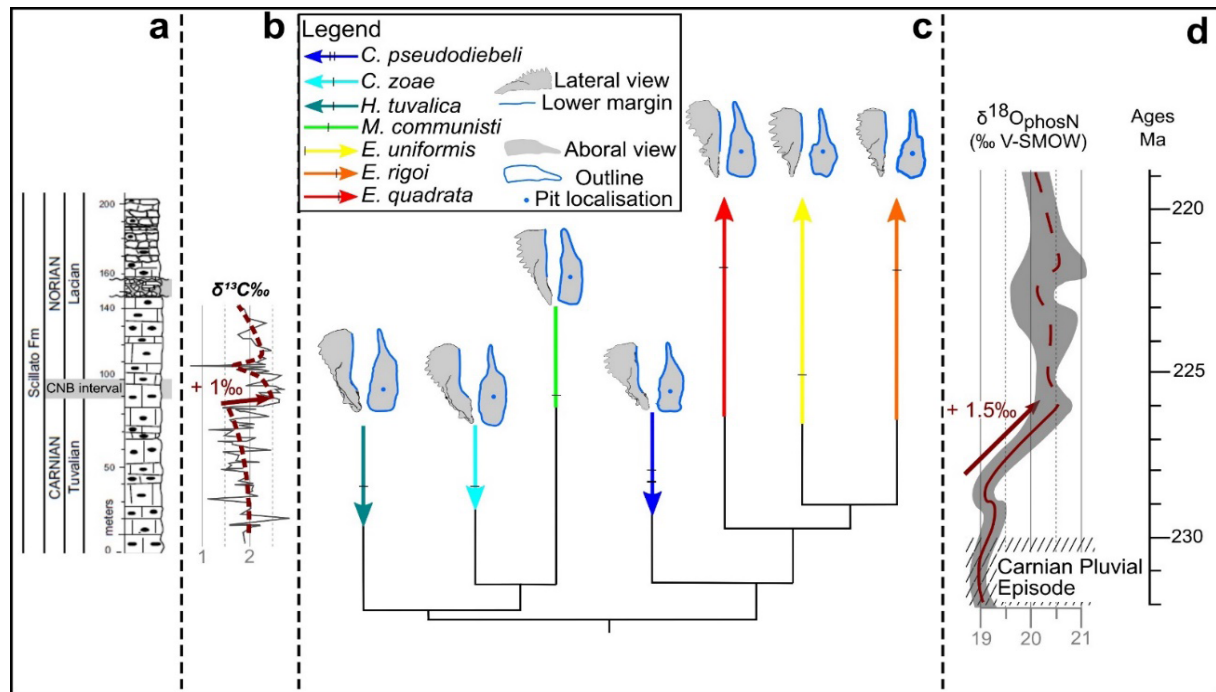


**Figure 7:** Synthetic illustration including sedimentologic, geochemical, stratigraphic and morphological data of the Pizzo Mondello section and at global scale. a) Log including the Carnian-Norian boundary interval, and a part of Late Carnian and Lower Norian (after Mazza and coworkers (2012b)); b)  $\delta^{13}\text{C}$  isotopic data got on carbonate bulk sample, including the 1‰ shift occurring just before the CNB interval (Mazza et al., 2010). The red dashed line and the red arrow highlight the shift (image modified after Mazza and co-workers (2010)); c) Global stratigraphically calibrated cladogram reduced to the studied seven species (modified after Rigo and collaborators (2018)). For each species its stratigraphic range, as well as the location of the samples used in this study, and its specimen consensus is represented; d) Global  $\delta^{18}\text{O}$  isotopic curve got on conodont elements and highlight of the 1.5‰ positive shift (modified after Trotter and co-workers (2015)). Absolute timing correlation was done following Kent and co-workers (2017).

*Paragondolella* specimens among *Carnepigondolella-Hayashiella* specimens consistent with this hypothesis (Figure 4).

As the Pizzo Mondello section is a GSSP candidate for the definition of the Carnian-Norian boundary (CNB), detailed geochemical and paleontological studies have been already carried out (Mazza et al., 2010; Mazza et al., 2012b), and their results can be interpreted in terms of paleoenvironments. The stable carbon isotope record (Mazza et al., 2010) of the Pizzo Mondello section shows a one permil positive excursion at the base of the CNB interval (Muttoni et al., 2004, fig. 3, at 84.5 m; Mazza et al., 2010, fig. 5, at 82 m). This + 1‰ shift coincides with the most conspicuous faunal turnover in this section: most of the carnepigondolellids get extinct and specimens of *Metapolygnathus* and *Epigondolella* become abundant (Figure 7). .

At the global scale, a 1.5 permil increase of the Tethyan subtropics stable oxygen isotope ratio ( $\delta^{18}\text{O}_{\text{apatite}}$ , measured on conodont elements) from the late Tuvalian (Late Carnian) to the early Ladian (Early Norian) was demonstrated by several authors (Rigo et al., 2012; Trotter et al., 2015), implying a decrease of 6°C in marine seawater temperature. This cooling followed the Wrangellian volcanism and the Carnian Pluvian Episode and marked a return to an arid climate. It coincided with low  $\text{pCO}_2$  values and a major faunal turnover at several trophic levels: replacement of almost all coral species, emergence and radiation of new phytoplankton lineages, as well as marine and terrestrial vertebrates including dinosaurs, pterosaurs, turtles, crocodilians and mammals. This suggests a major shift in food resources available for conodonts, hence a likely shift in their diet, which may explain the observed shift in the morphology of the  $P_1$  elements.

#### *The developmental mechanisms under the evolutionary shift*

As suggested previously (Mosher, 1968; Mazza et al., 2012a), the transition from Carnian to Norian forms involved modifications of the lower margin profile of the platform (captured in the ‘lower margin bending’ principal component above), a shortening of the platform relative to the entire element (see ‘brevicuneoellipticity’ and ‘posterior extension’ principal components), and a ‘shifting of the pit’ (i.e. a relative enlargement of the posterior part of the element; see ‘posterior extension’) (Figure 7, Figure 8). Moreover, even if it was not quantified

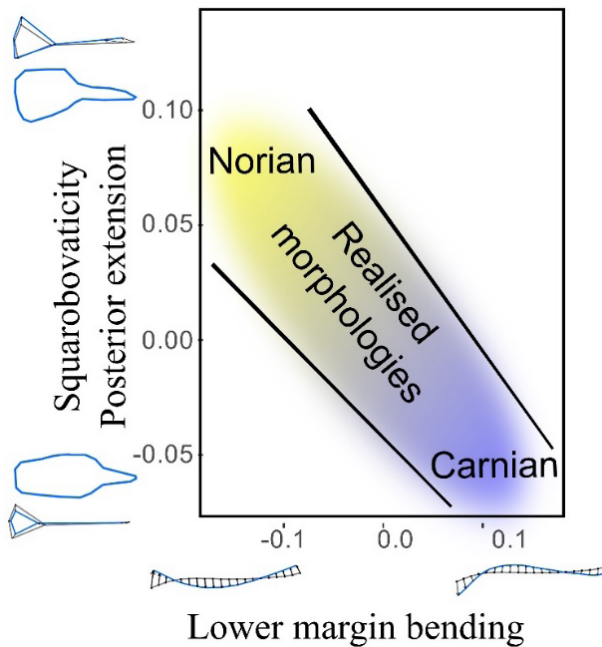


**Figure 8:** Illustration of the constrained morphologies of the conodont elements through the Carnian-Norian interval.

here, the ornamentation of the platform became more complex, showing a development from nodes restricted to the middle and anterior parts of the platform (Carnian) to nodes or denticles all over the platform (Norian) (Mazza et al., 2012a). These modifications, except for the lower margin profile of the platform, were also noted by Orchard (2014) with similar collections from the Black Bear Ridge section in Canada, and show a global evolutionary change in conodont elements at CNB. The fact that the very same evolutionary path was followed in two presumably distinct lineages at Pizzo Mondello section suggest that both morphologies of these lineages were constrained in a parallel way, and possibly by the same drivers.

Beyond the patterns of intraspecific and intergeneric variation, the correlations we demonstrated between, on one hand, the ‘lower margin bending’, ‘squarobovaticity’ and ‘posterior extension’ (and implicitly platform ornamentation), and, on the other hand, the ‘posterior width’ and ‘platform lateral expansion’, also highlight the existence of ‘restricted’ areas in the morphospace for which no realised morphology is observed (Figure 8, see also Figure 5). As far as P1 conodont elements are concerned, this suggests that general laws of covariation exist, that apply not only within species, but also at higher taxonomical levels. These laws may be the consequence of some developmental and/or functional constraints. For instance, the association of a wavy baseline and a large posterior platform (and/or a highly ornamented platform) is never observed in this assemblage. Whether such association of traits may correspond to

morphologies that are either developmentally ‘impossible’ or functionally ‘non-viable’ because they could prevent proper occlusion and hence proper feeding is still unclear and may be the subject of further work.

## 5. Conclusion

A parallel evolutionary path between two lineages, highlighted by a common pattern of intraspecific and intergeneric variation, suggests the existence of generic laws of morphological traits covariation in conodont elements. The transition between Carnian forms and their presumed Norian descendants corresponds to an axis in the morphospace that is very different from the axis of intraspecific variation affecting all pre- and post-CNB species, suggesting that the intergeneric evolution of these elements did not follow the expected evolutionary path of least resistance. This may reflect the consequences of an environmental perturbation as highlighted by the carbon and oxygen isotope records during that particular interval, and/or its ecological implications for conodonts such a complete diet change. This would have constituted a major selective pressure on conodont element’s shape. The present study is a first step toward a general quantification and better understanding of the patterns of variation and covariation in euconodonts, and allows to better constrain the causes of their morphological evolution. Due to their ~300 Myr-long widespread abundance in marine strata, conodont elements appear to be a useful model to study evolution in deep time.

## Acknowledgments

We thank Mathilde Bouchet (ENS Lyon, SFR Biosciences) for her invaluable help with the microtomography, and Sylvain Doledec and Gilles Escarguel (Université Lyon 1) for their advices in statistics. Gilles Escarguel is also thanked for having discussed several drafts of this manuscript. This research is supported by a French ANR @RAction grant to NG (ACHN project ‘EvoDevOdonto’).

## References

- Anderson, M.J., 2001. A new method for non-parametric multivariate analysis of variance. *Austral ecology* 26, 32–46.
- Barnett, S.G., 1972. The evolution of *Spathognathodus remscheidensis* in New York, New Jersey, Nevada, and Czechoslovakia. *Journal of Paleontology* 900–917.
- Blanc, L., Chessel, D., Dolédec, S., 1998. Etude de la stabilité temporelle des structures spatiales par analyses d'une série de tableaux de relevés faunistiques totalement appariés (in French). *Bulletin Français de la Pêche et de la Pisciculture* 1–21.
- Bonhomme, V., Picq, S., Gaucherel, C., Claude, J., others, 2014. Momocs: outline analysis using R. *Journal of Statistical Software* 56, 1–24.
- Chen, J., Beatty, T.W., Henderson, C.M., Rowe, H., 2009. Conodont biostratigraphy across the Permian–Triassic boundary at the Dawen section, Great Bank of Guizhou, Guizhou Province, South China: implications for the Late Permian extinction and correlation with Meishan. *Journal of Asian Earth Sciences* 36, 442–458.
- Chen, Y., Neubauer, T.A., Krystyn, L., Richoz, S., 2016. Allometry in Anisian (Middle Triassic) segminiplanate conodonts and its implications for conodont taxonomy. *Palaeontology* 59, 725–741.
- Croll, V.M., Aldridge, R.J., Harvey, P.K., 1982. Computer applications in conodont taxonomy: characterization of blade elements. Miscellaneous paper, in: Geological Society of London. pp. 237–246.
- Donoghue, P.C., 1998. Growth and patterning in the conodont skeleton. *Philosophical Transactions of the Royal Society of London B: Biological Sciences* 353, 633–666.
- Donoghue, P.C., Forey, P.L., Aldridge, R.J., 2000. Conodont affinity and chordate phylogeny. *Biological Reviews* 75, 191–251.
- Donoghue, P.C., Purnell, M.A., 1999. Growth, function, and the conodont fossil record. *Geol-*

ogy 27, 251–254.

Dray, S., Dufour, A.B., Chessel, D., 2007. The ade4 package-II: Two-table and K-table methods. *R news* 7, 47–52.

Epstein, A.G., Epstein, J.B., Harris, L.D., 1977. Conodont color alteration: an index to organic metamorphism.

Girard, C., Renaud, S., 2011. The species concept in a long-extinct fossil group, the conodonts. *Comptes Rendus Palevol* 10, 107–115.

Girard, C., Renaud, S., 2008. Disentangling allometry and response to Kellwasser anoxic events in the Late Devonian conodont genus *Ancyrodella*. *Lethaia* 41, 383–394.

Girard, C., Renaud, S., 2007. Quantitative conodont-based approaches for correlation of the Late Devonian Kellwasser anoxic events. *Palaeogeography, Palaeoclimatology, Palaeoecology* 250, 114–125. <https://doi.org/10.1016/j.palaeo.2007.03.007>

Girard, C., Renaud, S., Korn, D., 2004a. Step-wise morphological trends in fluctuating environments: evidence in the Late Devonian conodont genus *Palmatolepis*. *Geobios* 37, 404–415.

Girard, C., Renaud, S., Sérayet, A., 2004b. Morphological variation of *Palmatolepis* Devonian conodonts: species versus genus. *Comptes Rendus Palevol* 3, 1–8.

Goudemand, N., Orchard, M.J., Urdy, S., Bucher, H., Tafforeau, P., 2011. Synchrotron-aided reconstruction of the conodont feeding apparatus and implications for the mouth of the first vertebrates. *Proceedings of the National Academy of Sciences* 108, 8720–8724.

Hallam, A., 1996. Major bio-events in the Triassic and Jurassic, in: Global Events and Event Stratigraphy in the Phanerozoic. Springer, pp. 265–283.

Hammer, Ø., Harper, D.A.T., Ryan, P.D., 2001. Paleontological statistics software: Package for education and data analysis. *Palaeontologia Electronica*.

Hunt, G., 2007. Evolutionary Divergence in Directions of High Phenotypic Variance in the

Ostracode genus *Poseidonamicus*. Evolution 61, 1560–1576.

Joachimski, M.M., Pancost, R.D., Freeman, K.H., Ostertag-Henning, C., Buggisch, W., 2002. Carbon isotope geochemistry of the Frasnian–Famennian transition. Palaeogeography, Palaeoclimatology, Palaeoecology 181, 91–109.

Joachimski, M.M., von Bitter, P.H., Buggisch, W., 2006. Constraints on Pennsylvanian glacioeustatic sea-level changes using oxygen isotopes of conodont apatite. Geology 34, 277–280.

Jones, D., 2009. Directional evolution in the conodont *Pterospathodus*. Paleobiology 35, 413–431.

Jones, D., Purnell, M.A., von Bitter, P.H., 2009. Morphological criteria for recognising homology in isolated skeletal elements: comparison of traditional and morphometric approaches in conodonts. Palaeontology 52, 1243–1256.

Kent, D.V., Olsen, P.E., Muttoni, G., 2017. Astrochronostratigraphic polarity time scale (APTS) for the Late Triassic and Early Jurassic from continental sediments and correlation with standard marine stages. Earth-science reviews 166, 153–180.

Klapper, G., Foster Jr, C.T., 1993. Shape analysis of Frasnian species of the Late Devonian conodont genus *Palmatolepis*. Memoir (The Paleontological Society) 1–35.

Kuhl, F.P., Giardina, C.R., 1982. Elliptic Fourier features of a closed contour. Computer graphics and image processing 18, 236–258.

Lavit, C., Escoufier, Y., Sabatier, R., Traissac, P., 1994. The act (statis method). Computational Statistics & Data Analysis 18, 97–119.

Levins, R., Lewontin, R.C., 1985. The dialectical biologist. Harvard University Press.

Martinez-Perez, C., Purnell, M., Rayfield, E., Donoghue, P., 2016. Shedding light into the function of the earliest vertebrate skeleton, in: EGU General Assembly Conference Abstracts. p. 17108.

Mazza, M., Cau, A., Rigo, M., 2012a. Application of numerical cladistic analyses to the Carnian–Norian conodonts: a new approach for phylogenetic interpretations. *Journal of Systematic Palaeontology* 10, 401–422.

Mazza, M., Furin, S., Spötl, C., Rigo, M., 2010. Generic turnovers of Carnian/Norian conodonts: Climatic control or competition? *Palaeogeography, Palaeoclimatology, Palaeoecology* 290, 120–137.

Mazza, M., Martínez-Pérez, C., 2016. Evolutionary convergence in conodonts revealed by Synchrotron-based Tomographic Microscopy. *Palaeontologia Electronica* 19, 1–11.

Mazza, M., Martinez-Perez, C., 2015. Unravelling conodont (Conodonta) ontogenetic processes in the Late Triassic through growth series reconstructions and X-ray microtomography. *Bollettino della Società Paleontologica Italiana* 54, 161–186.

Mazza, M., Nicora, A., Rigo, M., (in press). *Metapolygnathus parvus* Kozur, 1972 (Conodonata): a potential primary marker for the Norian GSSP (Upper Triassic). *Bollettino della Società Paleontologica Italiana*. <https://doi.org/10.4435/BSPI.2018.06>

Mazza, M., Rigo, M., Gullo, M., 2012b. Taxonomy and biostratigraphic record of the Upper Triassic conodonts of the Pizzo Mondello section (western Sicily, Italy), GSSP candidate for the base of the Norian. *Rivista Italiana di Paleontologia e Stratigrafia* 118, 85–130.

Mosher, L.C., 1968. Evolution of Triassic platform conodonts. *Journal of Paleontology* 42, 947–954.

Murdock, D.J., Sansom, I.J., Donoghue, P.C., 2013. Cutting the first ‘teeth’: a new approach to functional analysis of conodont elements, in: Proc. R. Soc. B. The Royal Society, p. 20131524.

Murphy, M.A., Cebecioglu, M.K., 1984. The *Icriodus steinachensis* and *I. claudiae* lineages (Devonian conodonts). *Journal of Paleontology* 1399–1411.

Murphy, M.A., Springer, K.B., 1989. Morphometric study of the platform elements of

*Amydrotaxis praejohnsoni* n. sp.(Lower Devonian, Conodonts, Nevada). Journal of Paleontology 63, 349–355.

Muttoni, G., Kent, D.V., Olsen, P.E., Di Stefano, P., Lowrie, W., Bernasconi, S.M., Hernández, F.M., 2004. Tethyan magnetostratigraphy from Pizzo Mondello (Sicily) and correlation to the Late Triassic Newark astrochronological polarity time scale. Geological Society of America Bulletin 116, 1043–1058.

Nicora, A., Balini, M., Bellanca, A., Bertinelli, A., Bowring, S.A., Di Stefano, P., Dumitrica, P., Guaiumi, C., Gullo, M., Hungerbuehler, A., others, 2007. The Carnian/Norian boundary interval at Pizzo Mondello (Sicani Mountains, Sicily) and its bearing for the definition of the GSSP of the Norian Stage. Albertiana 36, 102–129.

Orchard, M.J., 2014. Conodonts from the Carnian-Norian boundary (Upper Triassic) of Black Bear Ridge, Northeastern British Columbia: Bulletin 64. New Mexico Museum of Natural History and Science.

Orchard, M.J., 2013. Five new genera of conodonts from the Carnian-Norian boundary beds of Black Bear Ridge, northeast British Columbia, Canada. The Triassic system: New Mexico Museum of Natural History and Science Bulletin 61, 445–457.

Pálfy, J., Demény, A., Haas, J., Carter, E.S., Görög, Á., Halász, D., Oravecz-Scheffer, A., Hetényi, M., Márton, E., Orchard, M.J., 2007. Triassic–Jurassic boundary events inferred from integrated stratigraphy of the Csövár section, Hungary. Palaeogeography, Palaeoclimatology, Palaeoecology 244, 11–33.

Purnell, M.A., 1994. Skeletal ontogeny and feeding mechanisms in conodonts. Lethaia 27, 129–138.

Purnell, M.A., Donoghue, P.C., Aldridge, R.J., 2000. Orientation and anatomical notation in conodonts. Journal of Paleontology 74, 113–122.

Renaud, S., Auffray, J.-C., Michaux, J., 2006. Conserved Phenotypic Variation Patterns, Evolution along Lines of Least Resistance, and Departure Due to Selection in Fossil Ro-

dents. *Evolution* 60, 1701–1717.

Renaud, S., Girard, C., 1999. Strategies of survival during extreme environmental perturbations: evolution of conodonts in response to the Kellwasser crisis (Upper Devonian).

*Palaeogeography, Palaeoclimatology, Palaeoecology* 146, 19–32.

Rigo, M., Mazza, M., Karádi, V., Nicora, A., 2018. New Upper Triassic Conodont Biozonation of the Tethyan Realm, in: *The Late Triassic World*. Springer, pp. 189–235.

Rigo, M., Preto, N., Roghi, G., Tateo, F., Mietto, P., 2007. A rise in the carbonate compensation depth of western Tethys in the Carnian (Late Triassic): deep-water evidence for the Carnian Pluvial Event. *Palaeogeography, Palaeoclimatology, Palaeoecology* 246, 188–205.

Rigo, M., Trotter, J.A., Preto, N., Williams, I.S., 2012. Oxygen isotopic evidence for Late Triassic monsoonal upwelling in the northwestern Tethys. *Geology* 40, 515–518.

Ritter, S.M., 1989. Morphometric patterns in Middle Triassic *Neogondolella mombergensis* (Conodonta), Fossil Hill, Nevada. *Journal of Paleontology* 63, 233–245.

Robert, P., Escoufier, Y., 1976. A unifying tool for linear multivariate statistical methods: the RV-coefficient. *Applied statistics* 257–265.

Roghi, G., Gianolla, P., Minarelli, L., Pilati, C., Preto, N., 2010. Palynological correlation of Carnian humid pulses throughout western Tethys. *Palaeogeography, Palaeoclimatology, Palaeoecology*, *Palaeoecology* 290, 89–106.

Roghi, G., Mirro, P., Dalla Vecchia, F.M., 1995. Contribution to the conodont biostratigraphy of the Dolomia di Forni (Upper Triassic, Carnian, NE Italy). *Memorie di Scienze Geologiche Universita di Padova* 47, 125–133.

Rohlf, F.J., 2007. tpsRelw version 1.45. Department of Ecology and Evolution, State University of New York, Stony Brook.

Rohlf, F.J., 2006. tpsDig, version 2.10. Department of Ecology and Evolution, State Universi-

ty of New York, Stony Brook.

Rohlf, F.J., Marcus, L.F., 1993. A revolution morphometrics. Trends in Ecology & Evolution 8, 129–132.

RStudio Team, 2015. RStudio: integrated development for R. RStudio, Inc., Boston, MA URL <http://www.rstudio.com>.

Schluter, D., 1996. Adaptive radiation along genetic lines of least resistance. Evolution 50, 1766–1774.

Siahsarvie, R., 2012. Comparaison de la divergence morphologique et génétique chez la souris domestique au cours de son expansion géographique (in French) (PhD Thesis). Montpellier 2.

Simms, M.J., Ruffell, A.H., 1990. Climatic and biotic change in the late Triassic. Journal of the Geological Society 147, 321–327.

Sun, Y., Joachimski, M.M., Wignall, P.B., Yan, C., Chen, Y., Jiang, H., Wang, L., Lai, X., 2012. Lethally hot temperatures during the Early Triassic greenhouse. Science 338, 366–370.

Thioulouse, J., Chessel, D., 1987. Les analyses multitableaux en écologie factorielle. I: De la typologie d'état à la typologie de fonctionnement par l'analyse triadique (in French). Acta Oecologica Oecologia Generalis 8, 463–480.

Tolmacheva, T., Löfgren, A., 2000. Morphology and paleogeography of the Ordovician conodont *Paracordylodus gracilis* Lindström, 1955: comparison of two populations. Journal of Paleontology 74, 1114–1121.

Trotter, J.A., Williams, I.S., Barnes, C.R., Lécuyer, C., Nicoll, R.S., 2008. Did cooling oceans trigger Ordovician biodiversification? Evidence from conodont thermometry. Science 321, 550–554.

Trotter, J.A., Williams, I.S., Nicora, A., Mazza, M., Rigo, M., 2015. Long-term cycles of Tri-

assic climate change: a new  $\delta^{18}\text{O}$  record from conodont apatite. *Earth and Planetary Science Letters* 415, 165–174.

Wenzel, B., Lécuyer, C., Joachimski, M.M., 2000. Comparing calcite and phosphate oxygen isotope paleothermometers— $\delta^{18}\text{O}$  of Silurian brachiopods and conodonts. *Geochim. Cosmochim. Acta* 64, 1859–1872.

Wickham, H., 2016. *ggplot2: elegant graphics for data analysis*. Springer.



## **Chapitre 4 :**

# **Forces évolutives et morphologie des conodonts: impact de l'environnement et des contraintes développementales**

Comme détaillé dans le chapitre 2, l'évolution est le produit de deux grands facteurs: l'environnement et le développement selection (Alberch, 1980; Alberch and Gale, 1985; Goodwin, 1988; Gould and Lewontin, 1979; Oster et al., 1988, 1988; Webster and Goodwin, 1982). Mais lorsque l'on s'intéresse à l'évolution morphologique d'un organe, faire la part des choses et déterminer l'impact de ces deux facteurs n'est pas chose aisée. D'un côté, la sélection naturelle filtre des phénotypes naturellement présents dans une population en fonction de leur valeur adaptative dans un environnement donnée. Ainsi, toute modification de l'environnement pourra modifier les modalités de sélection, résultant en un changement morphologique. D'un autre côté, la croissance des organismes est contrainte par les lois universelles de la physique, la chimie et la géométrie, ce qui limite les formes possibles qu'un organe peut prendre, ce qui peut canaliser l'évolution dans certaines directions privilégiées. Ainsi, face à une évolution morphologique donnée, comment déterminer si l'évolution est «simplement» canalisée par les contraintes développementales, ou véritablement une réponse à une pression de sélection? Pour répondre à cette question, il est utile d'étudier l'évolution en temps profond, seul moyen d'observer les mécanismes en action sur de longs intervalles de temps et les réponses à des variations climatiques majeures (Gould, 1980). Il est possible pour cela d'observer les patrons de variation morphologique au sein des populations, ainsi que l'arrangement des populations entre elles. Cela permet de mettre en évidence les distributions des phénotypes «réalisés», et ainsi de mettre en lumière leurs contours, séparant les zones «non-réalisées». Ces zones non réalisées peuvent alors correspondre à des phénotypes à plus faible valeur sélective, ou à des phénotypes impossibles à générer lors du développement. La distinction entre les deux peut alors être faite observant la réponse des populations à des changements environnementaux, et les changements de morphologies associées à ces nouvelles conditions.

Dans ce chapitre, les morphologies de deux assemblages d'éléments conodontes distants dans le temps, l'espace et l'évolution sont comparées pour démêler les effets de l'environnement et du développement dans leur évolution. Des patrons de variation morphologique communs aux deux groupes sont mis en évidence permettent de mettre en lumière un axe principal d'évolution hypothétiquement contraint par le développement des éléments. Mis en lien avec les variations de température se produisant à la même époque, l'évolution semble alors se diriger dans un sens ou dans l'autre le long de cet axe en fonction de l'environnement. La comparaison de ces patrons avec les séries ontogéniques proposées dans la littérature permettent de proposer un possible mécanisme d'hétérochronie, également en lien avec la température.

# **Developmental constraints and water temperature as major evolutionary forces driving the shape of conodont elements**

## **Authors**

Louise Souquet <sup>1\*</sup>, Pauline Guenser<sup>1,2</sup>, Catherine Girard<sup>3</sup>, Michele Mazza<sup>4</sup>, Manuel Rigo<sup>5</sup> and Nicolas Goudemand <sup>1</sup>

<sup>1</sup> Univ Lyon, Ecole Normale Supérieure de Lyon, Centre National de la Recherche Scientifique, Université Claude Bernard Lyon 1, Institut de Génomique Fonctionnelle de Lyon, UMR 5242, 46 Allée d'Italie, F-69364 Lyon Cedex 07, France

<sup>2</sup> Current address: Univ Lyon, CNRS, Université Claude Bernard Lyon 1, Laboratoire d'Écologie des Hydrosystèmes Naturels et Anthropisés, UMR 5023, 3-6 rue Raphaël Dubois – Bâtiments Forel, 69622 Villeurbanne Cedex 43

<sup>3</sup> Institut des Sciences de l'Evolution, Université de Montpellier, UMR5554 CNRS, IRD, EPHE, Place Eugène Bataillon, CC65, 34095 Montpellier Cedex, France

<sup>4</sup> Dipartimento di Scienze della Terra “Ardito Desio”, Università degli Studi di Milano, Via Mangiagalli 34, 20133 Milan, Italy

<sup>5</sup> Department of Geosciences, University of Padova, Via G. Gradenigo 6, 35131 Padova, Italy

\* Corresponding author

## **Keywords**

Development, environment, evolution, conodonts, geometrics morphometrics, fossils

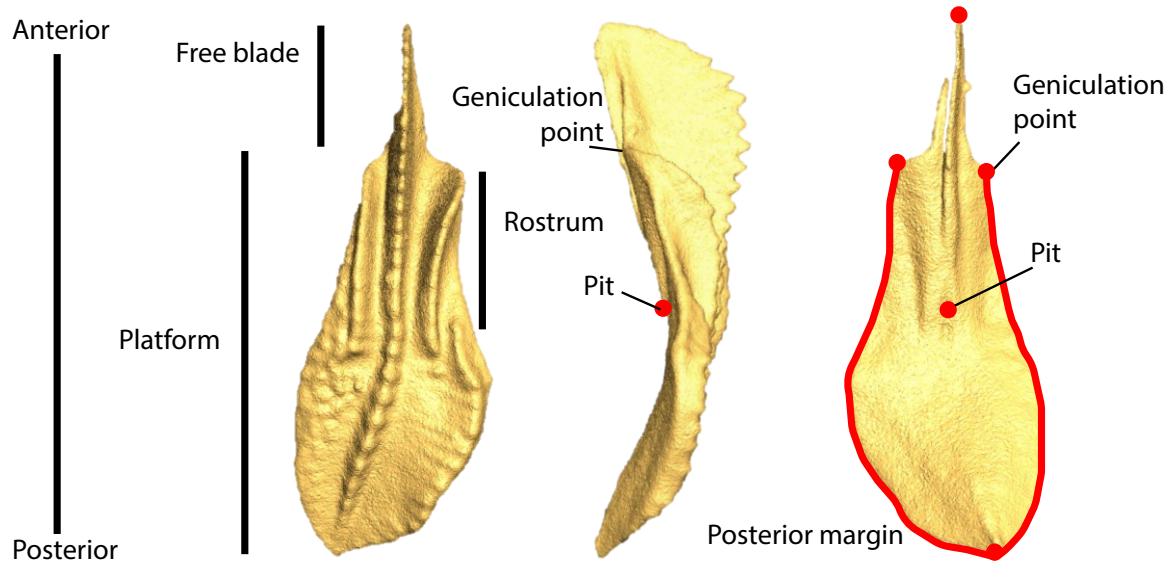
## 1. Introduction

The incredible diversity of organismal shapes and their evolution have always been a source of wonder and questions for biologists (His, 1888; Thompson 1917; Turing 1952; Foote 1997; Klingenberg 2010; Raff 2012). The term “evolution” actually designates both the empirically observed patterns of phenotypic change of an organism, and the processes that produce these patterns (Gingerich, 2001). Thanks to the recent rise of 3d imaging and shape characterization technics such as geometric morphometrics, a wealth of morphological data can be relatively easily obtained and associated patterns of phenotypic change can be analysed in detail. Yet, untangling the underlying evolutionary processes and their drivers remains elusive. Evolution is the result of two main processes: development and natural selection (Gould and Lewontin 1979 ; Alberch 1980 , 1989 ; Webster and Goodwin 1982 ; Alberch and Gale 1985 ; Goodwin 1988 ; Oster et al. 1988 ; Kauffman 1993). On one hand, within the now classical framework of the Neo-Darwinian synthesis, evolution is thought as the diffusion among a population of one or several selected characters that would confer a better fitness to its bearer. Primary variation within that population is assumed to be random and isotropic, that is equal in all directions, and the main driver of evolution is natural selection, which biases the modification of the population over several generations in one direction or the other. As a consequence, extrinsic (environmental) factors are expected to play a major role in evolution through the pressure exerted on organisms, whereas intrinsic (developmental) factors produce the primary variation but do not bias it significantly. In this line, many examples of morphological shifts related to environmental changes have been evidence in several families, including the famous example of the Galapagos finches whose beaks changed in size and shape in response to environmental changes and hence shifts in food resources (Darwin 1859, Grant & Grant 1989). On the other hand, the recent advances in evolutionary developmental biology (evo-devo) have challenged the Neo-Darwinian conception of evolution and evidenced that selection may not be the only significant source of non-randomness in evolutionary patterns: development does bias phenotypic variation and hence morphological evolution (Reiss *et al.*, 2008). In 1980, Alberch summarized this idea saying that “in evolution, selection may decide the winner of a given game but development non-randomly defines the players”. Indeed, the set of theoreti-

cally possible forms is bound by developmental ‘constraints’: e.g. the basic rules of physics, geometry and chemistry constrain organismal growth (Thompson 1917). Hence both intrinsic and extrinsic factors are expected to drive evolution. Yet, the respective roles of both types of factors are still a matter of debate.

To answer this question, studies in deep time are pivotal because they are the only way to provide evidence for “the actual course of life’s history” (Gould, 1980), in particular at times of great environmental changes, such as those observed to be contemporaneous of major biotic turnovers, i.e. when extrinsic factors may be expected to have had the largest impact on evolution. Abundant data about paleo-environmental fluctuations is nowadays available, which makes it possible to look for correlations between environmental parameters and organismal traits in an ever increasing level of detail. Yet, studying development in deep time is challenging, mostly because of the common lack of paleogenetic data and the impossibility to run developmental biology experiments. However, it is possible to infer developmental constraints indirectly from the fossil record (Urdy et al., 2013). One way is to analyse the phenotypic variation within populations to evidence the distribution of realized (observed) phenotypes in generic morphospace, and thereby the one of unrealized and possibly impossible ones. The constraints lie at the boundary between these two distributions. In this study, we explore the patterns of within-population variation and their evolution in assemblages of conodont elements during intervals of significant climatic changes. We selected conodont elements as our fossil model system because their fossil record combines the advantages of displaying: (1) one of the best resolution in time and space of any fossil, which allows, and this is critical, comparisons with commonly fast pacing environmental changes; (2) a ca. 300 Ma range (from Late Cambrian to Late Triassic), that encompasses several intervals of mass extinctions; and (3) relatively large populations throughout, which allows to quantify variation in a statistically meaningful way. Furthermore their high evolutionary rates have made them a standard for many biochronological scales, which means they allow for a direct estimation of time; and the resistance of their enamel-like crown tissue to taphonomic processes has rendered them invaluable for the reconstruction of paleo-environments via the techniques of geochemistry.

## Early Carboniferous (*Siphonodella*)



## Late Triassic (*Epigondolella*)

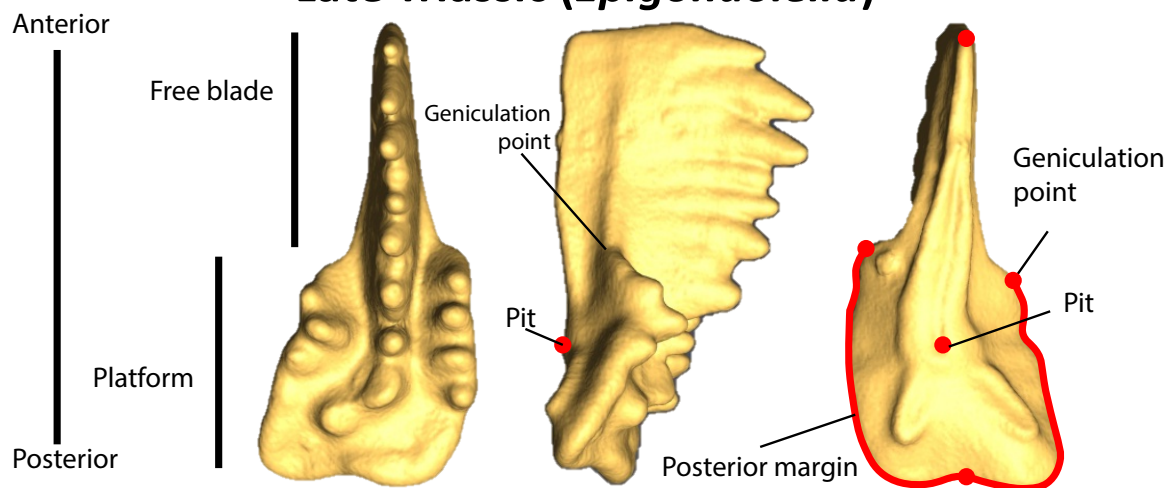


**Figure1:** P1 conodont elements in the three standard views with anatomical vocabulary and location of the used landmarks and sliding landmarks curves. The illustrated specimen belongs to *S. cooperi* for Carboniferous and *E. rigoi* for Triassic.

Conodonts are extinct marine jawless vertebrates (Samson 1992; Aldridge *et al.*, 1993; Purnell 1995; Purnell *et al.*, 1995; Donoghue *et al.*, 2000; Murdock *et al.*, 2013; Janvier 2015, see also Turner *et al.*, 2010). Their phosphatic feeding structures, called conodont elements, constitute most of their abundant fossil record. These elements are widely distributed and highly abundant in marine sedimentary rocks from the Late Cambrian to the Late Triassic. Their bilaterally symmetrical feeding apparatus was usually composed of 15 elements divided in two

groups: an anterior (rostral) set of ‘ramiform’ elements that they probably used to grasp food; and two pairs of posterior (dorso-caudal) elements that were probably used to process the food (e.g. Donoghue *et al.*, 1999; Goudemand *et al.*, 2011). The pair of elements occupying the most dorso-caudal position, the so-called P<sub>1</sub> elements (following Purnell *et al.*, 2000), display the highest evolutionary rates and experienced major morphological changes (Sweet, 1988). For this reason, conodont P1 elements have been the focus of most conodont studies, and they are considered an invaluable tool of (and are being used extensively in) biostratigraphy.

Conodont elements were grown by outer-apposition of apatite lamellae during the entire life of the animal (Sweet 1980; Purnell 1994; Donoghue 1998; Donoghue *et al.*, 2007). This mode of growth induces, among other morphological changes, a constant addition of new denticles on the element’s blade (see Figure X), which partly explains the spectacular variation in size and shape that can be observed within an assemblage of specimens of any conodont species (Mazza *et al.*, 2016; Zhuravlev 1995). This ontogenetic variation renders quantitative comparisons of the morphology of conodont elements particularly challenging because of the subsequent lack of biologically homologous landmarks between specimens of the same species (Jones & Purnell 2007; Hogancamp 2016). Nevertheless, several studies already incorporated such a quantitative framework for exploring morphology and evolution in conodonts (e.g. Barnett 1971, 1972; Murphy and Cebecioglu 1984; Murphy and Springer 1989; Ritter 1989; Girard *et al.* 2004a, b; Roopnarine *et al.*, 2004). Because conodont elements are part of the feeding apparatus of conodonts, their diverse morphologies likely reflect putative adaptations to specific diets, and hence their evolution is expected to be largely controlled by environmental factors. Therefore, most of the studies were focused on functional or environmental aspects and, despite their huge potential for deep time evolutionary studies, virtually nothing is known to date about developmental constraints in conodont elements.

In order to test for the existence of generic developmental constraints in conodont elements, we consider here not only one assemblage of conodont elements but two conodont assemblages (or groups of assemblages) that are separated by 200 Ma of evolution: an Early Carboniferous assemblage of siphonodellids and a Late Triassic assemblage of ‘epigondolel-

lids'. Both assemblages belong to the suborder Ozarkodinina (Dzik 1976) and share sufficient morphological similarities to be compared. Based on the suprageneric classification of Donoghue et al 2008, these assemblages belong to two distinct superfamilies that likely bifurcated in the Ordovician, which is about 100 Ma before the appearance of siphonodellids. In both assemblages, the  $P_1$  elements are segminiplanate (elements with one anterior and one posterior process), with a variably ornamented platform and a relatively high blade that is partly free at the anterior end (Fig. 1). This ensures that we can easily combine all samples in the same morphometric analysis (see Material and Methods), and compare their shapes within the same morphospace.

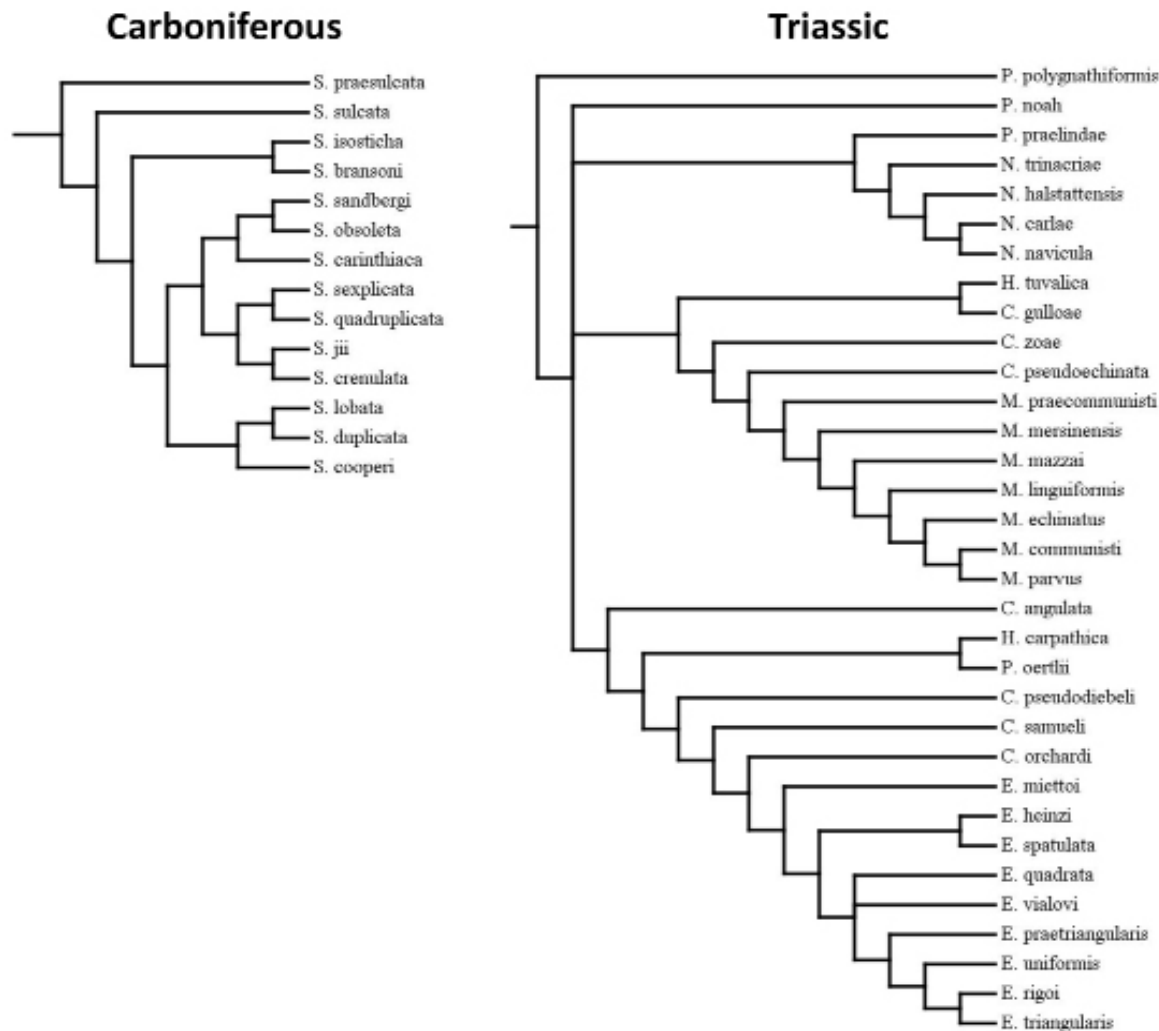


**Figure 2:** Simplified phylogenetic tree for the species considered in this study for Carboniferous (left) and for Triassic (right) (modified after Mazza et al. (2012) and Sandberg et al., (1978)). The taxonomy has been modified according to recent updates.

The first assemblage is composed of closely related species of *Siphonodella* from lower Tournaisian (Carboniferous) rocks of Montagne Noire, France. The second assemblage is composed of closely related species of *Carnepigondolella*, *Epigondolella*, *Hayashiella* and *Metapolygnathus* from upper Triassic rocks of Pizzo Mondello, Sicily, Italy. For both assemblages, phylogenetic hypotheses were available in the literature and we retained the ones we considered most likely and updated them using the latest taxonomical revisions (see Fig.2). Environmentally speaking, the two considered time intervals are characterized by a global shift in marine seawater temperature of similar amplitude but occurring in opposite direction.

## 2. Material & Methods

### *Material and environmental context*

The Carboniferous material comes from the Puech de la Suque section in the Montagne Noire, France, and is currently housed in the collections of the Institut des Sciences de l'Evolution de Montpellier, France. It includes elements of Early Carboniferous age, all belonging to the genus *Siphonodella*. Eight species have been identified: *Siphonodella praesulcata*, *S. sulcata*, *S. bransoni*, *S. duplicata*, *S. carinthiaca*, *S. isosticha*, *S. quadruplicata* and *S. cooperi* (see Table 1). The corresponding studied interval is characterized by a radiation event (Sandberg et al., 1978) that follows the biotic crisis of the Hangenberg event (Walliser 1996; Caplan & Bustin 1998). It corresponds to the very onset of the transition from a Devonian greenhouse to the ice-house modes of the Carboniferous and Permian (Buggish et al., 2008). In the Montagne Noire, the interval is marked by a regression-transgression cycle, with a shallowing into the photic zone followed by a slow deepening beyond the photic zone (Girard 1994). The stable oxygen isotope ratios ( $\delta^{18}\text{O}$ ) measured on conodont apatite from Europe and Laurentia evidence a mean global negative shift of about one permil during this interval, which corresponds to an average global 4°C warming of the ocean waters (Buggisch et al., 2008). This shift is associated with a coeval 0.5‰ drop of the stable carbon isotope ratio ( $\delta^{13}\text{C}$ ) measured on carbonates (Buggisch et al., 2008) (Fig. 3).

The Triassic material, housed in the collections of the Dipartimento di Scienze della Terra « A. Desio » (Università degli Studi di Milano), is from the Pizzo Mondello section, located in the Sicanes Mounts in Western Sicily, Italy. The elements belong to 4 genera, divided in seven species: *Carnepigondolella pseudodiebeli*, and *C. zoae*; *Hayashiella tuvalica*; *Epigondolella quadrata*, *E. rigoi* and *E. uniformis*; and *Metapolygnathus communisti* (Table 1). The corresponding studied interval spans the Carnian Norian boundary (Late Triassic). This interval corresponds to a major conodont turnover that follows the biotic crisis associated with the Carnian Pluvial Event (Rigo et al., 2007; Mazza et al., 2010). The  $\delta^{13}\text{C}$  record of the Pizzo Mondello section shows a one permil positive shift at the base of the CNB interval (Muttoni et al., 2004; Mazza et al., 2010). Locally there is no evidence for a drop in seawater temperatures (the  $\delta^{18}\text{O}$  signal is constant) or for variation of sea level, but at the wider scale of the sub-tropical Tethys, there is evidence of a 6°C cooling of the ocean (a positive shift of 1.5‰ in the  $\delta^{18}\text{O}$  signal; Trotter et al., 2015) (Fig. 3).

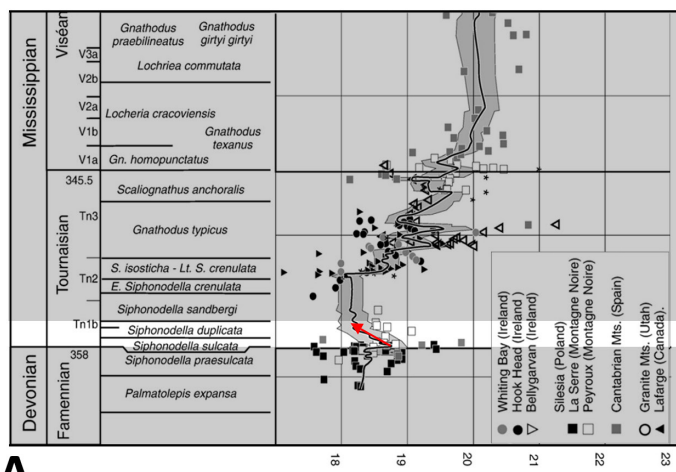
For the Carboniferous group, no cladistics-based phylogenetic hypotheses have been proposed so far. Following the most recurrent view (Sandberg et al., 1978, Sweet 1980), *S. praesulcata* would be the rootstock of all *siphonodellids*. A first radiation would have led to the appearance of *S. sulcata*, *S. duplicata* and *S. cooperi*. From those species, all the other siphonodellids emerged during a second burst of evolutionary radiation (Fig. 2).

For the Triassic group, our phylogenetic hypothesis (Fig. 2) is based on a cladistics analysis by Mazza et al. (2012). *Paragondolella polygnathiformis* and *P. praelindae* were presumably the only two species to survive the Carnian Pluvial event. They gave rise to the genera *Carnepigondolella* and *Norigondolella*. *Carnepigondolella* itself is a paraphyletic group that branched into, on one hand *Metapolygnathus* and, on the other hand, *Epigondolella*. Recently, Kilic et al (2015) reassigned ‘*Carnepigondolella*’ *tuvalica* to a new genus *Hayashiella*, from which, in their view, all carnepigondolellids stemmed. This is not supported by the analysis of Mazza et al (2012) as *Hayashiella* appears polyphyletic.

In the two groups, all elements are considered adults following the growth stages illustrated by Zhuravlev (1995) and Mazza & Martinez-Perez (2015).

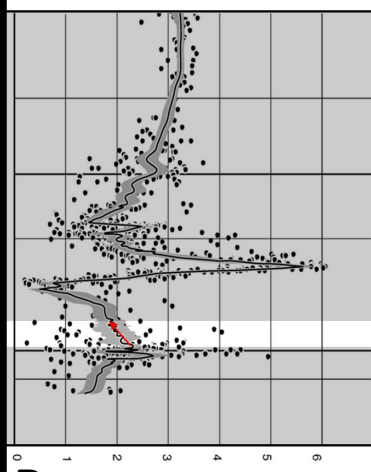
# Carboniferous

$\delta\text{O18}$



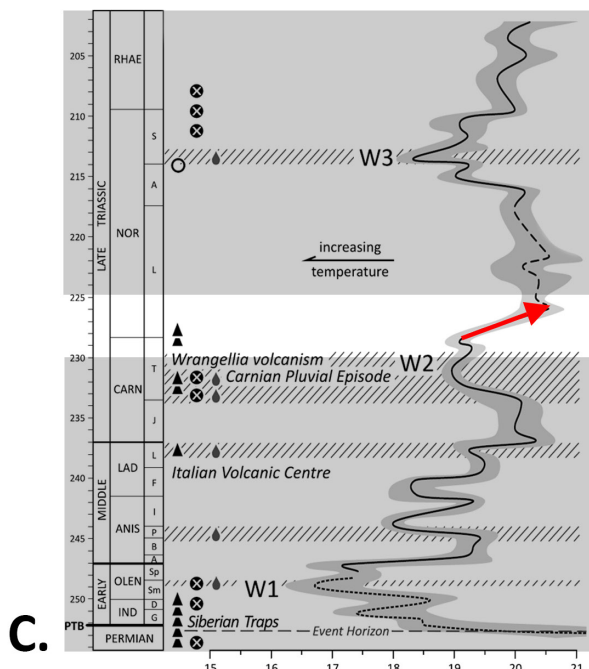
A.

$\delta\text{C13}$

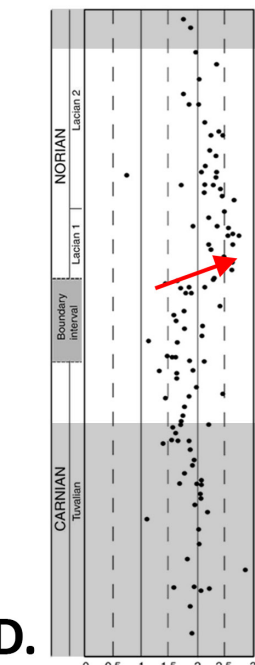


B.

# Triassic



C.



D.

**Figure 3:** Environmental context in the two considered time intervals. AB. Carboniferous environment C. D. Triassic environment. A. C. Global  $\delta\text{O18}$  isotopic curve got on conodont elements B. Global  $\delta\text{C13}$  isotopic data D. Local  $\delta\text{C13}$  isotopic data at Pizzo Mondello. The red arrows highlight the shifts during the considered time periods. Modified after Buggisch et al., 2008, Trotter et al., 2015 and Mazza et al., 2010.

In order to assess the validity of the observed evolutionary patterns across the corresponding evolutionary lineages, we considered additionally the holotypes of all the species that are thought to belong to the genera we analysed, including the species for which we have measured specimens. When the illustrations of the holotypes available from the literature were not appropriate for our analysis, we selected other representative specimens of the corresponding species (see details in Table 2).

### *Digitization*

All the elements were glued on wooden sticks and digitized using an X-ray microtomograph ( $\mu$ CT) Phoenix nanotomeS (AniRA-Immos platform, SFR Biosciences, UMS 3444, ENS Lyon) at  $1\mu\text{m}$  cubic voxel resolution. The element surfaces were reconstructed in 3d and pictures were taken in a standardized aboral view (Fig. 1) using the Amira<sup>®</sup> software (6.3.0). Because there were no systematic differences between sinistral and dextral elements according to a multivariate analysis of variance (MANOVA), data from both orientations were lumped together after first reflecting the dextral elements over the vertical axis.

### *Geometric morphometrics*

To quantify the shape of the elements, seven landmarks and twenty sliding landmarks (Fig. 1) were digitized using TPSDig 2.0 (Rohlf, 2010a). The seven landmarks were placed at the anterior and posterior extremities of the elements, at the growth center of the element (the so-called pit), and at the antero-lateral extremities of the platform called the geniculation points (Fig. 1). Two sets of ten equally-distributed sliding landmarks were digitized on the platform margins from the geniculation points to the posterior extremity, describing the platform outline (Fig. 1).

All measured individuals were subjected to a generalized full Procrustes superimposition using the two sets of landmarks using TPSRelw (Rohlf, 2010b). This procedure scales, translates and rotates all the configurations of landmarks with a least square calculation so that their shape can be compared without any scale or orientation effect. The resulting residuals (Procrustes coordinates) were used as shape variables in the subsequent analyses. Shape deformations along the Principal Components Analysis (PCA) axes were reconstructed using TPSRelw.

### *Statistics*

The Procrustes coordinates were analysed using a PCA on the variance-covariance matrices using the PAST software (Hammer et al., 2001). Shape differences between genera were tested on a set of significant PC axes representing more than 5% of variance using a PER-

MANOVA (non-parametric multivariate analysis of variance based on 9999 permutations) and associated pairwise post-hoc tests.

**Table 1.** Sampling considered in the geometric morphometrics analysis

Species	Age	Sample	Number of elements
			number
<i>Hayashiella tuvalica</i>	Late Carnian	NA15	23
<i>Carnepigondoella zoae</i>	Late Carnian	NA15	22
<i>Carnepigondolella pseudodiebeli</i>	Late Carnian	NA15a	9
		NA16	4
		PM11a	7
<i>Metapolygnathus communisti</i>	Carnian-Norian boundary interval	NA37	24
<i>Epigondolella uniformis</i>	Earliest Norian	NA42	8
<i>Epigondolella rigoi</i>	Early Norian	NA59	21
<i>Epigondolella quadrata</i>	Early Norian	NA60	14
<i>Siphonodella praesulcata</i>	Early Carboniferous	PS17	2
		PS18	1
		PS19	3
		PS20	4
		PS21	3
		PS24	1
<i>Siphonodella sulcata</i>	Early Carboniferous	PS17	6
		PS18	2
		PS19	10
		PS21	1
		PS24	1
		PS26	1
<i>Siphonodella bransoni</i>	Early Carboniferous	PS16	1
		PS17	4
		PS18	1
		PS19	4
		PS20	2
		PS21	2
		PS24	2

<i>Siphonodella duplicata</i>	Early Carboniferous	PS17	2
		PS18	2
		PS19	3
		PS20	2
		PS21	1
		PS24	2
		PS25	3
		PS26	5
		PS27	12
		PS28	2
<i>Siphonodella isosticha</i>	Early Carboniferous	PS25	3
<i>Siphonodella cooperi</i>	Early Carboniferous	PS19	1
		PS25	6
		PS26	5
		PS27	8
		PS28	3
<i>Siphonodella quadruplicata</i>	Early Carboniferous	PS25	1
		PS28	5

**Table 2.** List of holotype considered in the geometric morphometric analysis

Species	Nature	Source
<i>Carnepigondolella angulata</i>	Holotype	(Mazza et al., 2012a) Fig.9A
<i>Carnepigondolella carpathica</i>	Holotype	(Mock, 1979) Pl.1
<i>Carnepigondolella nodosa</i>	Representative specimen	(Mazza et al., 2012b) Pl.2 figs.4a-c
<i>Carnepigondolella orchardi</i>	Representative specimen	(Mazza et al., 2012b) Pl.2 figs. 2a-c
<i>Carnepigondolella pseudodiebeli</i>	Representative specimen	Mazza et al. 2012, Pl. 2 fig. 8
<i>Carnepigondolella pseudoechinata</i>	Representative specimen	(Balini et al., 2010) Pl.2, fig.6
<i>Carnepigondolella samueli</i>	Holotype	(Orchard, 1991) Pl.1, figs.10-12
<i>Carnepigondolella tuvalica</i>	Holotype	(Mazza et al., 2012b) Pl.3, figs.4a-c
<i>Carnepigondolella zoae</i>	Holotype	Orchard 1991
<i>Epigondolella heinzi</i>	Holotype	(Mazza et al., 2012a) Fig. 9C
<i>Epigondolella miettoi</i>	Holotype	(Mazza et al., 2012a) Fig. 9F
<i>Epigondolella praetriangularis</i>	Holotype	(Moix et al., 2007) Pl.1, figs.9;10
<i>Epigondolella quadrata</i>	Holotype	(Orchard, 1991) Pl.2, figs.1-3
<i>Epigondolella rigoi</i>	Holotype	(Noyan and Kozur, 2007) Fig.6.4
<i>Epigondolella spatulata</i>	Representative specimen	(Mazza et al., 2010) Pl.III, figs. 6a-c
<i>Epigondolella triangularis</i>	Representative specimen	(Balini et al., 2010) Pl.4, figs 7a-c
<i>Epigondolella uniformis</i>	Holotype	(Orchard, 1991) Pl.3, figs.1-3
<i>Epigondolella vialovi</i>	Representative specimen	(Balini et al., 2010) Pl.3, figs 6a-c
<i>Metapolygnathus mazzai</i>	Holotype	(Mosher, 1970) Mazza et al., 2012, Pl. 8, Fig. 12
<i>Metapolygnathus communisti</i>	Holotype	(Hayashi, 1968) reillustrat- ed by mazza and co-work- ers(Mazza et al., 2011) Fig.2B
<i>Carnepigondolella gulloae</i>	Holotype	Mazza et al. 2012
<i>Metapolygnathus echinatus</i>	Representative specimen	(Mazza et al., 2012b) Pl.8 figs.7a-c
<i>Metapolygnathus linguiformis</i>	Representative specimen	(Balini et al., 2010) Pl.4, fig.1
<i>Metapolygnathus mersinensis</i>	Holotype	(Moix et al., 2007) Pl.1, fig.14

<i>Metapolygnathus parvus</i>	Holotype	(Kozur, 1972) Pl.6, fig.2
<i>Metapolygnathus praecommunisti</i>	Holotype	(Mazza et al., 2011) Fig.2C
<i>Paragondolella noah</i>	Holotype	(Hayashi, 1968) reillustrated by Mazza and co-workers
		(Mazza et al., 2011) Fig.2A
<i>Paragondolella oertlii</i>	Holotype	(Rigo et al., 2018) Fig.2
<i>Paragondolella polygnathiformis</i>	Representative specimen	(Rigo et al., 2007) Fig.4.6a-c
<i>Paragondolella praelindae</i>	Representative specimen	(Mazza et al., 2012b) Pl.7 figs 13a-c. Sample NA4a
<i>Siphonodella praesulcata</i>	Holotype	Sandberg et al., 1972 Pl.1, fig.3
<i>Siphonodella sulcata</i>	Representative specimen	Sandberg et al., 1972 Pl.2, fig.4
<i>Siphonodella duplicata</i>	Lectotype	Branson & Mehl, 1934
<i>Siphonodella isosticha</i>	Holotype	Cooper, 1939 reillustrated in Klapper 1971 Pl.1, fig.16
<i>Siphonodella jii</i>	Representative specimen	Cigler, 2017 Fig.5.4
<i>Siphonodella cooperi</i>	Paratype	Hass, 1959 Pl.48, fig.35
<i>Siphonodella obsoleta</i>	Representative specimen	Klapper, 1971 Pl.1, fig.25
<i>Siphonodella carinthiaca</i>	Holotype	Schönlaub, 1969 Pl.2 fig.1
<i>Siphonodella sandbergi</i>	Holotype	Klapper, 1966 Pl.4, fig.14
<i>Siphonodella quadruplicata</i>	Representative specimen	Klapper, 1971 Pl.1. fig.24
<i>Siphonodella lobata</i>	Representative specimen	Klapper, 1966 Pl.2, fig.3
<i>Siphonodella crenulata</i>	Holotype	Cooper, 1939 reillustrated in Klapper 1971 Pl.2, fig.14
<i>Siphonodella sexplicata</i>	Representative specimen	Klapper, 1966 Pl.4, fig.18

**Table 3.** Difference of shape between genus in P1 conodont elements. P-values of a peranova on the first four axes of a PCA on the Procrustes coordinates are provided. In bold: significant probabilities ( $P < 0.05$ ).

	<i>Carnepigondolella</i>	<i>Epigondolella</i>	<i>Metapolygnathus</i>	<i>Siphonodella</i>
<i>Carnepigondolella</i>		<b>0.0001</b>	<b>0.0001</b>	<b>0.0001</b>
<i>Epigondolella</i>	<b>0.0001</b>		<b>0.0001</b>	<b>0.0001</b>
<i>Metapolygnathus</i>	<b>0.0001</b>	<b>0.0001</b>		<b>0.0001</b>
<i>Siphonodella</i>	<b>0.0001</b>	<b>0.0001</b>	<b>0.0001</b>	

### 3. Results

#### *Main morphological variations*

Four axes explained more than 5% of the total variance (PC1: 49.82%, PC2: 22.24%, PC3: 8.04%, PC4: 7.29%) in the PCA performed on the Procrustes coordinates (Fig. 4). Based on this set of axes, significant morphological differences were evidenced between the four considered genera (Table 3). PC1, PC2 and PC4 correspond to a gradual variation of the length of the platform relative to the entire element, though associated with distinct trends in the posterior shape of the platform and the relative position of the pit. Along PC1 the anterior extension of the platform is associated with a similar anterior shift of the pit (so that the distance between the pit and the plane of the geniculation points remains approximately the same, relative to the entire element) and a sharpening of the posterior margin (from wide and squared to circular, to narrow and pointy). Along PC2 the anterior extension of the platform is associated with a posterior shift of the pit (so that the distance between the pit and the plane of the geniculation points increases) and a corresponding unsharpening of the posterior margin (from pointy to circular to squared). Along PC4 the platform extends mostly laterally: a shorter free blade is associated with a wider, biconvex platform whose maximal width is reached more posteriorly (teardrop shaped), whereas a longer free blade is associated with a narrower, and posterior constricted (partly biconcave) platform. Finally PC3 corresponds to variation in the lateral bending of the element: the platform of straight elements tends to be subsymmetrical, with biconvex lateral margins, whereas the inner side of the platform of bent elements is narrower and its lateral margin is straighter.

Interestingly, the first two principal components seem to highlight a positive correlation between the relative distance of the pit to the posterior margin and the sharpening of the posterior margin, quantified as the curvature of the posterior margin at the posterior end (flat to circular to pointy geometry corresponding to a gradient from low to high curvature at the tip) (Fig. 4). In other words, when the pit is closer to the posterior margin, the posterior margin tends to be more squared; when the pit is more anteriorly located, the posterior margin tends to taper; in between, the posterior margin is sub-circular.

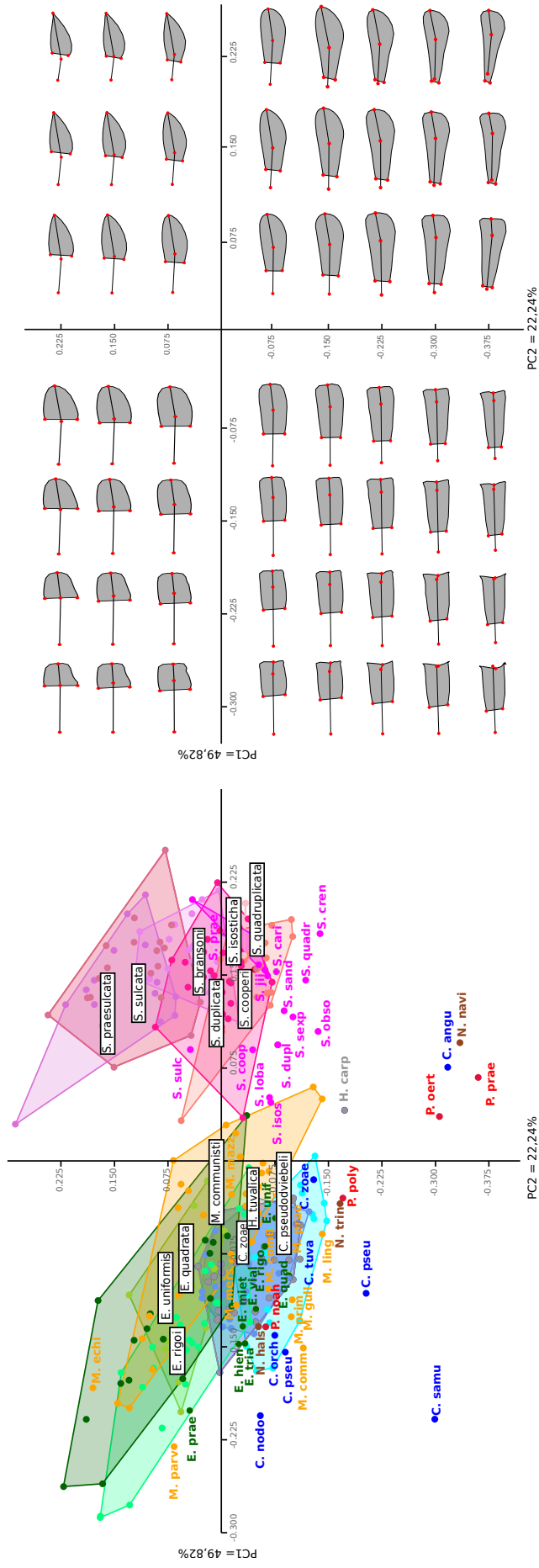


**Figure 4:** Shape variations of the dataset. Position of the species in the two first axis of the component analysis (left) and associated shape deformation (right). Convex hulls highlight the variability of the considered dataset for Carboniferous (Siphonodella = pink colors) and Triassic (Paragondolella = red; Norigondolella = brown; Epigondolella = blue; Metapolygnathus = green colors). The lonely points associated with a short name correspond to the holotypes of the species.

### *Shape changes in phylogeny*

The two groups are well separated on the first PC axis with the Triassic group corresponding to negative values and the Carboniferous group to positive values (Fig. 4). The Carboniferous species are characterized by an ovate platform with a pointed posterior extremity. The Triassic species are characterized by an oblong to sub-cuneate platform with a rounded to sub-squared posterior extremity. As mentioned above, a pit located posteriorly and aligned with the antero-posterior axis of the conodont element is associated with a squared platform. A pit located more anteriorly, and offset from the antero-posterior axis of the conodont element is associated with an elongated, pointy platform. This morphological trend highlights the main division between the two groups and is consistent with the diagnoses of the considered Carboniferous and Triassic genera.

Within both groups, interspecific variation tends to align with PC2, although most species cannot be differentiated using PC2 only (Fig. 4). PC2 is characterized by a change in the position of the pit relative to the entire element that is opposed to the movement of the anterior end of the platform.

Furthermore, for both groups, the inferred order of appearance of the considered species seems to be correlated with PC2. For the Carboniferous group, *S. praesulcata* and *S. sulcata* correspond to the PC2 maxima of the group, whereas *S. cooperi* and *S. quadruplicata* correspond to the PC2 minima. Similarly, in the Triassic group, *Carnepigondolella pseudodiebeli* corresponds to the PC2 minima and *Epigondolella uniformis* to the PC2 maxima.

The same trends are observed when considering the holotypes of all species included in those intervals, not only the species for which we analysed the intraspecific variation. The position of the species in the morphospace is strongly correlated with phylogeny (permutation test; two groups: p-value<0,001; Carboniferous group: p-value=0,0093; Triassic group: p-value=0,0002). Note that the holotypes of the latter species are offset in the PC1-PC2 morphospace from the assemblages we measured (Fig. 4). This can be partly explained by the fact the digitization of the landmarks on the holotypes was based on photographs from the literature, hence without being able to control for the orientation, and for some without access to an aboral view,

which meant guessing the position of the pit from the position of the cusp in oral view. It may also be due to the fact that the holotypes are from a different region or a slightly different time interval as the elements we measured (most of the holotypes were sampled in North America). This suggests that the types of the species considered here have a slightly broader range in the PC1-PC2 morphospace than what the material analysed in this study can possibly capture. Although we analysed only elements that are considered typical, note that they can be typical on the basis of other traits than the ones captured by the first two principal components and/or this particular set of landmarks. When considered the ellipses corresponding to the inferred 95% variance of the species present in our dataset, the holotypes are included in the range of variation of their corresponding species, allowing interpretation of their relative position. Finally note that the observed trend in the Triassic group involves two separate lineages, indicating parallel evolution. This strongly supports our assumption that this trend is not driven by random walk.

Both groups parallel an environmental shift: the species succession toward lower PC2 values in the Carboniferous group is associated with a coeval (from *S. sulcata* Zone to Late *S. duplicita* Zone) 4°C warming of the oceans (Fig. 3A); the species succession towards higher PC2 values in the Triassic group as associated with a 6°C cooling of the oceans (Fig. 3C). In other words, evolution in both groups parallels the PC2 axis and is associated with a shift in seawater temperature, lower PC2 values corresponding to higher temperatures.

#### 4. Discussion

##### *A main axis of morphological variation*

Considering this dataset, the main morphological variation of the elements is concentrated in three characters: (1) the relative length of the blade compared to the entire element; (2) the posterior shape of the element: round, pointed or sub-quadratus; (3) the position of the pit (center of growth of the element) along the anteroposterior axis. The first principal component of the morphospace separates the elements of the two time periods, whilst inside each group the

species are distributed along the second principal component.

The pattern of morphological variation between species highlights a common main axis channelling evolution in the two groups, sub-parallel to PC2. Yet, the direction of evolution is different, going in one way (toward positive PC2 values) in all 3 Triassic lineages, but in the other direction in the Carboniferous lineage. In other words, the main axis of evolution during the two considered time intervals is similarly constrained and driven. It is not clear yet whether this reflects the fact that some characters combinations might be impossible to realize during morphogenesis (for example no P1 element with a pointy posterior platform associated to a posterior pit and a short free blade is observed) or whether this reflects similar although opposite, environmental pressures, during these two time intervals. Indeed, as conodont elements are part of the animal feeding apparatus, they are in direct interaction with the environment and therefore they are expected to be under high selective pressures so that their morphology may adapt to the available food resources

Because the groups considered here are distant in phylogeny, time, geography, and possibly ecology, it is likely that the commonality of their evolutionary response to climate change reflects some generic aspect of conodont evolution. We propose here that at least some generic aspect of conodont element's development depends directly or indirectly on seawater temperature, which would explain this commonality between distant taxa. Indeed, as mentioned above, these two time intervals both correspond to a significant shift in the stable oxygen isotope ratio: a global negative shift of 1‰ corresponding to a 4°C warming of the ocean during the Carboniferous considered interval (Fig. 3A), and a global positive shift of 1.5‰ corresponding to a 6°C cooling of the ocean during the Triassic considered interval (Fig. 3B). Such variations, if not as spectacular as others in conodont's history, likely had a significant impact on the corresponding ecosystems. Similarly, Balter et al., (2008) showed that some aspects of the morphology of P<sub>1</sub> elements in Frasnian Famenian palmatolepids correlate with the stable oxygen isotope ratio: during the two cooling episodes of 3 to 7 degrees that they discuss, the posterior part of the platform appears to become pointier, which is, by the way, in accordance with the pattern presented in the present study (further comparisons with the present study are restricted

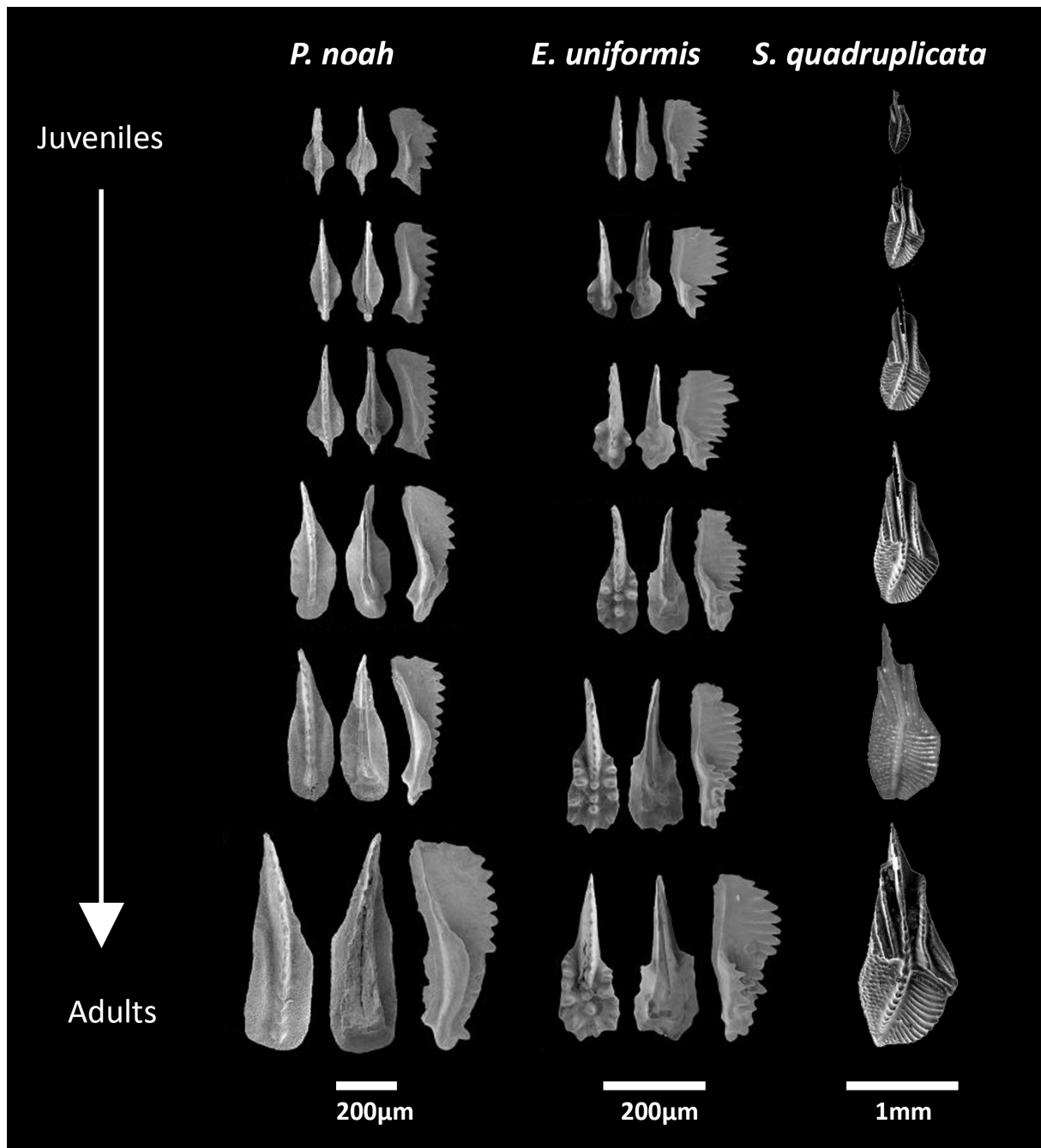


**Figure 5:** Ontogenetic series for *Paragondolella noah* (left), *Epigondolella uniformis* (center) and *Siphonodella quadruplicata* (right). Development from juveniles (top) to adult (bottom) morphologies. Modified after Mazza and Martinez-Perez, (2015) and Zhuravlev et al., (2018).

because Balter et al used an outline analysis and did not analyse the position of the pit). Balter et al (2008) hypothesized the shape variation to be adaptive to a change in the trophic position of palmatolepids during that Frasnian-Fasmenian interval. They further argue that during that very same interval, the morphology of genera *Icriodus* (Girard & Renaud 2007) and *Ancyrodella* (Girard and Renaud 2008) evolved also in a similar way. Environmental conditions and

presumably seawater temperature in particular appear to be important, consistent drivers for the direction of morphological evolution in conodonts. One way to test this hypothesis would be to perform a similar morphometrical analysis to quantify the morphological evolution of the P1 conodont elements in further distinct taxa such as e.g. polygnathids, neognathodids, cypridodelids or idiognathodids in similar or, on the contrary, different environmental contexts.

#### *Heterochrony and effect of temperature on development*

What comes immediately in mind when considering the possible effects of temperature on organismal development is that temperature may affect the growth rates of organisms (Bachmann, 1969; Blaxter, 1969; Brown, 1976, 1975, 1967; Kuramoto, 1975; McLaren, 1965; Needham and Biochemiker, 1931; Reiss, 1989). It is known for instance that some organisms and especially aquatic ectotherms experience temperature-based phenotypic plasticity (Bizuayehu et al., 2015; Drinkwater, 2005; Eagderi et al., 2015; Hollowed et al., 2013; Petitgas et al., 2013; Rowiński et al., 2015) and some of this plasticity may arise from decreased or increased growth rate, which is arguably one the fastest ways to affect morphology at any given size. The dataset we considered here consists only in adult elements (or considered so based on their size and morphology). Hence it is worth discussing the possibility that evolution along the PC2 axis corresponds to modifications of the element's growth rate. Interestingly, the morphologies associated with more positive values along PC2 do indeed bear similarities with those of juvenile elements of the two groups, as described and illustrated in the literature (Fig. 5).

In the considered Triassic taxa, ontogeny has been studied in details by Mazza *et al.* Martinez-Perez (2015): using synchrotron-based imaging techniques, they were able to test hypothetical ontogenetic series by virtually subtracting growth lamellae and analysing the evolution of the morphology within single adult specimens. The ontogeny in these species is marked by a relatively higher growth rate of the platform laterally and of both platform and blade towards the anterior side, which corresponds to a relative posterior shift of the pit. Mazza & Martinez-Perez (2015) already noted that this ontogenetic pattern parallels the evolutionary trend observed in these species: namely a drop in the relative growth rate of the platform to the anterior, and hence an apparent forward shifting of the pit and a relative lengthening of the free blade.

Mazza et al further suggested the evolution of this group in the late Norian occurred by progenesis; that is, an earlier maturation or the acceleration of developmental processes such that the juvenile forms become sexually mature adults. This is also concordant with the evolutionary pattern observed in the present study, although, due to a lack of independent proxy for the age, it is unclear what paedomorphogenetic process (progenesis or neoteny) may have been involved.

Similarly and symmetrically, the evolutionary trend we described for the Carboniferous group toward more anteriorly developed platforms, apparent posterior shift of the pit and relative shortening of the free blade, is also concordant with a heterochronic shift, in this case with peramorphosis; that is, delayed maturation or faster development. Indeed, the ontogenetic series (though not yet confirmed by synchrotron-based analyses) proposed by Zhuravlev (1995, 2018) for siphonodellids (especially *Siphonodella quadruplicata*) seems to display the same morphological changes along ontogeny. This led Zhuravlev to consider that some of the previously described *Siphonodella* species might in fact correspond to different ontogenetic stages of *Siphonodella quadruplicata*.

The role of heterochrony in evolution has been the focus of many debates and controversies: from “heterochrony . . . explains everything” (Mc-Namara, 1997) to “It’s not all heterochrony” (Raff, 1996) (see discussion in McKinney, 1999). Indeed, for a long time, proponents of the modern synthesis had been arguing that natural variation was essentially random and neutral. But with the recognition of the developmental process as source of non-randomness in evolution, the role of heterochrony has been reconsidered. The morphologies produced by heterochrony processes are considered part of the normal phenotypic variation of a species (Cock 1966; Larson 1980; Travis 1981), and if one of those morphologies confers a good enough fitness to its bearer, selection may favour the fixation of this phenotype in a population, and potentially lead to speciation (McNamara, 1982). If this process is repeated across phylogeny, heterochrony may orientate morphological variation of a species along a particular pathway producing directional evolution (Ede 1978; Gould 1980; Alberch 1980; Levinton & Simon 1980; McNamara 1982).

In conodont elements, adulthood is not defined by the age of sexual maturity since we

cannot access this type of information in a fossil. Instead adulthood is estimated using the size of the element, as compared to the size distribution in assemblages. As conodont elements are ever-growing organs, assessing adulthood is not trivial and the distinction between juveniles and adults may be somewhat arbitrary. One way to overcome this problem is to analyse the number and the relative thickness of the growth lamellae (Dzyk, 2008), or their relative strontium content (Shirley et al 2018).

Several authors already suggested a correlation between heterochrony and environmental conditions (Gould 1977; McKinney & Gittleman 1995; McKinney 1994, 1986; Allmon 1994; Wei 2994). In particular, temperature is known to have a major impact on the development of organisms, higher temperatures inducing higher developmental rates (Needham 1931; McLaren 1965; Brown 1967, 1975a,b, 1976; Bachmann 1969; Blaxter 1969; Kuramoto 1975; Reiss 1989). The latter is particularly true for aquatic ectotherms (e.g. Drinkwater 2005; Hollowed et al., 2013; Petitgas et al., 2013; Pörtner et al., 2001; Biziayehu et al., 2015; Eagderi et al., 2015; Rowinski et al., 2015). Therefore, ocean temperature is expected to have played an overriding role in the development of conodont elements, especially in terms of developmental dynamics: acceleration or deceleration of growth. Hence it is maybe not surprising that gradually more juvenile-like morphologies appeared during a cooling event, while gradually more adult-like morphologies appeared during a warming event. Although temperature could have induced physiological changes in conodonts and may alone explain the observed trends, it is also possible that these morphological changes were, as suggested by Balter et al (2008), ecology-driven; that is, via a shift in the composition of food resources, itself likely induced by the temperature change . The considered Late Triassic interval follows the so-called Carnian Pluvial Event, and there is evidence for replacement of most of the coral species, emergence and radiation of new phytoplankton lineages, as well as marine and terrestrial vertebrates including dinosaurs, pterosaurs, turtles, crocodilians and mammals (Roghi *et al.*, 2010; Simms & Ruffel 1990; Hallam 1996). Similarly, the considered early Carboniferous interval follows the well-studied Frasnian-Famennian mass extinction and the Hangenberg event (Walliser 1996; Caplan & Bustin 1998) and it corresponds to a biotic recovery marked by a large diversification event in the tetrapods, actinopterygians, and chondrichthyans (Sallan & Coates 2010).

Conodonts were likely impacted by the disruption of the marine trophic web during both intervals. Because the discussed morphological changes affected similarly very different taxa with potentially different ecologies, this scenario is not the one we favour. Nevertheless, functional analyses could be performed to test for this alternative hypothesis.

If, as we suggest, temperature acted instead as a direct accelerator/decelerator of development in conodont elements, the re-analysis of conodont distributions in terms of facies *versus* morphology may deliver important new insights into their ecology and evolutionary history.

## Acknowledgments

We warmly thank Mathilde Bouchet for her assistance with the microtomography. This research is supported by a French ANR @RAction grant to NG (project “EvoDevOdonto”).

## References

- Alberch, P., 1980. Ontogenesis and morphological diversification. *American zoologist* 20, 653–667.
- Alberch, P., Gale, E.A., 1985. A developmental analysis of an evolutionary trend: digital reduction in amphibians. *Evolution* 39, 8–23.
- Aldridge, R.J., Briggs, D.E.G., Smith, M.P., Clarkson, E.N.K., Clark, N.D.L., 1993. The anatomy of conodonts. *Phil. Trans. R. Soc. Lond. B* 340, 405–421.
- Allmon, W.D., 1994. Patterns and processes of heterochrony in lower Tertiary turritelline gastropods, US Gulf and Atlantic coastal plains. *Journal of Paleontology* 68, 80–95.
- Bachmann, K., 1969. Temperature adaptations of amphibian embryos. *The American Naturalist* 103, 115–130.
- Balini, M., Bertinelli, A., Di Stefano, P., Guaimi, C., Levera, M., Mazza, M., Muttoni, G., Nicora, A., Preto, N., Rigo, M., 2010. The late carnian-rhaetian succession at Pizzo Mondello (Sicani Mountains). *Albertiana* 39, 36–57.
- Balter, V., Renaud, S., Girard, C., Joachimski, M.M., 2008. Record of climate-driven morphological changes in 376 Ma Devonian fossils. *Geology* 36, 907–910.
- Barnett, S.G., 1972. The evolution of *Spathognathodus remsciedensis* in New York, New Jersey, Nevada, and Czechoslovakia. *Journal of Paleontology* 900–917.
- Barnett, S.G., 1971. Biometric determination of the evolution of *Spathognathodus remsciedensis*: a method for precise intrabasinal time correlations in the Northern Appalachians. *Journal of Paleontology* 274–300.

- Bizuayehu, T.T., Johansen, S.D., Puvanendran, V., Toftsen, H., Babiak, I., 2015. Temperature during early development has long-term effects on microRNA expression in Atlantic cod. *BMC genomics* 16, 305.
- Blaxter, J., 1969. Development: Eggs and Larvae, in: *Fish Physiology*. Elsevier, pp. 177–252.
- Brown, H.A., 1976. The time–temperature relation of embryonic development in the northwestern salamander, *Ambystoma gracile*. *Canadian Journal of Zoology* 54, 552–558.
- Brown, H.A., 1975. Temperature and development of the tailed frog, *Ascaphus truei*. *Comparative Biochemistry and Physiology Part A: Physiology* 50, 397–405.
- Brown, H.A., 1967. Embryonic temperature adaptations and genetic compatibility in two allopatric populations of the spadefoot toad, *Scaphiopus hammondi*. *Evolution* 21, 742–761.
- Buggisch, W., Joachimski, M.M., Sevastopulo, G., Morrow, J.R., 2008. Mississippian  $\delta^{13}\text{C}_{\text{carb}}$  and conodont apatite  $\delta^{18}\text{O}$  records—their relation to the Late Palaeozoic Glaciation. *Palaeogeography, Palaeoclimatology, Palaeoecology* 268, 273–292.
- Caplan, M.L., Bustin, R.M., 1999. Devonian–Carboniferous Hangenberg mass extinction event, widespread organic-rich mudrock and anoxia: causes and consequences. *Palaeogeography, Palaeoclimatology, Palaeoecology* 148, 187–207.
- Cock, A.G., 1966. Genetical aspects of metrical growth and form in animals. *The Quarterly Review of Biology* 41, 131–190.
- Darwin, C., 1859. *On the origins of species by means of natural selection*. London: Murray 247.
- Donoghue, P.C., Forey, P.L., Aldridge, R.J., 2000. Conodont affinity and chordate phylogeny. *Biological Reviews* 75, 191–251.
- Donoghue, P.C., Purnell, M.A., 1999. Growth, function, and the conodont fossil record. *Geology* 27, 251–254.
- Donoghue, P.C., Purnell, M.A., Aldridge, R.J., Zhang, S., 2008. The interrelationships of ‘complex’ conodonts (Vertebrata). *Journal of Systematic Palaeontology* 6, 119–153.
- Drinkwater, K.F., 2005. The response of Atlantic cod (*Gadus morhua*) to future climate change. *ICES Journal of Marine Science* 62, 1327–1337.
- Dzik, J., 1976. Remarks on the evolution of Ordovician conodonts. *Acta Palaeontologica Polonica* 21.
- Dzik, J., 2008. Evolution of morphogenesis in 360-million-year-old conodont chordates calibrated in days. *Evolution & development*, 10(6), 769–777.
- Eagderi, S., Poorbagher, H., Parsazade, F., Mousavi-Sabet, H., 2015. Effects of rearing temperature on the body shape of swordtail (*Xiphophorus hellerii*) during the early development using geometric morphometrics. *Poeciliid Research* 5, 24–30.
- Ede, D.A., 1978. *Introduction to developmental biology*. Wiley.
- Foote, M., 1997. The evolution of morphological diversity. *Annual Review of Ecology and Systematics* 28, 129–152.
- Gingerich, P.D., 2001. Rates of evolution on the time scale of the evolutionary process, in: *Microevolution Rate, Pattern, Process*. Springer, pp. 127–144.
- Girard, C., 1994. Conodont biofacies and event stratigraphy across the D/C boundary in the stratotype

- area (Montagne Noire, France). *Courier Forschungsinstitut Senckenberg* 168, 299–309.
- Girard, C., Renaud, S., 2008. Disentangling allometry and response to Kellwasser anoxic events in the Late Devonian conodont genus *Ancyrodella*. *Lethaia* 41, 383–394.
- Girard, C., Renaud, S., 2007. Quantitative conodont-based approaches for correlation of the Late Devonian Kellwasser anoxic events. *Palaeogeography, Palaeoclimatology, Palaeoecology* 250, 114–125.
- Girard, C., Renaud, S., Korn, D., 2004. Step-wise morphological trends in fluctuating environments: evidence in the Late Devonian conodont genus *Palmatolepis*. *Geobios* 37, 404–415.
- Goodwin, B.C., 1988. Morphogenesis and heredity. *Evolutionary processes and metaphors* 145–162.
- Goudemand, N., Orchard, M.J., Urdy, S., Bucher, H., Tafforeau, P., 2011. Synchrotron-aided reconstruction of the conodont feeding apparatus and implications for the mouth of the first vertebrates. *Proceedings of the National Academy of Sciences* 108, 8720–8724.
- Gould, S.J., 1980. The evolutionary biology of constraint. *Daedalus* 39–52.
- Gould, S.J., 1977. *Ontogeny and phylogeny*. Harvard University Press.
- Gould, S.J., Lewontin, R.C., 1979. The spandrels of San Marco and the Panglossian paradigm: a critique of the adaptationist programme. *Proc. R. Soc. Lond. B* 205, 581–598.
- Grant, B.R., Grant, P.R., 1989. Natural selection in a population of Darwin's finches. *The American Naturalist* 133, 377–393.
- Hallam, A., 1996. Major bio-events in the Triassic and Jurassic, in: *Global Events and Event Stratigraphy in the Phanerozoic*. Springer, pp. 265–283.
- Hammer, Ř., Harper, D.A.T., Ryan, P.D., 2001. PAST: Paleontological Statistics Software Package for Education and Data Analysis—Palaeontol. Electron. 4: 9pp.
- Hayashi, S., 1968. The Permian conodonts in chert of the Adoyama Formation, Ashio mountains, central Japan. *Earth Science* 22, 63–77.
- His, W., Murray, J., 1888. On the Principles of Animal Morphology: Letter to Mr. John Murray.
- Hogancamp, N.J., Barrick, J.E., Strauss, R.E., 2016. Geometric morphometric analysis and taxonomic revision of the Gzhelian (Late Pennsylvanian) conodont *Idiognathodus* simulator from North America. *Acta Palaeontologica Polonica* 61, 477–502.
- Hollowed, A.B., Barange, M., Beamish, R.J., Brander, K., Cochrane, K., Drinkwater, K., Foreman, M.G., Hare, J.A., Holt, J., Ito, S., 2013. Projected impacts of climate change on marine fish and fisheries. *ICES Journal of Marine Science* 70, 1023–1037.
- Janvier, P., 2015. Facts and fancies about early fossil chordates and vertebrates. *Nature* 520, 483.
- Jones, D., Purnell, M., 2007. 14 A New Semi-Automatic Morphometric Protocol for Conodonts and Taxonomic Application.
- Kılıç, A.M., Plasencia, P., Ishida, K., Hirsch, F., 2015. The case of the Carnian (Triassic) conodont genus *Metapolygnathus* Hayashi. *Journal of Earth Science* 26, 219–223.
- Klingenberg, C.P., 2011. MorphoJ: an integrated software package for geometric morphometrics. *Molecular ecology resources* 11, 353–357.

- Klingenberg, C.P., 2010. Evolution and development of shape: integrating quantitative approaches. *Nature Reviews Genetics* 11, 623.
- Kozur, H., 1972. Die Conodontengattung *Metopolygnathus* (Hayashi, 1968) und ihr stratigraphischer Wert [Conodont genus *Metopolygnathus* (Hayashi, 1968) and their stratigraphic values] (en Allemand). Institut für Geologie und Paläontologie.
- Kuramoto, M., 1975. Embryonic temperature adaptation in development rate of frogs. *Physiological Zoology* 48, 360–366.
- Larson, A., 1980. Paedomorphosis in relation to rates of morphological and molecular evolution in the salamander *Aneides flavipunctatus* (Amphibia, Plethodontidae). *Evolution* 34, 1–17.
- Levinton, J.S., Chris, M.S., 1980. A critique of the punctuated equilibria model and implications for the detection of speciation in the fossil record. *Systematic Biology* 29, 130–142.
- Mazza, M., Cau, A., Rigo, M., 2012a. Application of numerical cladistic analyses to the Carnian–Norian conodonts: a new approach for phylogenetic interpretations. *Journal of Systematic Palaeontology* 10, 401–422.
- Mazza, M., Furin, S., Spötl, C., Rigo, M., 2010. Generic turnovers of Carnian/Norian conodonts: Climatic control or competition? *Palaeogeography, Palaeoclimatology, Palaeoecology* 290, 120–137.
- Mazza, M., Martinez-Perez, C., 2015. Unravelling conodont (Conodonta) ontogenetic processes in the Late Triassic through growth series reconstructions and X-ray microtomography. *Bollettino della Società Paleontologica Italiana* 54, 161–186.
- Mazza, M., Rigo, M., Gullo, M., 2012b. Taxonomy and biostratigraphic record of the Upper Triassic conodonts of the Pizzo Mondello section (western Sicily, Italy), GSSP candidate for the base of the Norian. *Rivista Italiana di Paleontologia e Stratigrafia* 118, 85–130.
- Mazza, M., Rigo, M., Nicora, A., 2011. A new *Metopolygnathus* platform conodont species and its implications for Upper Carnian global correlations. *Acta Palaeontologica Polonica* 56, 121–131.
- McKinney, M.L., 1999. Heterochrony: beyond words. *Paleobiology* 25, 149–153.
- McKinney, M.L., 1986. Ecological causation of heterochrony: a test and implications for evolutionary theory. *Paleobiology* 12, 282–289.
- McKinney, M.L., Gittleman, J.L., 1995. Ontogeny and phylogeny: tinkering with covariation in life history, morphology and behaviour. *Evolutionary change and heterochrony*. John Wiley & Sons, Chichester 21–47.
- McLaren, I.A., 1965. Some Relationships Between Temperature and EGG Size, Body Size, Development Rate, and Fecundity, of the Copepod PSEUDOCALANUS1. *Limnology and Oceanography* 10, 528–538.
- McNamara, K.J., 1982. Heterochrony and phylogenetic trends. *Paleobiology* 8, 130–142.
- McNamara, K.J., McNamara, K., 1997. Shapes of time: the evolution of growth and development. Johns Hopkins University Press Baltimore.
- Mock, R., 1979. *Gondolella carpathica* n. sp., eine wichtige tuvalische Conodontenart. *Geol. Paläont. Mitt. Innsbruck* 9, 171–174.
- Moix, P., Kozur, H.W., Stampfli, G.M., Mostler, H., 2007. New paleontological, biostratigraphical

- and paleogeographic results from the Triassic of the Mersin Mélange, SE Turkey. The Global Triassic. New Mexico Museum of Natural History Science Bulletin 41, 282–311.
- Mosher, L.C., 1970. New conodont species as Triassic guide fossils. Journal of Paleontology 44, 737–742.
- Murdock, D.J., Dong, X.-P., Repetski, J.E., Marone, F., Stampanoni, M., Donoghue, P.C., 2013. The origin of conodonts and of vertebrate mineralized skeletons. Nature 502, 546.
- Murphy, M.A., Cebecioglu, M.K., 1984. The *Icriodus steinachensis* and *I. claudiae* lineages (Devonian conodonts). Journal of Paleontology 1399–1411.
- Murphy, M.A., Springer, K.B., 1989. Morphometric study of the platform elements of *Amydrotaxis praejohnsoni* n. sp. (Lower Devonian, Conodonts, Nevada). Journal of Paleontology 63, 349–355.
- Muttoni, G., Kent, D.V., Olsen, P.E., Stefano, P.D., Lowrie, W., Bernasconi, S.M., Hernández, F.M., 2004. Tethyan magnetostratigraphy from Pizzo Mondello (Sicily) and correlation to the Late Triassic Newark astrochronological polarity time scale. Geological Society of America Bulletin 116, 1043–1058.
- Needham, J., Biochemiker, R., 1931. Chemical embryology. University Press Cambridge.
- Noyan, Ö.F., Kozur, H.W., 2007. Revision of the late Carnian–early Norian conodonts from the Stefanion section (Argolis, Greece) and their palaeobiogeographic implications. Neues Jahrbuch für Geologie und Paläontologie-Abhandlungen 245, 159–178.
- Orchard, M.J., 1991. Upper Triassic conodont biochronology and new index species from the Canadian Cordillera. Bulletin of the Geological Survey of Canada 417, 299–335.
- Oster, G.F., Shubin, N., Murray, J.D., Alberch, P., 1988. Evolution and morphogenetic rules: the shape of the vertebrate limb in ontogeny and phylogeny. Evolution 42, 862–884.
- Petitgas, P., Rijnsdorp, A.D., Dickey-Collas, M., Engelhard, G.H., Peck, M.A., Pinnegar, J.K., Drinkwater, K., Huret, M., Nash, R.D., 2013. Impacts of climate change on the complex life cycles of fish. Fisheries Oceanography 22, 121–139.
- Purnell, M.A., 1995. Large eyes and vision in conodonts. Lethaia 28, 187–188.
- Purnell, M.A., 1994. Skeletal ontogeny and feeding mechanisms in conodonts. Lethaia 27, 129–138.
- Purnell, M.A., Aldridge, R.J., Donoghue, P.C., Gabbott, S.E., 1995. Conodonts and the first vertebrates. Endeavour 19, 20–27.
- Purnell, M.A., Donoghue, P.C., Aldridge, R.J., 2000. Orientation and anatomical notation in conodonts. Journal of Paleontology 74, 113–122.
- Raff, M.C., 1996. Size control: the regulation of cell numbers in animal development. Cell 86, 173–175.
- Raff, R.A., 2012. The shape of life: genes, development, and the evolution of animal form. University of Chicago Press.
- Reiss, J.O., 1989. The meaning of developmental time: a metric for comparative embryology. The American Naturalist 134, 170–189.
- Rigo, M., Mazza, M., Karádi, V., Nicora, A., 2018. New Upper Triassic Conodont Biozonation of the

- Tethyan Realm, in: The Late Triassic World. Springer, pp. 189–235.
- Rigo, M., Preto, N., Roghi, G., Tateo, F., Mietto, P., 2007. A rise in the carbonate compensation depth of western Tethys in the Carnian (Late Triassic): deep-water evidence for the Carnian Pluvial Event. *Palaeogeography, Palaeoclimatology, Palaeoecology* 246, 188–205.
- Ritter, S.M., 1989. Morphometric patterns in Middle Triassic *Neogondolella mombergensis* (Conodont), Fossil Hill, Nevada. *Journal of Paleontology* 63, 233–245.
- Roghi, G., Gianolla, P., Minarelli, L., Pilati, C., Preto, N., 2010. Palynological correlation of Carnian humid pulses throughout western Tethys. *Palaeogeography, Palaeoclimatology, Palaeoecology* 290, 89–106.
- Rohlf, F.J., 2010a. tpsDig v2. 16. Department of Ecology and Evolution, State University of New York, Stony Brook, New York.
- Rohlf, F.J., 2010b. tpsRelw, relative warps analysis. Department of Ecology and Evolution, State University of New York at Stony Brook, Stony Brook, NY.
- Roopnarine, P.D., Murphy, M.A., Buening, N., 2004. Microevolutionary dynamics of the Early Devonian conodont *Wurmiella* from the Great basin of Nevada. *Palaeontologia Electronica* 8, 1–16.
- Rowiński, P.K., Mateos-Gonzalez, F., Sandblom, E., Jutfelt, F., Ekström, A., Sundström, L.F., 2015. Warming alters the body shape of European perch *Perca fluviatilis*. *Journal of fish biology* 87, 1234–1247.
- Sallan, L.C., Coates, M.I., 2010. End-Devonian extinction and a bottleneck in the early evolution of modern jawed vertebrates. *Proceedings of the National Academy of Sciences* 107, 10131–10135.
- Sandberg, C.A., Ziegler, W., Leuteritz, K., Brill, S.M., 1978. Phylogeny, speciation, and zonation of *Siphonodella* (Conodonta, upper Devonian and lower Carboniferous). *Newsletters on Stratigraphy* 102–120.
- Sansom, I.J., Smith, M.P., Armstrong, H.A., Smith, M.M., 1992. Presence of the earliest vertebrate hard tissue in conodonts. *Science* 256, 1308–1311.
- Shirley, B., Grohganz, M., Bestmann, M., Jarochowska, E., 2018. Wear, tear and systematic repair: testing models of growth dynamics in conodonts with high-resolution imaging. *Proc. R. Soc. B* 285.
- Simms, M.J., Ruffell, A.H., 1990. Climatic and biotic change in the late Triassic. *Journal of the Geological Society* 147, 321–327.
- Sweet, W.C., 1988. The Conodonta: morphology, taxonomy, paleoecology, and evolutionary history of a long-extinct animal phylum. Clarendon Press Oxford.
- Thompson, D.W., 1917. On growth and form. On growth and form.
- Travis, J., 1981. Control of larval growth variation in a population of *Pseudacris triseriata* (Anura: Hylidae). *Evolution* 35, 423–432.
- Trotter, J.A., Williams, I.S., Nicora, A., Mazza, M., Rigo, M., 2015. Long-term cycles of Triassic climate change: a new  $\delta^{18}\text{O}$  record from conodont apatite. *Earth and Planetary Science Letters* 415, 165–174.
- Turing, A.M., 1952. The chemical basis of morphogenesis. *Phil. Trans. R. Soc. Lond. B* 237, 37–72.

- Turner, S., Burrow, C.J., Schultze, H.-P., Blieck, A., Reif, W.-E., Rexroad, C.B., Bultynck, P., Nowlan, G.S., 2010. False teeth: conodont-vertebrate phylogenetic relationships revisited. *Geodiversitas* 32, 545–594.
- Urdy, S., Wilson, L.A., Haug, J.T., Sánchez-Villagra, M.R., 2013. On the unique perspective of paleontology in the study of developmental evolution and biases. *Biological Theory* 8, 293–311.
- Walliser, O.H., 1996. Global events in the Devonian and Carboniferous, in: *Global Events and Event Stratigraphy in the Phanerozoic*. Springer, pp. 225–250.
- Webster, G., Goodwin, B.C., 1982. The origin of species: a structuralist approach. *Journal of Social and Biological Structures* 5, 15–47.
- Wei, K.-Y., 1994. Allometric heterochrony in the Pliocene-Pleistocene planktic foraminiferal clade *Globoconella*. *Paleobiology* 20, 66–84.
- Zhuravlev, A.V., 1995. Ontogeny and trophic types of some Tournaisian Polygnathacea (Conodonta). *Courier Forschungsinstitut Senckenberg* 182, 307–312.
- Zhuravlev, A.V., Plotitsyn, A.N., 2018. Taxonomical reassignment of some siphonodellids (conodonts, Early Carboniferous) from W. Hass's collection.

## **Chapitre 5:**

# **Utiliser la morphométrie géométrique et l'analyse de clusters pour démêler la taxonomie des neogondolellides du Griesbachien.**

Ce chapitre constitue un travail préliminaire visant à utiliser les méthodes de morphométrie géométrique et de clustering pour faciliter l'assignation taxonomique des conodontes de la famille des neogondolellides au Griesbachien. En effet, les neogondolellides ont survécus à la crise biologique majeure marquant la fin du Permien, ce qui a fait d'eux un sujet d'étude de choix notamment dans le domaine de la biostratigraphie. Cet intérêt a mené à la reconnaissance de nombreuses espèces différentes au sein de cette famille. Mais en pratique, la reconnaissance de certaines de ces espèces peut s'avérer très compliqué, et mener à de nombreuses erreurs d'identification augmentant la confusion autour de cette famille, ce qui a finalement conduit à les écarter lors du choix des fossiles indexés en biostratigraphie. L'idée à l'origine de ce chapitre est donc de tester s'il est possible d'utiliser la morphométrie géométrique et les méthodes d'analyse multivariées et de clustering pour reconnaître les différentes espèces présentes dans un assemblage de neogondolellides, et pour déterminer quels caractères permettent une meilleure discrimination de ces espèces. Le but est alors d'utiliser ces résultats pour contraindre la taxonomie actuelle des neogondolellides et en faciliter l'accès. Pour cela, une matrice de caractères a été construite sur tous les individus sans aprioris de l'espèce, et une analyse de contours a été effectuée. Les méthodes utilisées ici ne permettent pas de séparer les différentes espèces décrites dans la littérature, ni de trouver de caractères taxonomiques vraiment pertinents associés aux groupes observés. Une discussion de la validité de ces espèces et de certains caractères taxonomiques est alors proposée.

## **Untangling the taxonomy of Griesbachian neogondolellids using morphometrics and cluster analyses**

### **Authors**

Louise Souquet<sup>a</sup>, Morgane Brosse<sup>b</sup>, Nicolas Goudemand<sup>a</sup>

<sup>a</sup>Univ. Lyon, ENS de Lyon, CNRS, Univ. Claude Bernard Lyon 1, Institut de Génomique Fonctionnelle de Lyon, UMR 5242, 46 Allée d’Italie, F-69364 Lyon Cedex 07, France.

<sup>b</sup>Paläontologisches Institut und Museum der Universität Zürich, Karl Schmid-Strasse 4, CH-8006 Zürich, Switzerland. morgane.brosse@pim.uzh.ch

## **Abstract**

In the aftermath of the Permian-Triassic boundary mass extinction, the most dramatic biotic crisis in the history of the Earth, conodonts thrived: they had been declining throughout the Permian but at the onset of the Triassic they were experiencing a new evolutionary radiation. Two conodont families particularly drove this radiation: the anchignathodontids who went extinct shortly after, at the end of the Griesbachian (early Induan, Early Triassic), and the neogondolellids, which are thought to be the rootstock of most Early Triassic conodonts. Neogondolellids had been around since the Carboniferous and were to remain until the end of the Triassic, and the extinction of conodonts, the most successful group of conodonts in post-Carboniferous times. The many biostratigraphical studies that focused at the elucidation of the Permian-Triassic Boundary crisis led to the description of numerous species of Griesbachian neogondolellids. Yet, the taxonomic determination of most Griesbachian neogondolellids remains puzzling and it is not clear how many of these species are actually valid in practice. Here we used a cohort of 183 neogondolellids specimens retrieved from Griesbachian rocks of the Guryul Ravine section, Kashmir, India, and thought to belong to about ten distinct neogondolellids species, in order to quantify variability in terms of trait associations and shape outline and to assess the sharpness (or fuzziness) of the corresponding species boundaries. The methods used in this study failed to recognize the different species described in the literature, nor to found truly appropriate taxonomically discriminant morphological characters. We discuss the relevance of those species and characters, and suggest the need of some clarifications to avoid as much confusions as possible in the species identification, allowing easier conodont based studies by non-taxonomical specialists in wider topics of interest.

## **Keywords:**

Classification, cladistics, morphology, statistics, hierarchical clustering.

## 1. Introduction

The Permian-Triassic boundary (PTB,  $251.956 \pm 0.033$  Ma; Baresel et al., 2016) marks the most devastating of all mass extinctions in the history of life. The great abundance, global spatial distribution and high evolutionary rates of conodont marine microfossils make them one of the main biochronological tools for the Palaeozoic and the Triassic. Contrary to most organisms, conodonts remained comparatively unscathed across the Permian-Triassic boundary and therefore became prominent fossil indexes for this time interval.

Among all conodont genera that survived the PTB mass extinction, neogondolellids and anchignathodontids are of paramount importance for Late Permian and lowermost Triassic biostratigraphical scales (see Orchard, 2007 and references therein). Contrary to anchignathodontids who thrived during the Griesbachian (early Induan, see for instance Brosse et al 2015, 2016) but went extinct shortly after the PTB (at the end of the Griesbachian), neogondolellids are thought to have been the rootstock of most Early Triassic conodonts. Neogondolellids were ubiquitous and abundant across the PTB, but it has been argued that their high morphological variability precludes establishing reliable fossil indexes (Kozur et al., 1995), which eventually led to elect instead an anchignathodontid, *Hindeodus parvus*, as index fossil for the base of the Triassic (Yin et al., 1996). This interpretation has later been contested by Orchard and Krystyn (1998), who, based on material from Spiti, Himashal Pradesh, India, proposed a high-resolution Griesbachian biozonation based exclusively on neogondolellids, which they compared to an anchignathodontid-based biozonation. Indeed, neogondolellids are thought to have inhabited mostly deeper and colder environments than anchignathodontids during the Griesbachian (Joachimski et al., 2012), and hence neogondolellid-based biochronological scales are key to correlate sections worldwide across facies.

Like most conodont workers, Orchard and Krystyn (1998) adopted a typological approach and distinguished four new neogondolellids species that are nowadays commonly used for the biostratigraphy of the Griesbachian (*Neogondrella discreta*, *C. kazi*, *C. krystyni*, and *C. nassichuki*), as well as six new morphotypes of previously existing species (*Clarkina tulongensis*  $\alpha$ ,  $\beta$ ,  $\gamma$  and *Clarkina taylorae*  $\alpha$ ,  $\beta$ ,  $\gamma$ ). In systematics, taxonomic diagnoses are meant to highlight specific *diagnostic* characters or associations of characters. For Griesbachian neogondolellids,

Orchard and Krystyn (1998) summarized those diagnostic characters in a convenient table reproduced here (Table 1). Yet, note that this table is not *sensu stricto* an *identification key* that would allow the user to identify an element based on a fixed or interactive series of identification steps at which the user chooses from two or more alternatives about a particular diagnostic character. In particular it is not entirely clear to what extent the set of proposed diagnostic features is sufficient to make unambiguous identifications. As a general rule, one would expect the diagnostic characters to be truly *diagnostic*: they should be common to all individuals of a particular taxa, and unique to that group. Ideally they should be also *differential*; that is, they should separate taxa from each other. Yet, because conodont elements are relatively integrated organs with a relatively limited number of characters, both conditions are rarely met, and identifications usually rely on associations of characters. Moreover, diagnostic characters are often qualitative ('a relatively broad platform' for instance), not discrete nor quantitative, which precludes objective reassessments; and they are mostly based on large, presumably adult, specimens, which means many variants, especially smaller, presumably juvenile, specimens are not properly taken into account. As a result the identification of many elements of a particular assemblage may remain ambiguous or indeterminate. In biostratigraphy this is possibly less of an issue because within a particular assemblage one may find at least one very 'typical' individual of a particular index fossil and that may be sufficient to date the rocks and conduct the study to some meaningful conclusion. If, on the other hand, the focus is, for example, on the specific diversity of an assemblage in order to discuss the dynamics of a biotic recovery, or on the microevolutionary patterns of some population and its bearing on macroevolutionary processes, then a more rigorous assessment of diagnostic characters is needed. Note that this issue is not specific to Griesbachian neogondolellids (nor to conodonts only actually). Instead the present case is considered iconic of some of the frequent problems encountered by many taxonomists. Within the frame of Early Triassic conodonts, the case of Griesbachian neogondolellids is, in our opinion, one of the trickiest.

Brosse et al. (2017) recently retrieved from the Member E of the Guryul Ravine section (Vihi district of Kashmir) abundant conodont assemblages. Those assemblages are dominated by neogondolellids and encompass most of the Griesbachian time interval. A comparison in terms

of species composition with the reference material from Spiti, India, described by Orchard and Krystyn (1998), suggests they are very similar. Hence the Guryul Ravine material is here considered to be representative of the Griesbachian neogondolellids of the Northern Indian Margin (NIM) and possibly of Griesbachian neogondolellids in general.

In the following we perform multiple correspondence and clustering analyses to assess the ‘classificability’ of the specimens of our assemblage based on their morphological description using Elliptic Fourier analysis of their outline, and a set of discretized diagnostic characters that in our opinion represents the full spectrum of traits used in traditional diagnoses of neogondolellids. By doing so, we can assess the relative weight of the considered characters for discriminating the specimens and discuss the ‘biological validity’ (not their merit as index taxa for biochronology) of the considered species.

For comparison purposes, we also include in our analyses the holotypes of 16 typical latest Permian and Griesbachian species of neogondolellids.

## 2. Material and methods

### 2.1. Selection of variables for analyses

All analyses are run exclusively on the  $P_1$  element, which is considered the diagnostic element within the group of taxa we are considering. We have selected 19 variables based on the standard upper and lateral views of the  $P_1$  element. These variables are common diagnostic characters used in diagnoses of neogondolellids species and are thought to cover the full spectrum of traits used in descriptions of these species. When possible, we attempted to translate continuous characters into ratio-based discrete characters. For instance, the platform width character is expressed as the length/width ratio ( $L/W$ ) and split into two categories: “wide” ( $L/W \geq 3$ ) and “narrow” ( $L/W < 3$ ) categories. Table 2 shows the list of variables with their different categories.

The cohort contains 215 specimens (199 from the Guryul Ravine population and 16 previously published holotypes). The specimens were retrieved from different horizons but are all of Griesbachian age. Complete data for all 19 variables are available for 183 specimens

<i>Ng. carinata</i>	broad platform, maximum width medially, posteriorly indented
<i>Ng. discreta</i>	narrow platform; high discrete carinal denticles
<i>Ng. kazi</i>	broad posteriorly rounded platform; high and fused carinal denticles
<i>Ng. krystyni</i>	platform margins parallel to undulose; elevated posterior carina
<i>Ng. meishanensis</i>	upturned platform margins, straight carina, high terminal cusp
<i>Ng. nassichuki</i>	narrow, evenly tapered platform with maximum width medially
<i>Ng. nevadensis</i>	broad platform, maximum width near posterior end; carina extends to or beyond posterior end
<i>Ng. orchardi</i>	narrow, curved and pointed platform with terminal cusp
<i>Ng. planata</i>	broad, evenly tapered platform with maximum width medially
<i>Ng. taylorae</i>	broad, rounded posterior margin, prominent cusp with posterior brim
<i>Ng. taylorae</i> $\alpha$	as holotype; length:width ratio = 2:1
<i>Ng. taylorae</i> $\beta$	relatively short bulbous platform due to anterior narrowing
<i>Ng. taylorae</i> $\gamma$	relatively narrow, long platform; length:width ratio = 3:1
<i>Ng. tulongensis</i>	subquadrate platform +/-sinuous margin
<i>Ng. tulongensis</i> $\alpha$	symmetrical quadrate platform
<i>Ng. tulongensis</i> $\beta$	platform with sinuous inner margin
<i>Ng. tulongensis</i> $\gamma$	form with strongly deflected posterior carina
<i>Ng. zhejiangensis</i>	elongate-oval platform, rounded posterior margin, low carinal nodes, indistinct cusp +/-accessory posterior denticles
<i>Ng. sp. A</i>	oblong platform, high carina, sinuous margin

Table 1: Summary of diagnostic morphological characteristics of *Neogondolella* (Ng.) species occurring in the lowermost Triassic. After Orchard and Krystyn, 1998.

only. The remaining 32 specimens, which we consequently excluded from the analyses, consist in poorly preserved elements or partial illustrations. The holotypes of *Clarkina carinata*, *Neogondolella discreta*, *Clarkina griesbachensis*, *Clarkina kazi*, *Clarkina krystyni*, *Clarkina nassichuki*, *Clarkina orchardi*, *Clarkina planata*, *Clarkina taylorae* and *Clarkina zhejiangensis* were considered.

## 2.2. Factorial analyses and hierarchical classification

Factorial analyses were conducted using the R “FactoMineR” package (Lê et al. 2008), dedicated to multivariate data analysis.

The relationships between the 19 categorical variables were studied using multiple correspondence analyses (MCA; see Husson et al., 2016 for detailed description of the function). In a multidimensional dataset of non-linear data, MCA identify associations between multiple categorical variables. Similarly to other multivariate methods, it is dimension reducing: it represents the data as points in a space of two to four dimensions that best capture the variance of the dataset.

Variables are clustered using hierarchical classification (HCPC; see Husson et al., 2016 for detailed description of the function). The cluster analysis produces a hierarchical tree that sorts

view of the P1 considered	N°	variables	categories
upper view	V1	indentation on lateral margin	(0) no indentation (1) weak indentation (2) strong indentation
upper view	V2	symmetrical indentations of posterior platform	(0) no indentation (1) weak indentation (2) strong indentation = posterior platform
upper view	V3	platform width	(0) narrow: L/maximalW>3 (1) wide: L/maximalW<=3
upper view	V4	location of the platform maximal width	(0) parallel platforms (1) anterior 3/5th (2) posterior 2/5th
upper and lateral view	V5	thickness of the posterior platform brim	(0) no platform brim (cusp terminal) (1) bulge (cusp subterminal) (2) thin brim (< cusp diametre) (3) thick brim (>=)
upper view	V6	occurrence of a free anterior blade	(0) no free blade (1) one denticle free (2) more than one denticle free
upper view	V7	occurrence of a free posterior blade	(0) absence (1) occurrence
upper view	V8	deflection of the carina (main process)	(0) no deflection (1) weak deflection (2) strong deflection
upper view	V9	accessory denticle after the cusp	(0) absence (1) occurrence of exactly one denticle
upper view	V10	accessory process after the cusp	(0) absence (1) at least 2 denticles after the cusp (2) 2 extensions
lateral view	V11	denticle fused (only tip free)	(0) denticles discrete or space between denticle' tip <= 2*height (1) closely appressed to weakly fused (2) strongly fused
lateral view	V12	cusp projects posteriorly further than the posterior margin	(0) absence (1) occurrence
upper and lateral view	V13	space between cusp and carina	(0) equal to space between other denticles (1) larger
lateral view	V14	relative size of denticles (without cusp)	(0) denticles lowest at midlength or decreasing posteriorly (1) denticles subequal
lateral view	V15	high denticles (midlength)	(0) low denticle (1) high denticles
upper and lateral view	V16	broad cusp	(0) cusp diametre smaller or equal than adjacent denticles (1) diametre larger
lateral view	V17	cusp higher than adjacent denticle	(0) absence (1) occurrence
upper view	V18	Posterior platform shape	(0) rounded (1) subquadrate to quadrate (2) constricted to pointy
lateral view	V19	lateral shape of the attachment scar	(0) flat: angle between anterior part and posterior part >= 150° (1) angulate: <150°

Table 2: list of the 19 variables and their categories.

individuals according to their coordinates within the MCA's principal components morphospace. The hierarchical clusters are presented in a dendrogram.

### 2.3. Elliptic Fourier analysis

An elliptic Fourier analysis (Kuhl and Giardina, 1982) was conducted on the outline of the element in oral view using the Momocs package (Bonhomme et al., 2014) in the R software

(RStudio Team, 2015). This method decomposes the outline signal into harmonics, each of them described by four Fourier coefficients which are used as shape variable in further statistical analysis. In this study, 8 harmonics were kept, which together describe 99% of the original outlines. The mean outline of each species was reconstructed using the Momocs package. The morphological variation of the assemblage was explored using a Principal Component Analysis on the variance-covariance matrix of the Fourier coefficients. Differences between species have been tested using a pairwise PERMANOVA (non-parametric multivariate analysis of variance based on 9999 permutations) and associated pairwise post-hoc tests.

### 3. Results

#### 3.1. Cluster analysis

The components generated by the MCA are presented in Table 3. The first three components account for 28.32% of the total variance (respectively for 12.53, 8.52, and 7.17%, see Table 3).

We calculated the pairwise Euclidian distances between all individuals based on their scores on the 16 first dimensions of the MCA (accounting for 80% of the total variance).

The dendrogram resulting from the analysis using these 16 dimensions is indexed by the within-inertia gain. The total inertia (total variance) is the sum of the between- and within-group variance and characterizes the homogeneity of a cluster. It is decomposed thanks to the Ward's criterion detailed in Husson et al. (2010). We based the initial number of clusters on the optimal growth of inertia calculated by the HCPC function. The optimal growth of inertia being four, the population is grouped into five clusters (Fig. 1).

Each cluster is described in Table 4. The clusters are unequal in number of individuals, from 7 in Cluster 5 to 81 in Cluster 3. The population of each cluster can be described thanks to the categories that are most frequently displayed (Table 4). For instance, 100% of the individuals in Cluster 2 show a weak constriction of the posterior platform and the other categories are not much represented. 100% of the individuals in Cluster 1 have a free posterior blade (including the holotype of *Ng. discreta*). 100% of the individuals in Cluster 5 have one or two extensions

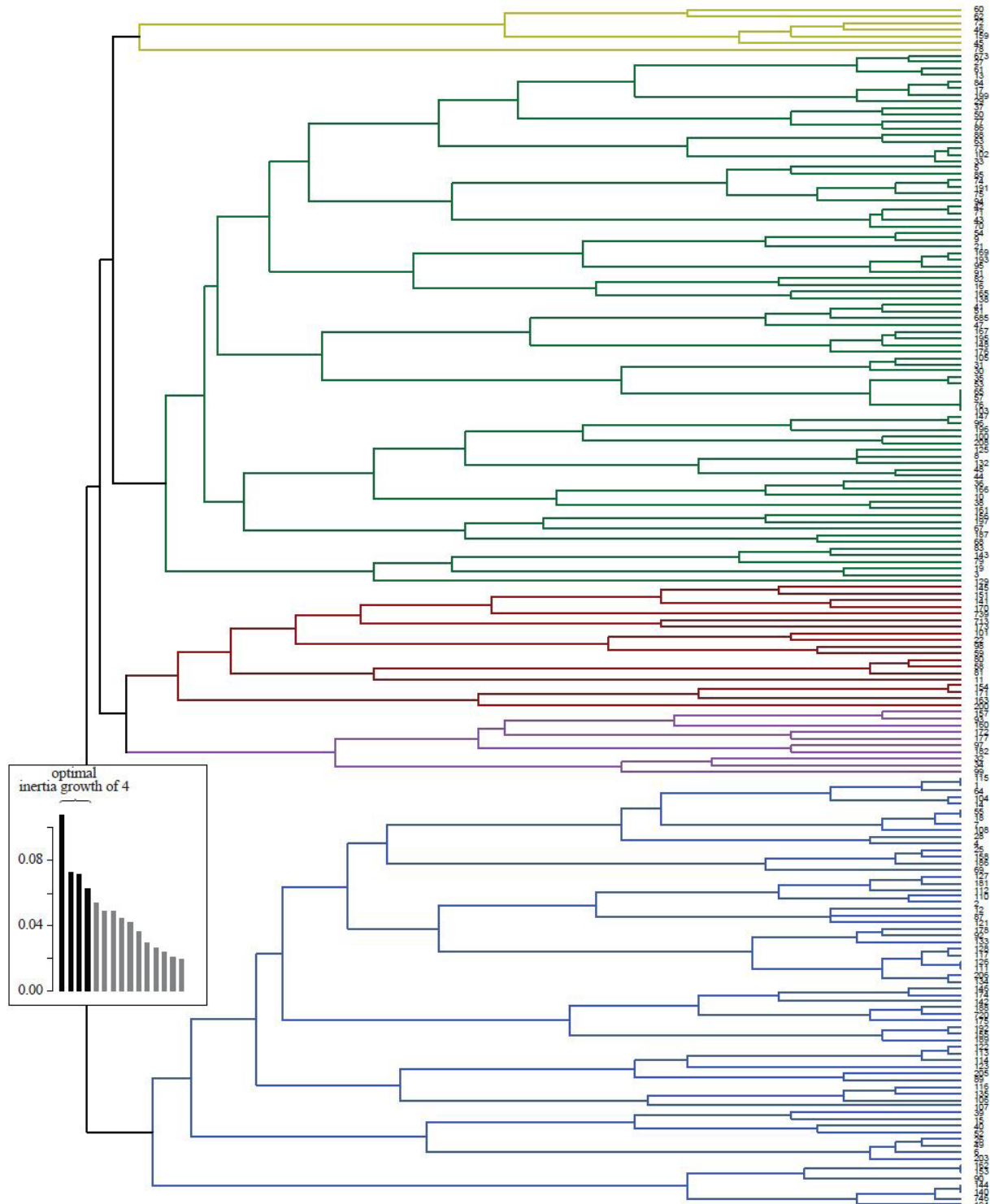


Figure 1: Dendrogram illustrating the results of the cluster analysis of morphological variables. Each horizontal line represents an individual. The original individuals are optimally grouped into five major clusters highlighted by the different colours.

Components	Eigenvalues	% Variance	Cum % Variance
1	0.19	12.53	12.53
2	0.13	8.52	21.06
3	0.11	7.27	28.32
4	0.09	5.84	34.16
5	0.08	5.31	39.47
6	0.08	5.13	44.60
7	0.07	4.55	49.15
8	0.07	4.37	53.53
9	0.06	4.19	57.72
10	0.06	3.61	61.33
11	0.05	3.49	64.82
12	0.05	3.44	68.26
13	0.05	3.18	71.44
14	0.05	2.96	74.40
15	0.04	2.69	77.08
16	0.04	2.65	79.73
17	0.04	2.32	82.05
18	0.03	2.12	84.17
19	0.03	2.04	86.20

Table 3: Eigenvalue, % of variance explained and cumulated % of variance for each component generated by the MCA. The part highlighted by the grey shade indicates the 16 first components that were used to compute the hierarchical classification.

of the carina behind the cusp. 80% of the individuals in Cluster 4 have a secondary posterior platform (including the holotype of *C. carinata*). 85% of the individuals in Cluster 3 feature an asymmetrical weak indentation of the lateral margin and 71% have a thin posterior brim (including the holotype of *C. taylorae*, *C. nassichuki* and *C. yini*).

For each variable, we can observe the repartition of all categories in the morphospace, to evaluate their potential to discriminate the different species. Some variables display categories which do not or slightly overlap (e.g. accessory process after the cusp, posterior platform shape vs free anterior blade, upturned platform margins). These categories are thus more likely to discriminate individuals in different species (Fig. 7). Differences between each pair of species have been tested with a PERMANOVA (Table 5). The degree of morphological identity of each species has been calculated as the number of statistically valid differences ( $p\text{-value}<0.05$ ) with the other species. The species with the stronger morphological identity is *Ng. discreta*. Then, from the strongest to the weakest morphological identity we have: *C. meishanensis*, *C. griesbachensis*, *Sw. kummeli*, *C. tulongensis*, *C. zejiangensis*, *C. taylorae*, *C. krystyni*, *C. planata*, *C. kazi*, *C. nassichuki*, *C. orchard*, and finally *C. carinata*.

### 3.2 Outline analysis

Only the first two principal component (PC) axis explained more than 5% of morphological variation (PC1= 80,3%; PC2=12%). All the species are overlapping each other, presenting a morphological continuum along PC1. Only *N. discreta* tends to separate from the other species towards negative PC1 values, and *C. tulongensis* along positive PC1 values (Fig.8). The main

Clusters	Variable_category	Considered variables and categories (for each cluster)	% of individuals included within the cluster (>=50%)	Holotypes included within the cluster
1 (n=66)	V7_1	occurrence of a free posterior blade	100	<i>Ng. discreta</i> <i>Ng. griesbachensis</i> <i>Ng. planata</i> <i>Ng. nevadensis</i>
	V18_2	constricted to pointy posterior platform	85	
	V5_0	no platform brim (cusp terminal)	78.87	
	V12_1	cusp projects posteriorly further than the posterior margin	73.77	
	V4_0	parallel platform margins	66.67	
	V8_0	no deflection of the carina (main process)	51.81	
2 (n=10)	V2_1	Weak constriction of the posterior platform	100	
3 (n=81)	V1_2	weak indentation on lateral margin	85.71	<i>Ng. taylorae</i> <i>Ng. yini</i> <i>Ng. nassichuki</i>
	V5_2	thin posterior brim (< cusp diametre)	71.05	
	V18_0	posterior platform rounded	68.42	
	VV5_1	posterior bulge (cusp subterminal)	66.67	
	V17_0	cusp not higher than adjacent denticle	64.58	
	V11_1	denticles closely appressed to weakly fused	62.07	
	V12_0	cusp does not project posteriorly	60.66	
	V13_1	space between cusp and carina larger than space between other denticles	60.00	
	V5_3	thick posterior brim	57.45	
	V8_1	weak deflection of the carina	56.52	
	V16_0	cusp diameter smaller or equal than adjacent denticles	53.75	
	V15_0	low denticles at midlength	53.62	
4 (n=19)	V19_1	attachment scar angulate laterally	52.73	
	V2_2	secondary posterior platform	80.00	<i>Ng. carinata</i> <i>Ng. krystyni</i> <i>Ng. kazi</i>
	V9_1	occurrence of exactly one extra denticle posteriorly	59.09	
5 (n=7)	V11_2	denticles strongly fused	56.25	
	V10_2	two posterior extension of the carina	100.00	
	V10_1	one posterior extension	85.71	

Table 4: description of the 5 computed clusters. The column to the right corresponds to the percentage of individuals showing the corresponding category. We only show here the categories that are represented by at least 50% of the cluster population.

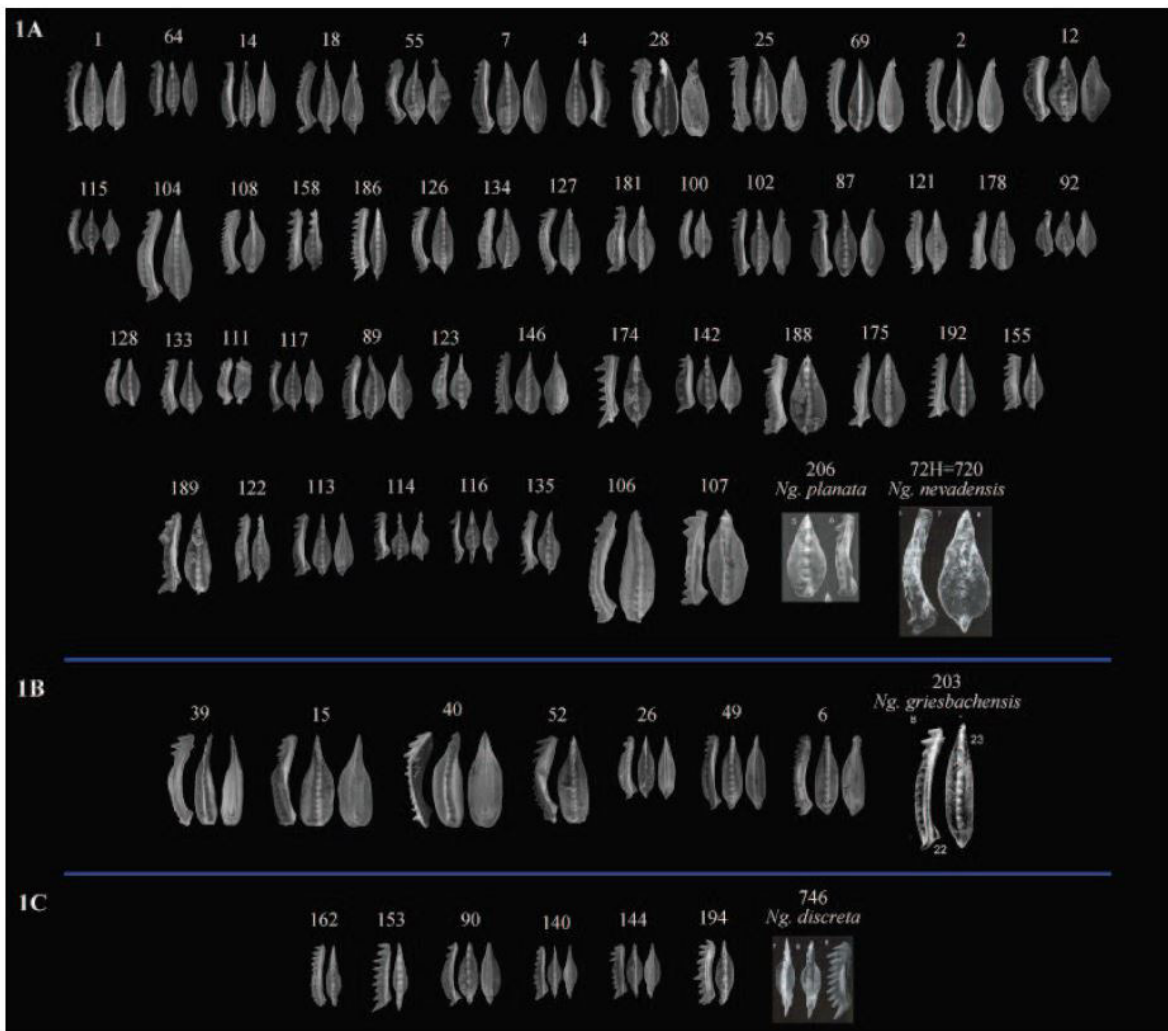


Figure 2: cluster 1 (blue on the dendrogram), including 66 individuals. Numbers above the individuals correspond to the number in figure 2.

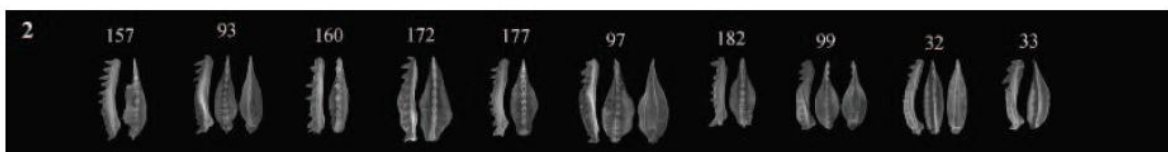


Figure 3: cluster 2 (purple on the dendrogram), including 10 individuals. Numbers above the individuals correspond to the number in figure 2.

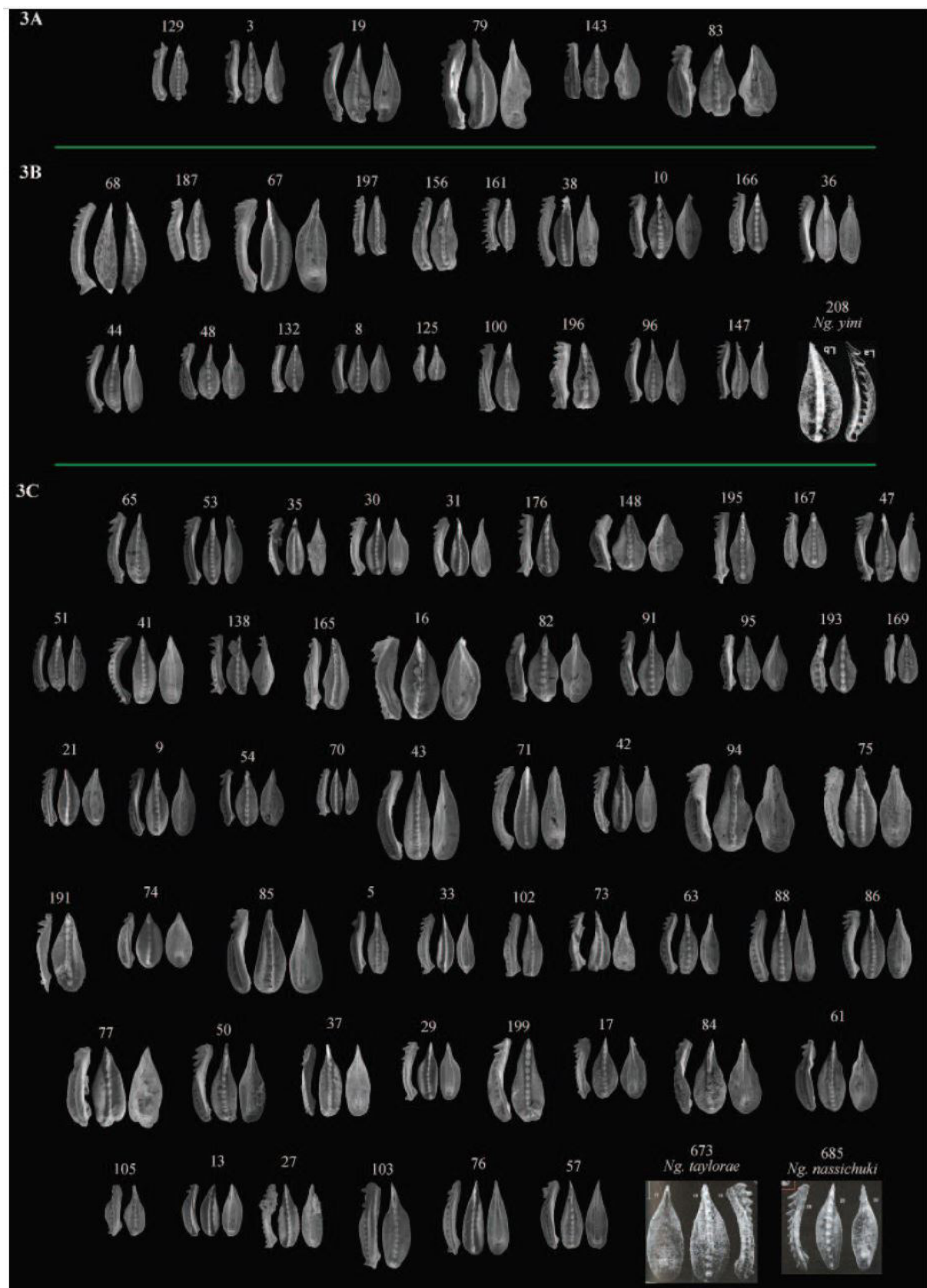


Figure 4: cluster 3 (green on the dendrogram), including 81 individuals. Numbers above the individuals correspond to the number in figure 2.

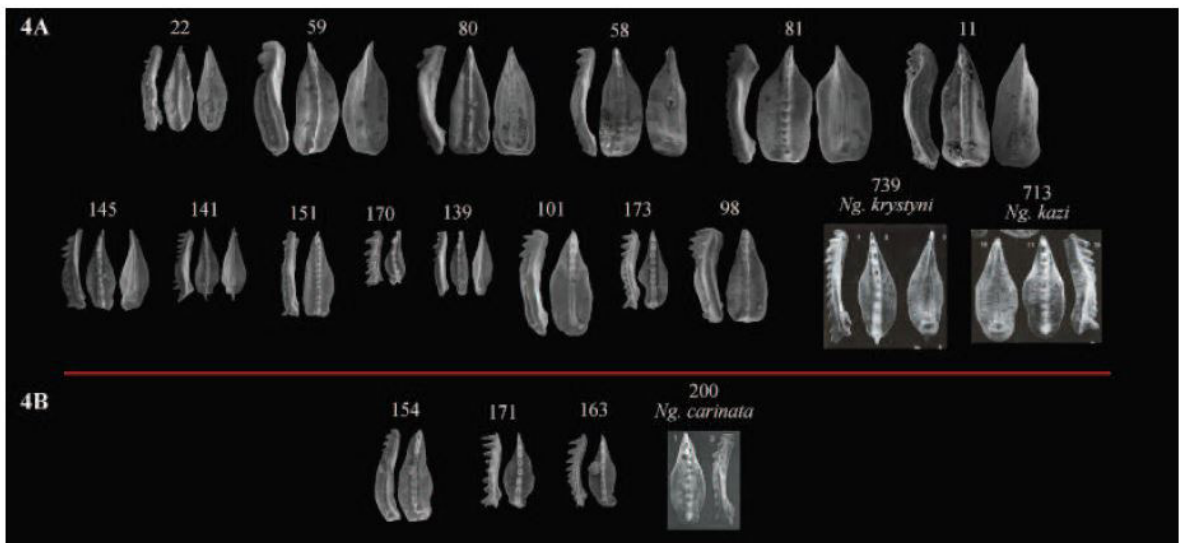


Figure 5: cluster 4 (red on the dendrogram), including 19 individuals. Numbers above the individuals correspond to the number in figure 2.



Figure 6: cluster 5 (yellow on the dendrogram), including 7 individuals. Numbers above the individuals correspond to the number in figure 2.

	orchardi	zhejiangensis	meishanensis	griesbachensis	taylorae	nassichuki	tulongensis	kazi	krystyni	planata	carinata	kummeli	discreta	
orchardi	0,8742		<b>0,0347</b>	<b>0,0017</b>	0,1148	0,5608	0,1754	0,1268	0,1818	0,0935	0,2687	<b>0,0412</b>	0,0005	
zhejiangensis	0,8742		<b>0,0012</b>	<b>0,0001</b>	<b>0,0249</b>	0,6478	<b>0,0272</b>	<b>0,02</b>	0,1088	<b>0,0148</b>	0,1029	<b>0,0051</b>	0,0001	
meishanensis	<b>0,0347</b>	<b>0,0012</b>			0,0681	<b>0,0002</b>	<b>0,0156</b>	<b>0,0001</b>	<b>0,0001</b>	<b>0,0076</b>	<b>0,0004</b>	0,0741	<b>0,0122</b>	0,0001
griesbachensis	<b>0,0017</b>	<b>0,0001</b>		0,0681		<b>0,0002</b>	<b>0,0044</b>	<b>0,0002</b>	<b>0,0001</b>	<b>0,0023</b>	<b>0,0005</b>	<b>0,0477</b>	0,2892	0,0006
taylorae	0,1148	<b>0,0249</b>	<b>0,0002</b>		<b>0,0002</b>		<b>0,0441</b>	0,2544	0,3503	<b>0,0005</b>	0,1581	<b>0,0134</b>	<b>0,0107</b>	0,0001
nassichuki	0,5608	0,6478	<b>0,0156</b>		<b>0,0044</b>	<b>0,0441</b>		<b>0,0268</b>	0,1561	0,5749	0,0704	0,5249	0,045	0,0001
tulongensis	0,1754	<b>0,0272</b>	<b>0,0001</b>		0,0002	<b>0,2544</b>	<b>0,0268</b>		0,0926	<b>0,0001</b>	<b>0,0169</b>	<b>0,006</b>	0,0093	0,0001
kazi	0,1268	<b>0,02</b>	<b>0,0001</b>		<b>0,0001</b>	0,3503	0,1561	0,0926		<b>0,0138</b>	<b>0,517</b>	0,0876	<b>0,0311</b>	0,0002
krystyni	0,1818	0,1088	<b>0,0076</b>		<b>0,0023</b>	<b>0,0005</b>	0,5749	<b>0,0001</b>	<b>0,0138</b>		<b>0,0151</b>	0,536	<b>0,0114</b>	0,0001
planata	0,0935	<b>0,0148</b>	<b>0,0004</b>		<b>0,0005</b>	0,1581	0,0704	<b>0,0169</b>	<b>0,517</b>	<b>0,0151</b>		0,0549	<b>0,0063</b>	0,0001
carinata	0,2687	0,1029	0,0741		<b>0,0477</b>	<b>0,0134</b>	0,5249	<b>0,006</b>	0,0876	0,536	0,0549		0,1732	0,0007
kummeli	<b>0,0412</b>	<b>0,0051</b>	<b>0,0122</b>		0,2892	<b>0,0107</b>	0,045	0,0093	0,0311	0,0114	0,0063	0,1732		<b>0,0013</b>
discreta	<b>0,0005</b>	<b>0,0001</b>	<b>0,0001</b>		<b>0,0006</b>	<b>0,0001</b>	0,0001	0,0001	0,0002	0,0001	0,0001	<b>0,0007</b>	<b>0,0013</b>	

Table 5: p-values of a pairwise PERMANOVA analysis considering the species as described in the literature on the shape characters (matrix)

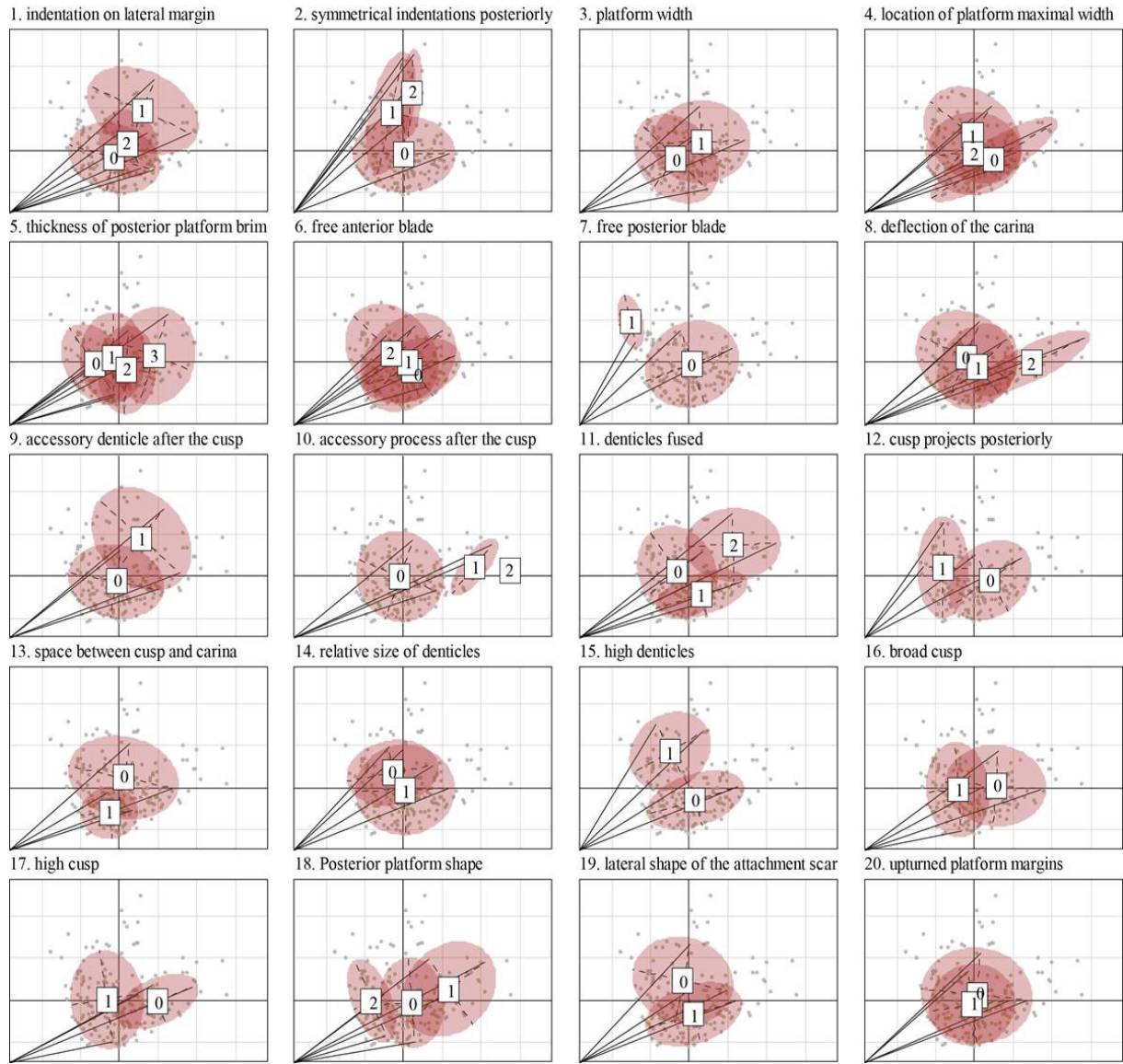


Figure 7: Illustrations of the 20 variables and their categories within the two first axis of the MCA. The red ellipse corresponds to each categories.

morphological variation present in the assemblage is associated with PC1, and evidenced a morphological continuum between lanceolate and sub-quadrangular posterior platform margin. PC2 is characterized by the fluctuating asymmetry of the platform between the elements. *C. tulongensis* and *C. taylorae* are the two species presenting the more important morphological variation, which is not surprising as they have been divided in different morphotypes in the literature (Orchard and Krystyn 1998).

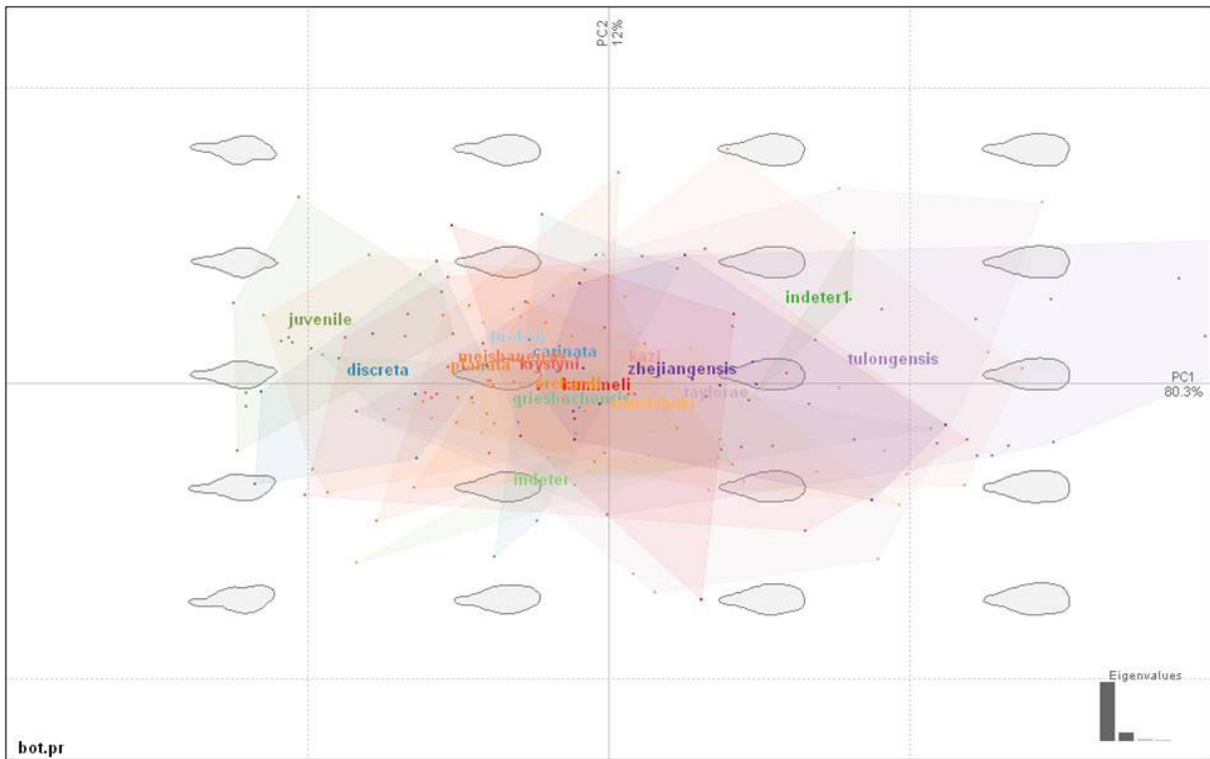


Figure 8: Conodont elements (P1) shape differentiation between species on the two first and significant axis on the principal component analysis. The different species are represented in colored convex hulls. The reconstruction of theoretical outline shape in the morphospace are displayed.

#### 4. Discussion

Following the standard typological approach, Orchard and Krystyn (1998) detected 13 species of neogondolellids in Spiti and Brosse et al. (2017) identified 13 species in the Griesbachian material from Guryul Ravine. Both localities have 10 species in common. In contrast, using the optimal inertia growth generates five clusters only, i.e. about 40% of the expected number of species. Morphotypes that are clearly separated by the typological approach are here grouped, such as the holotypes of *C. planata* and *Ng. discreta* in Cluster 1 (Fig. 2).

If we split the hierarchical tree to get closer from the expected number of 10-13 species, for instance by choosing an inertia growth of 10 that splits the hierarchical tree accordingly into 11 subgroups, then Cluster 1 is divided into 3 subgroups 1A-C, Cluster 3 into 3 sub-groups 3A-C, Cluster 4 into 2 subgroups 4A-B, and Cluster 5 into 2 subgroups 5A-B. The five clusters and their subgroups are displayed in Figures 2-6. Interestingly, in this new partition the holotypes

of *C. planata* and *Ng. discreta* are now separated into two different subgroups (1A and 1C). In fact, the subgroup including the holotype of *Ng. discreta* appears to be the most consistent, as all individuals feature the posterior free blade that is considered as a good diagnostic character of this species. Another relatively consistent subgroup of Cluster 1 includes the holotype of *C. griesbachensis* and individuals with parallel platform margins (subgroup 1B). The partitioning of Cluster 3 also presents interesting result, as the new sub-division allows to separate the holotype of *C. yini* with terminal cusp (subgroup 3B) and the holotypes of *C. taylorae* and *C. nassichuki* with a posterior platform brim (subgroup 3C).

Cluster 3A is clearly discriminated mostly on the base of an asymmetrical lateral indentation of the platform margins. It is worth noting that from every diagnosis of neogondolellids species that are mentioned here (see the summary in Table 1), the asymmetrical indentation is never used as a diagnostic character, although being plainly featured on the holotype of *C. kazi* (Orchard and Krystyn, 1998; Pl. 2, Fig. 10-12). The overall platform shape itself is however often considered as a major diagnostic character: *C. tulongensis* (Tian, 1982) is identified thanks to a squared posterior platform and a rectangular platform outline; the holotype of *C. carinata* (Clark, 1959; Pl. 44, Fig. 16-17) features a strong constriction of the platform posteriorly considered diagnostic by some authors (Orchard et al., 1994; Orchard and Krystyn, 1998); *C. krystyni* (Orchard and Krystyn, 1998) is characterized by “undulose margins”. Mei (1996) introduced the square-, rounded- and narrow-morphotypes when referring to neogondolellids species. The square-morphotype has a squared and oblique posterior end and includes *C. tulongensis*; the rounded-morphotype has a teardrop platform outline and includes *C. changxingensis*, *C. zhejiangensis* and *C. taylorae*; the narrow-morphotype has a narrow posterior end and a lenticular platform outline and includes *C. meishanensis* and *C. orchardi*. Mei et al. (1998) in their re-evaluation of the taxonomy of Permian-Triassic conodonts from China, also used the three morphotypes, but concluded that “the general configuration of the denticles is the most consistent and reliable characteristic”. This hypothesis was independently proposed in Krystyn and Orchard (1996) and in Orchard and Krystyn (1998), who argued that Griesbachian neogondolellids species are mostly distinct by the axial part (blade-carina-cusp).

One limitation of this study is the sampling size of the dataset. The small number of

individuals in certain species might lead to a lack of statistical power to recognize the different species. However, at the interspecific level, the differences between the morphospecies are expected to be strong enough to be visualized on the morphospace, even with a small sampling size. It would be interesting to add more specimens into the analysis to improve the statistical power, and see if this helps to differentiate the species or on the contrary add variability that would reinforce the morphological continuum.

Regarding the cluster and the outline analysis, *Ng. discreta* appears to be the more consistent morphospecies in this assemblage. As its range of existence is much reduced during the Griesbachian, this easily recognizable species is considered as a potential good and useful biostratigraphic tool. Interestingly, *C. meishanensis*, *C. griesbachensis*, *Sw. kummeli*, *C. tulongensis*, *C. zejiangensis* and *C. taylorae* are individually significantly different from at least half of the other species of the assemblage. These species might therefore have been used carefully for biostratigraphy or other kind of evolutionary analysis, but the characters used for taxonomy need to be clarified and when possible quantified. Concerning the remaining species, the characters studied here didn't succeed to evidence enough differences between them. Their distinction appears to be quite arbitrary and author dependent, which increase the risk of taxonomical errors and confusions in further studies. Their validity and use as a biostratigraphic tool might therefore be reconsidered.

This study evidence that all the taxonomical characters usually used in taxonomy are not equally useful, and some reconsideration could be useful to avoid some confusions. Some characters are not used for the construction of any cluster, such as the platform width, the occurrence of a free anterior blade, or the relative size of denticles (without cusp). Those characters seem to be widespread and variable in the assemblage, and therefore do not constitute a good taxonomic character. On the opposite, the thickness of the posterior platform brim is used in three different clusters, and can therefore be considered of taxonomical importance. Based on the position of the categories for each variable in the morphospace, the presence of an accessory process after the cusp could also be useful.

According to Mei et al. (1998), to Krystyn and Orchard (1996) and to Orchard and Krystyn (1998), Griesbachian neogondolellids species are mostly distinguished by the axial part. By this

standards, a subgroup mostly defined by the occurrence of a lateral indentation like subgroup 3A is considered a taxonomical dead-end. Although this has never been quantified, it is generally admitted that the platform margins in neogondolellids display a high variability (Kozur et al., 1995), and that asymmetrical lateral indentation is occurring independently in different species. The data presented in this study do not seem to corroborate this theory, as *Ng. discreta* can be recognized only with the outline of the element in oral view. Would the axial part bear the most important diagnostic features, it would be interesting to tune the relative weight of the considered taxonomical characters in the analysis to give more importance to the blade-carina-cusp than to the platform shape, and see if the species are better discriminated. Such analysis would incorporate a strong a priori in the analysis, which was not the aim of the present study.

To summarize, although the size of the cohort does not allow a statistical partitioning into more than five groups, we observe that even non-statistical groups can separate the holotypes in different clusters. Increasing the sample size would achieve a higher statistical power, but we also propose here a number of perspectives and solutions in order to improve the method in future analyses. The difficulty to interpret continuous characters as categorical variables led to approximations that generate “noise” within the final signal, resulting into high within-group inertia. A multivariate method including quantitative measurements would lead to a more objective classification. The diagnostic characters are eventually the authors’ own choice, and the relative importance of the platform shape or the axial part in taxonomy is still matter to debate. Some clarification needs to be done in the description of some species and taxonomical characters to avoid as much confusions as possible. This would ease the species recognition by non-taxonomical specialists, and allows a wider use of conodonts in different topic of interest, e.g. studies in evolution, biogeography, diversity, evo-devo, histology or ecology.

## Acknowledgments

This work is supported by the French ANR @RAction grant (project EvoDevOdonto to N.G.) and a Swiss NSF project 200021\_135446. We are very grateful to IE P. Joncour (IGFL, ENS Lyon, France) for her help with statistics.

## References

- Brosse, M., Baud, A., Bhat, G. M., Bucher, H., Leu, M., Vennemann, T., & Goudemand, N., 2017. Conodont-based Griesbachian biochronology of the Guryul Ravine section (basal Triassic, Kashmir, India). *Geobios*, 50(5-6), 359-387.
- Clark, D., 1959. Conodonts from the Triassic of Nevada and Utah. *Journal of Paleontology*, 33(2), 305-312.
- Husson, F., Josse, J., and Pages, J., 2010. Principal component methods-hierarchical clustering-partitional clustering: why would we need to choose for visualizing data. Applied Mathematics Department.
- Husson, F., Josse, J., Lê, S., Mazet, J., and Husson, F., 2016. Package ‘FactoMineR’.
- Kozur H., Ramovs A., Wang E. and Zakharov Y., 1995. The importance of *Hindeodus parvus* (Conodontata) for the definition of the Permian-Triassic boundary and evaluation of the proposed sections for a global stratotype section and point (GSSP) for the base of the Triassic. *Geologija*, 37(8), 173-213, Ljubljana.
- Krystyn, L., and Orchard, M., 1999. Lowermost Triassic ammonoid and conodont biostratigraphy of Spiti, India. *Albertiana*, 17, 10-21.
- Lê, S., Josse, J., and Husson, F., 2008. FactoMineR: an R package for multivariate analysis. *Journal of statistical software*, 25(1), 1-18.
- Mei, S., 1996. Restudy of conodonts from the Permian-Triassic boundary beds at Selong and Meishan and the natural Permian-Triassic boundary. Centennial memorial volume of Professor Sun Yunzhu (Sun YC). *Stratigraphy and palaeontology*, 141-148.
- Mei, S., Zhang, K., and Wardlaw, B., 1998. A refined succession of Changhsingian and Griesbachian neogondolellid conodonts from the Meishan section, candidate of the global stratotype section and point of the Permian-Triassic boundary. *Palaeogeography, Palaeoclimatology, Palaeoecology*, 143(4), 213-226.
- Orchard, M., 2007. Conodont diversity and evolution through the latest Permian and Early

- Triassic upheavals. *Palaeogeography, Palaeoclimatology, Palaeoecology*, 252(1), 93-117.
- Orchard, M.J., and Krystyn, L., 1998. Conodonts of the lowermost Triassic of Spiti, and new zonation based on Neogondolella successions. *Rivista Italiana di Paleontologia e Stratigrafia*, 104(3), 341-368.
- Orchard, M., Nassichuk, W. W., and Rui, L., 1994. Conodonts from the Lower Griesbachian Otoceras Latilobatum Bed of Selong, Tibet and the Position of the Permian-Triassic Boundary. *Canadian Society of Petroleum Geologists, memoire* 17, 823-843.
- Tian, C., 1982. Triassic conodonts in the Tulong section from Nyalam County, Xizang (Tibet), China. *Contribution to Geology of Qinghai, Xizang (Tibet) Plateau*, vol. 10.
- Yin, H., Wu, S., Ding, M., Zhang, K., Tong, J., Yang, F., and Lai, X., 1996. The Meishan section, candidate of the global stratotype section and point of Permian-Triassic boundary. *The Paleozoic-Mesozoic Boundary Candidates of the Global Stratotype Section and Point of the Permian-Triassic Boundary*, 31-48.





## Conclusion et perspectives

Tout au long de cette étude, nous avons démontré le potentiel du conodonte en tant qu'organisme modèle pour étudier l'évolution en temps profond.

Le premier chapitre présente la découverte des premiers spécimens du Trias avec préservation exceptionnelle du corps basal sur tous les éléments de l'appareil masticatoire. Jusqu'alors, seuls quelques éléments P1 avaient été trouvés au Trias avec un corps basal préservé et aucun élément S ou M. Ainsi, il avait été proposé une perte progressive du corps basal ou une tendance à la faible minéralisation pour expliquer cet absence. Nous montrons ici que seul un biais de préservation (encore mal compris) en est, semble-t-il, responsable. Cette découverte nous a permis également de discuter de la morphologie du corps basal : sa taille et sa forme sont en accord avec prédictions antérieures associées à un modèle fonctionnel de l'appareil en mouvement, que nous ne pouvons donc pas infirmer. En comparant les morphologies du corps basal entre éléments P d'un côté et S et M de l'autreau travers des âges, nous avons aussi pu émettre l'hypothèse que leur forme répondait probablement à des contraintes fonctionnelles liées à la mécanique de la mastication. Pour aller plus loin, il serait nécessaire de scanner les éléments à haute résolution, par exemple au synchrotron, pour pouvoir quantifier en trois dimensions la forme du corps basal afin de tenter de la corrélérer à celle de la couronne. Cela pourrait permettre de mieux comprendre le développement de l'élément dans son intégralité, et nous informer sur la macroévolution des conodontes.

La méthodologie présentée dans le chapitre 2 et appliquée dans les chapitres trois et quatre démontre la possibilité, et surtout l'utilité des méthodes de morphométrie géométrique pour quantifier la forme des éléments conodontes. Ce protocole est exportable à plusieurs autres familles d'éléments conodontes. Dans le chapitre 3, nous proposons également une méthode originale permettant de scanner rapidement un grand nombre d'éléments à l'aide d'un microtomographe, permettant par la suite de contrôler l'orientation des éléments lors de la prise d'images servant aux analyses de morphométrie en 2D. Cette méthodologie nous a permis d'étudier de manière quantitative l'évolution morphologique des conodontes, et ses réponses à des perturbations en-

vironnementales. Par la suite, des analyses en trois dimensions pourraient être utilisées, notamment pour caractériser certaines structures impossibles à quantifier en deux dimensions comme l'ornementation de la plateforme par exemple. Pour cela, des techniques de topologie dentaire ou de système d'information géographique (SIG) devraient être transposées aux conodontes.

Dans le chapitre 3, nous avons pu mettre en évidence l'existence d'un axe principal de variation phénotypique au sein de différentes espèces de conodontes du Trias supérieur. Il était attendu que l'évolution soit orientée préférentiellement selon cet 'axe de moindre résistance'. Nous avons pu démontrer que si cela semble vrai à l'échelle intraspécifique ou intra-genre, l'évolution entre les genres pendant des périodes de grands changements environnementaux peut être au contraire dirigée par des facteurs environnementaux plutôt que développementaux. Néanmoins, nous avons établi aussi l'existence de lois potentiellement génériques de covariation entre certains traits morphologiques, illustrant ainsi l'effet des contraintes développementales sur l'évolution. A l'avenir, l'incorporation dans l'analyse de caractères morphologiques supplémentaires (notamment grâce aux analyses en trois dimensions) permettrait une meilleure compréhension des corrélations entre les caractères morphologiques, permettant une étude des patrons d'intégration et de modularité de ces éléments, et à terme le développement d'une théorie mécaniste de ces lois de covariation.

Dans le chapitre 4, nous avons mis en évidence l'existence d'un axe privilégié d'évolution, commun à deux lignées de conodontes très distantes phylogénétiquement, spatialement et temporellement, ce qui nous a permis de discuter du rôle des contraintes développementales et de l'environnement dans l'évolution des deux groupes de conodontes considérés. En particulier, nous avons démontré un lien potentiellement général entre changements de température des océans et changement morphologique chez les conodontes : en effet les deux groupes considérés évoluent tous les deux selon le même axe morphologique mais dans des directions opposées, ce qui est consistant avec le fait que les espèces concernées sont apparues pendant un réchauffement dans un cas et pendant un refroidissement dans l'autre. Nous proposons que la température ait un effet important sur la physiologie des conodontes, en particulier sur leur vitesse de croissance et que des températures plus basses correspondent à un développement

plus lent (ou plus court) et donc à la maturation de morphologies plus juveniles. En intégrant d'autres familles de conodontes ayant subi des changements climatiques similaires ou différents, et en considérant des mesures indépendantes de l'âge des éléments (taux de strontium dans les lamelles de croissance de la couronne) nous pourrions tester la validité de ces hypothèses, et trancher certaines questions laissées en suspens, notamment concernant les mécanismes développementaux à l'œuvre.

Le chapitre 5 présente une tentative d'utilisation de la morphométrie géométrique ainsi que des analyses multivariées et de clustering pour clarifier la taxonomie des neogondolellides au Trias inférieur. Si les méthodes utilisées ici ont échoué à séparer les espèces décrites dans la littérature et à identifier des caractères discriminants pouvant être utilisés en taxonomie, les résultats permettent cependant de discuter de la validité des espèces décrites et des caractères morphologiques diagnostiques associés. Dans l'avenir, il serait intéressant d'attribuer des poids différents aux caractères taxonomiques utilisés en suivant l'opinion des spécialistes de la taxonomie afin de recréer virtuellement la hiérarchie utilisée par ceux-ci lors de l'identification des espèces, et ainsi établir une méthode permettant une meilleure reconnaissance numérique des espèces.

